UNIVERSITA' DEGLI STUDI DI PADOVA

Sede Amministrativa: Università degli Studi di Padova

Dipartimento di Scienze Biomediche Sperimentali

SCUOLA DI DOTTORATO DI RICERCA IN: BIOSCIENZE
INDIRIZZO: BIOLOGIA CELLULARE
CICLO XX

IMMUNOLOGICAL EVENTS INDUCED BY INTRAPULMONARY ADMINISTRATION OF LTK63 OR CpG IN MICE

Direttore della Scuola : Ch.mo Prof. Tullio Pozzan
Supervisore : Ch.mo Prof. Cesare Montecucco
Supervisore esterno : Dott. Andreas Wack

Dottorando : Dott.ssa Isabella Pesce

31 gennaio 2008

Summary

The synthetic oligodeoxynucleotides containing unmethylated CpG dinucleotides (CpG ODNs) and LTK63, a detoxified mutant of the *E. coli* the heat labile enterotoxin (LT), are potent mucosal adjuvants. In addition, CpG ODNs and LTK63 provide generic protection, in the absence of co-administered antigen, to respiratory infections. CpG ODNs act through a well-defined molecular pathway, but little is known about immune modulation induced by CpG ODNs in the lung. Similarly, it is clear that LTK63 is immunogenic and functions efficiently as adjuvant, but the mechanism of action in both adjuvanticity and in generic protection is largely unknown. In order to study *ex vivo* and compare the immunological events induced by CpG ODNs and LTK63, the B-type CpG 1826 or LTK63 were administered intrapulmonary in BALB/c mice. Lungs, sera and spleens were monitored from 3 hours to 14 days after intrapulmonary administration by combining different approaches, comprising multiplex analysis of cytokine protein expression and flow cytometric analysis of lung immune cell populations. In addition, alveolar macrophage (AM) sensitivity to CpG ODNs and the effect of LTK63 on DC recruitment into the lung and on the function of DCs isolated from LTK63 treated and control mice were tested.

The cytokine analysis of lung homogenates shows that CpG ODNs induce an early cytokine response and that the earliest cytokines detected in the lung are KC at 1 hr followed by IL-1α and β, IL-12(p40) and IL-6 at 3 hrs and by G-CSF, MCP-1, MIP-1α and β, and RANTES at 6 hrs. Most but not all of these cytokines are found systemically in the serum in a narrow peak at slightly later time points compared to their appearance in the organ, suggesting a spillover from the lung into the blood, and several of those cytokines are released by AMs after *in vitro* stimulation with CpG ODNs. Flow cytometric analysis of lung immune cells shows that intrapulmonary administration of CpG ODN induces activation of plasmacytoid DCs (pDCs), myeloid DCs (mDCs), CD4 T cells, CD8 T cells and NK cells in a time period of 12 hours to 4 days after treatment, as well as recruitment into the lung of pDCs at 2 days and of mDC starting at 4 days, respectively.

LTK63 treatment, in contrast, acts more slowly and induces two phases of activation in the lung: an early phase, which extends from 1 to 2 days, and a second phase, which extends from 6 to 8 days. In the first phase, LTK63 intrapulmonary administration induces up-regulation of IL-1β, G-CSF and KC, which represent granulocyte chemoattractants and growth factors, and consistent with this, accumulation of granulocytes and mDCs in the lung is observed. In the second phase, LTK63 induces in the lung the up-regulation of a complex mixture of cytokines involved in

inflammation and cell recruitment, which are produced in part by $CD11c^+$ cells, as shown in *in vitro* experiments with these cells isolated from the lungs of LTK63 treated mice. Flow cytometric analysis of lung immune cells shows that at 6-8 days after LTK63 treatment, the number of mDCs and pDCs, CD8+ and CD4+ T cells, granulocytes, NK cells and B cells increase, and CD8+ and CD4+ T cell subsets are activated. In vivo migration assays indicate that at least part of the LTK63-induced increase in mDC numbers is due to the recruitment of differentiated DCs from the blood. In order to understand the nature of the increased immune responsiveness in the lung, the T cell stimulatory ability of lung myeloid cells was analyzed. The studies of the mixed population of total lung $CD11c^+$ cells show that cells isolated from LTK63 treated mice are more efficient at stimulating allogeneic T cell responses than those from untreated mice. When we tested the T cell stimulatory ability of cells sorted into $CD11c^+$MHC-II^{high} mDCs and $CD11c^{high}$MHC-II^{int} cells comprising alveolar macrophages and immature mDCS, we found no difference on a per cell basis between LTK63 treated and control mice. Since I find a strong accumulation of $CD11c^+$MHC-II^{high} mDCs after LTK63 treatment, I conclude that the enhanced immune responsiveness induced by LTK63 is partly due to increased numbers of $CD11c^+$MHC-II^{high} mDCs with a strong potential to prime T cells.

In conclusion, while both CpG ODNs and LTK63 studied here appear to act mainly through APCs such as AMs and DCs, the kinetics of this process greatly differ between the two. The response to CpG ODNs is much faster, probably due to the direct activation of receptor-bearing innate immune cells present in the lung, among which mDCs and pDCs. The earliest event in the response to LTK63, in contrast, is detectable only after 24 hrs, which suggests either that the initial steps are too subtle to be detected here, and that chemokine production and cell influx observed at 1 to 2 days has to be considered the distal result of a sequence of small events preceding those detected here. Alternatively, due to the nature of the interaction between LTK63 and target cells, the phenomena observed at 24 hrs may in fact be the very first to take place, which would suggest a very slow onset of cell activation by LTK63. On the other hand, the response to LTK63 lasts longer, and a second wave of events are observed at 6-8 days. The explanation that is most plausible and compatible with known kinetics of immune responses is that this second wave is driven at least partly by the adaptive immune response to LTK63 and that in fact, LTK63 acts by mimicking infection by a pathogen. At 8 days, we do not detect any response to CpG ODNs anymore, which again would be compatible with the fact that in the absence of a protein Ag component, the immune response is limited to the initial innate phase and not prolonged. This is in line with the studies on generic protection indicating that this protective effect is less durable for CpG ODNs than for LTK63.

Esposizione riassuntiva

Gli oligonucleotidi sintetici contenenti motivi CpG (CpG ODNs) e LTK63, un mutante privo di tossicità della tossina termolabile di *E. Coli* (LT), sono potenti adiuvanti mucosali. Inoltre, CpG ODNs e LTK63 conferiscono protezione generica, senza la contemporanea somministrazione di un antigene, alle infezioni respiratorie. CpG ODNs funzionano attraverso un ben definito "pathway" molecolare, ma poco è noto sull'immuno modulazione indotta da CpG ODNs nel polmone. In modo simile, è chiaro che LTK63 è immunogenico e funziona in maniera efficiente come adiuvante, ma il meccanismo d'azione è completamente sconosciuto sia nel ruolo adiuvante che nella protezione generica. Allo scopo di studiare *ex vivo* e comparare gli eventi immunologici indotti da CpG ODNs e LTK63, sono stati somministrati per via intrapolmonare nel topo il CpG ODNs 1826 di tipo B ed LTK63. Polmoni, sieri e milze sono stati monitorati da 3 ore a 14 giorni dopo la somministrazione intrapolmonare combinando differenti approcci, che comprendono l'analisi "multiplex" dell'espressione a livello proteico delle citochine a l'analisi citofluorimetrica delle popolazioni di cellule del sistema immunitario del polmone. Inoltre, sono stati testati la responsività dei macrofagi alveolari (AMs) al trattamento con CpG ODNs e gli effetti di LTK63 sul reclutamento e la funzionalità delle cellule dendritiche (DCs) isolate sia da topi trattati che da topi di controllo.

L'analisi delle citochine negli omogenati di polmone mostra che CpG ODNs inducono una risposta veloce delle citochine e che la prima citochina osservata è KC ad 1 ora seguita da IL-1α and β, IL-12(p40) and IL-6 a 3 ore e da G-CSF, MCP-1, MIP-1α and β, and RANTES a 6 ore. La maggior parte ma non tutte queste citochine sono state trovate a livello sistemico nel siero con un picco più stretto e a tempi leggermente più tardivi rispetto alla comparsa nell'organo, suggerendo lo "spillover" dal polmone nel sangue, e diverse di queste citochine sono rilasciate dai AMs dopo la stimolazione *in vitro* con CpG ODNs. L'analisi citofluorimetrica delle cellule del sistema immunitario del polmone mostra la somministrazione intrapolmonare di CpG ODNs induce in un arco temporale da 12 ore a 4 giorni dopo il trattamento attivazione delle DCs plasmacitoidi (pDCs), delle DCs mieloidi (mDCs), dei linfociti T CD4+, dei linfociti T CD8+ e delle cellule natural killer, come anche il reclutamento nel polmone a 2 giorni delle pDCs e a 4 giorni delle mDCs.

Al contrario, LTK63 agisce più lentamente e induce due fasi di attivazione nel polmone: un fase veloce, che si estende da 1 a 2 giorni, ed una seconda fase, che si estende da 6 a 8 giorni. Nella prima fase, la somministrazione intrapolmonare di LTK63 induce up-regolazione di IL-1β, G-CSF and KC, che rappresentano dei chemoattrattanti e dei fattori di crescita per i granulociti, e consistente con questo è stato osservato nel polmone accumulo di granulociti e mDCs. Nella seconda fase, LTK63 induce up-regolazione di un complesso insieme di citochine coinvolte nell'infiammazione e nel reclutamento cellulare, che sono prodotte in parte da cellule $CD11c^{+}$,

come mostrato negli esperimenti *in vitro* con queste cellule isolate dai polmoni di topi trattati con LTK63. L'analisi citofluorimetrica delle cellule del sistema immunitario del polmone mostra che 6-8 giorni dopo il trattamento con LTK63 aumenta il numero di mDCs e pDCs, dei linfociti T CD8+ e CD4+, dei granulociti, delle cellule natural killer e dei linfociti B. Le misurazioni della migrazione *in vivo* indicano che almeno in parte l'aumento del numero di mDCs indotto da LTK63 è dovuto al reclutamento di DCs differenziate dal sangue. Allo scopo di capire la natura dell'aumentata responsività del sistema immunitario nel polmone, è stata analizzata la capacità delle cellule mieloidi del polmone di stimolare i linfociti T. Gli studi della popolazione mista di cellule $CD11c^{+}$ del polmone mostrano che le cellule isolate da topi trattati con LTK63 sono più efficienti di quelle isolate da topi non trattati a stimolare i linfociti T allogenici. Quando abbiamo testato la capacità stimolatoria delle cellule sortate come $CD11c^{+}MHC\text{-}II^{high}$ mDCs e delle cellule $CD11c^{high}MHC\text{-}II^{int}$, che comprendono AMs e DCs immature, noi non abbiamo trovato differenze a parità di numero di cellule tra le cellule di topi trattati con LTK63 e di controllo. Poiché ho trovato un forte accumulo di mDCs dopo il trattamento con LTK63, concludo che l'aumentata responsività del sistema immunitario indotta da LTK63 è in parte dovuta all'aumentato numero di mDCs $CD11c^{+}MHC\text{-}II^{high}$ con un forte potenziale di "priming" dei linfociti T.

In conclusione, mentre sia CpG ODNs che LTK63 qui studiati sembrano agire principalmente tramite cellule presentanti l'antigene come AMs e DCs, la cinetica di questo processo è molto differente tra i due. La risposta a CpG ODNs è più veloce, probabilmente per la diretta attivazione delle cellule del sistema immunitario innato, tra cui mDCs e pDCs. Al contrario, il più veloce evento in risposta a LTK63, è rivelabile solo dopo 24 ore e questo suggerisce sia che gli eventi iniziali siano troppo impercettibili, sia che la produzione di chemochine e l'influsso di cellule osservato a 1-2 giorni possa considerarsi il risultato distale di un sequenza di piccoli eventi che precedono quelli rivelati qui. Alternativamente, a causa della natura dell'interazione tra lTK63 e le cellule target, il fenomeno osservato a 24 ore potrebbe essere il primo ad accadere e questo suggerirebbe un inizio molto lento dell'attivazione cellulare indotta da LTK63. D'altra parte, la risposta a LTK63 dura più a lungo, è una seconda ondata di eventi è stata osservata a 6-8 giorni. La spiegazione più plausibile e compatibile con le note cinetiche delle risposte immunitarie è che questa seconda ondata sia guidata almeno in parte dalla risposta adaptativa e che LTK63 agisca mimando l'infezione di un patogeno. A 8 giorni, non abbiamo rivelato alcuna risposta a CpG ODNs, che di nuovo potrebbe essere compatibile con il fatto che in assenza di un antigene la risposta immunitaria sia limitata alla fase iniziale. Questo è in accordo con gli studi di protezione generica che indicano che l'effetto protettivo di CpG ODNs dura meno di quello di LTK63.

Contents

Figures

Tables

1. Introduction

1.1. Lung immune response

The lungs, in order to facilitate gas exchange, represent the largest epithelial surface in the body in contact with the outside environment. During respiration, the upper and lower airways are continuously exposed to microorganisms and organic and inorganic particulate material.

During evolution, strategies to recognize material from the outside environment and to distinguish potentially harmful agents from the vast majority of innocuous foreign material have developed. It is well known that the immune system in the lungs, similar to the gut mucosa, is tolerogenic to avoid deleterious responses to harmless antigens.

However, in order to protect the host against pathogens, a complex defense system has evolved. The lungs offer physical barriers to the entry of microorganisms, then the antigen-independent recognition of pathogens by the innate immune system and finally, the adaptive immune responses, highly regulated and specific, mediated by antigen specific T and B lymphocytes. The innate immune responses are responsible for the clearance of foreign particles deposited on the surface of the airways and the rapid detection and elimination of invading pathogens from the alveolar spaces. In contrast, adaptive immune responses take time to become effective, but provide the antigen specificity required for complete eradication of pathogens and have a memory component lacking in the innate immune systems.

1.1.1. Innate immunity in the lungs

Innate immune mechanisms defend the air spaces from the array of microbial products that enter continuously the respiratory tract. The physical barriers represent the first obstacles to the invasion of the lung by infectious agents. Large particles are generally trapped in the upper airways by mucins and then cleared by ciliary movements. Particles 1 μm in size and smaller, the size of bacteria and viral particles, generally bypass these physical barriers and gain access to the alveolar surface where they interact with soluble components in the alveolar fluids, alveolar macrophages (AMs) and airway epithelial cells[1].

The soluble constituents of airway and alveolar fluids have an important role in innate immunity in the lungs. These constituents include a variety of proteins, peptides and

organic molecules, which either possess direct antimicrobial activity or facilitate the elimination of infectious pathogens by phagocytic cells. Lysozyme and Lactoferrin are soluble proteins that limit bacterial growth; lysozyme is lytic to many bacterial membranes and lactoferrin excludes iron from bacterial metabolisms. Immunoglobulin G (IgG) is the most abundant immunoglobulin in the alveolar fluid, and complement proteins and surfactant associated proteins serve as additional microbial opsonins. In particular, surfactant proteins A (SP-A) and surfactant proteins D (SP-D) that are members of the collectin family, promote phagocytosis by alveolar macrophages (AMs)[2].

Defensins are antimicrobial peptides with a broad spectrum of microbicidal activity against gram positive and negative bacteria, fungi and certain enveloped viruses. The microbicidal activity of defensins depends on their ability to permeabilize or form pores within biological membranes [2,3].

Moreover, the cells of the innate immune system express many key protective factors called pattern recognition receptors (PRRs). The PRRs mediate the antigen independent recognition of pathogens by cells of the innate immune systems[1]. During the innate immune response, through the PRRs, these cells recognize and respond to conserved structures that are shared by bacteria (e.g. lipopeptides, peptidoglycan, lipopolisaccharide and bacterial DNA) or viruses (e.g. single-stranded or double-stranded RNA) and are collectively known as pathogen associated molecular patterns (PAMPs). However, the PAMPs are not restricted in their expression to pathogens, but are expressed also in commensal organisms. The anatomic or intracellular location of the PAMPs allow to distinguish a pathogen from a commensal organism; for example, the PAMPs of commensal organisms are not be expected to stimulate a PRR on a basolateral epithelial surface, or to reach an intracellular PRR [4]. To date, the Toll-like receptor (TLR) family is the best characterized class of PRRs in mammalian species.

AMs have important phagocytic, microbicidal and secretory functions and play a prominent role in lung innate immunity [5]. Under normal conditions, AMs account for approximately 95% of the leukocytes in the alveolar spaces, whereas during inflammation, the percentage of macrophages is reduced and the percentage of lymphocytes and polymorphonuclear leukocytes increases [6]. AMs ingest all types of inhaled particulates that evade the physical barriers of the lungs and reach the alveolar spaces without triggering inflammatory responses. When bacteria are opsonized by IgG, complement, or SP-A and SP-D, they are ingested by Ams, and the phagosomal membrane provides discrimination among the various microbial products entering the cell [7]. In the event that AMs are not

capable to contain invading pathogens, they communicate with other cells of the innate immune system to mount a protective response. Cytokines produced by AMs play a critical role, not only to initiate, but also to localize and reinforce this protective response. The proinflammatory cytokines produced by AMs, notably IL-8 and CXC chemokines, initiate a localized inflammatory response by recruiting neutrophils into the airway lumen in response to invading pathogens. G-CSF acts both locally to activate and recruit neutrophils and systemically to stimulate the neutrophil proliferation and the release from the bone-marrow[2]. CC chemokines such MCP-1 and RANTES recruit activated monocytes and lymphocytes into the sites of inflammation in the lungs[1].

Other cells that have a key role in innate immune responses in the lung are airway epithelial cells, which prevent microbial colonization by several different mechanisms. The first mechanism is that the ciliated epithelial cells move fluid, mucus, and trapped particulates upward and out of the lungs, offering a physical barrier to the microbial ingress. Another mechanism is that airway epithelial cells, in response to pathogens, directly induce the production in the airway fluids of soluble proteins that contain bacterial growth, and the production of antimicrobial defensins [8]. In addition, airway epithelial cells express PRRs such as TLR1-6 and TLR-9 and sense bacteria, using the same TLR-dependent mechanisms used by leukocytes. After engagement of PRRs, epithelial cells enhance the production of antimicrobial defensins and are stimulated to produce CXC and CC chemokines, which recruit neutrophil into the airway lumen[1,9]. For example, in airway epithelial cells recognition of unmethylated bacterial DNA by TLR-9 lead to NF-κB activation and production of IL-6, IL-8 and β2-defensin [1,10]. Therefore, after infectious agents and inflammatory stimuli, airway epithelial cells produce IL-1β, IL-6, IL-8, RANTES, GM-CSF, and TGF-β, in addition to other proinflammatory cytokines, and the production of these cytokines initiate an inflammatory response in the lung and induce the recruitment of innate immune cells[8].

1.1.2. Adaptive immunity in the lungs

Adaptive immunity to infection in the lungs, as at other sites in the body, depends on the specific recognition of microbial antigens that is required for complete elimination of the pathogen and the generation of immunological memory.

During respiration, the lungs become exposed to a variety of environmental toxins, allergens, and pathogens. The fate of inhaled antigenic material, including infectious

agents, depends on their ability to resist enzymatic degradation and to penetrate physical, chemical, and immunologic barriers. When an antigen penetrates these defense barriers, the first step necessary to mount an adaptive immune response is the acquisition of the antigen by an antigen presenting cell (APC). The APCs are a group of cells which are able to take up antigens, to present antigens in the form recognizable by T cells and to produce co-stimulatory signals necessary for T cell activation. There are three types of professional APCs in the lung: alveolar macrophages, B cells and dendritic cells. AMs are abundant in the alveolar space and are likely first to encounter the antigen. AMs ingest all types of inhaled particulates that reach the alveolar spaces by phagocytosis and soluble antigen by fluid–phase pinocytosis [5]. Potential APCs are also antigen specific memory B cells, capable of acquiring antigen via cell-surface immunoglobulins [11]. DCs are also optimally located for antigen exposure: in the upper airways, DCs are found within the epithelial layer and beneath the epithelial layer; and in the lower respiratory tract, DCs are found in the interstitial space, or beneath the epithelial layer, as well as in the lumen of the alveoli [4]. DCs have several mechanisms for acquiring antigens: through micropinocytosis, endocytosis or phagocytosis [12]. In addition, DCs or the other cells capable of presenting antigens can be actively infected by some microrganisms [13-15]. DCs are thought to be the main APCs responsible for sensitization to inhaled antigens and induction of adaptive immunity in the lung.

Although direct evidence for DC involvement in lung T cell responses exists in only a limited number of cases [16-20], it is generally believed that DCs are the requisite APCs for initiation of T cell responses. A significant advance to the studies of the role of APCs in T cell responses is the use of CD11c-DTR model to deplet selectively DCs, but the use of this model is limited in the lung because in the respiratory tract and spleen macrophages express CD11c and are depleted by DT treatment of transgenic mice[17,21]. Nonetheless, confocal and intravital imaging analysis is beginning to provide views of T cell and DC interactions in situ and in real time [22-24]. From these studies several evidences indicate that DCs are the main initiators of T cell responses in the lung, although in some cases other APCs may partecipate in T cell activation.

DCs in the respiratory tract have a sentinel function and this implies that DCs are continuosly replenished, that DCs have the capacity to capture and to sense inhaled antigens and that DCs efficiently trasport processed antigens to the draining pulmonary lymph nodes (LNs), where DCs induce either tolerance or immunity.

Even in the absence of inflammation, DCs or their precursors are constantly recruited from the blood into the lung. Holt and coworkers were the first to demonstrate that respiratory tract DCs are continuosly replenished [25]. DCs can populate the lung through different mechanisms: chemokine-driven recruitment of differentiated DCs from the circulation; recruitment of DC precursors, which then differentiate into DCs after exposure to local cytokines, and, albeit less documented, proliferation of intrapulmonary DC progenitors and transdifferentiation of pulmonary macrophages into DCs [26]. Inflammatory stimuli have a profound impact on this steady state dynamic; for example, a very rapid influx of DCs into the airways of rat was described by McWilliam and colleagues after the inhalation of bacteria or viral particles [27].

In the airways, the superficial network of DCs, as introduced above, is ideally positioned to capture inhaled antigens. At this stage, DCs have high capacity to capture and process incoming antigens and to sense pathogens through the PRRs, but are functionally immature and unable to stimulate T cells [28]. Under steady state conditions, immature DCs continuosly capture antigens and increase their expression of the chemokine receptor CCR7, which enables them to become attracted to the chemokine CCL21 produced from the T cell areas of local lymphoid organs [29,30]. During the migration via afferent lymphatics to the LNs draining the low respiratory tract, antigen bearing DCs upregulate the costimulatory molecules and express high levels of MHC class II molecules enabling them to activate naïve T cells [29]. In the lung, the mediastinal lymph nodes (MLNs), which drain the lower respiratory tract, are the major sites of T cell priming [29,31,32]. After arriving into the MLNs, encounter of antigen-bearing DCs with T cells can result in multiple outcomes depending on the nature, form and dose of the antigen, the type and activation status of DCs, as well as the environmental factors present at the time of antigen encounter [11].

In response to inflammatory signals at antigen exposed surfaces, the number of DCs increase, as mentioned before. Under conditions in which exposure to inhaled antigen is accompanied by an inflammatory stimulus, such as recognition of pathogens through PRRs expressed on DCs, the signals transduced as a result of this recognition induces the expression of DC genes required for DCs full maturation [33]. In addition, inflammatory stimuli induce accelerated migration of antigen bearing DCs towards LNs. For example, airway inflammation induced by virus infection recruits airway DCs and induces their full maturation after arrival in the MLNs [31].

In the absence of PRRs ligands and/or inflammatory cytokines, DCs fail to mature and therefore are unable to provide sufficient costimulation to the T cells, and the functional

outcome of DCs encounter with T cells is the induction of a state of tolerance. For example, intranasal administration of protein antigens such as ovalbumin (OVA) induce T cell tolerance [34-36].

Fully mature DCs are able to activate naïve T cells in the MLNs, as observed when high doses of LPS or infection with influenza virus are administrated at the time of exposure to OVA [37,38].

Few studies have directly addressed the outcome of T cell priming by airway DCs. Early events during T cell activation in response to inhaled antigens has been investigated after the adoptive transfer of antigen pulsed DCs into the trachea of naïve animals [16,39]. It emerged from these studies that DCs select specific T cells from the polyclonal repertoire and that the encounter with T cells lead, within 4 days, to clonal expansion of antigen-specific T lymphocytes. After proliferation and differentiation, antigen-specific T cells leave the LNs and home back to the lung as cytokine producing effector T cells [16,40]. After two to four days, T cells also recirculate to non-draining lymph nodes and to the spleen, representing most probably the central memory T cells that have been described in vitro [41]. Moreover, activated T cells move towards the germinal centres where B cells are located to induce maturation of antigen-specific immunoglobulin secreting B cells. These studies indicate that DCs prime the T cell response not only by providing antigenic and costimulatory signals to lymphocytes, but also by imprinting in them the ability to home back to the lung by upregulation of chemokine and homing receptors [11].

1.2. Mucosal adjuvants

Many pathogens gain access and infect the host across a mucosal surface, in particular the respiratory or gastrointestinal mucosa. Although vaccines have traditionally been administered by injection, there are several important reasons for using a mucosal route of vaccination instead of a systemic route. The primary reason is that the majority of infections occur at or take their departure from a mucosal surface, and therefore, in these infections, local application of a vaccine is often required to induce a protective immune response. In fact, traditional vaccine strategies do not prevent initial phases of infection, while a vaccine administered by a mucosal route induce an immune response that can prevent the attachment and colonization at the mucosal epithelium of infectious agents or the penetration and replication of infectious agents in the mucosa. Moreover, mucosal vaccines, inducing local secretion of IgA, can block the binding and action of microbial

toxins, that could bind to mucosal epithelial cells and damage the host. In addition, there are also pratical and logistic reasons for using a mucosal route of vaccination, and these reasons include easier administration, greater acceptability, the potential for frequent boosting and the elimination in the developing world of the infections due to re-use of needles [42,43].

However, delivery of antigens via mucosal routes generally does not stimulate any immune responses, and this is due to a combination of factors including tight immune regulation at mucosal surfaces, which controls unnecessary T cell responses against innocuous antigens, and antigen dilution or denaturation. Therefore, induction of immune responses following mucosal immunization usually requires the codelivery of an appropriate adjuvant. Vaccine adjuvants are defined by their functional ability to enhance the immunogenicity of an antigen.

The number of known mucosal adjuvants is limited, and the best studied and most potent adjuvants are the *Escherichia coli* and *Vibrio Cholerae* secreted enterotoxins, heat labile enterotoxin (LT) and cholera toxin (CT) respectively, synthetic oligodeoxynucleotides containing unmethylated CpG dinucleotides (CpG ODNs) and monophosphoryl lipid A [42-44].

1.2.1. CpG ODNs

1.2.1.1. Structure & function of CpG ODNs

Synthetic oligodeoxynucleotides containing unmethylated CpG dinucleotides (CpG ODNs) are promising mucosal adjuvants. Small CpG ODNs are able to perfectly mimic the immunostimulatory activity of bacterial DNA and to activate host defense mechanisms leading to innate and adaptive immune responses [45-47].

Bacterial DNA, in comparison with vertebrate DNA, contains a higher proportion of unmethylated CpG dinucleotide motifs that act as pathogen-associated molecular patterns (PAMPs). The vertebrate immune system, as a result of evolutionary selections, recognizes and responds to bacterial unmethylated CpG motifs using Toll-like receptor 9 (TLR9) [48-50]. CpG ODNs that contain unmethylated CpG dinucleotide motifs that are similar to those found in bacterial DNA are recognized by the TLR9 and stimulate a similar response.

CpG ODNs are rapidly internalized by immune cells and interact with TLR9 that is present in endocytic vesicles, a process controlled by phosphatidylinositol 3 kinases (PI3Ks)[48,51]. Interaction between unmethylated CpG motifs and TLR-9 triggers the recruitment of

myeloid differentiation primary response gene (MyD88) adaptor molecule, followed by activation of signalling mediators and culminating with the activation of several transcription factors. This results in production of proinflammatory cytokine/chemokine and up-regulation in expression of co-stimulatory molecules [52-56].

B cells and plasmacytoid DCs (pDCs) are the main human cell types that express TLR9 and respond directly to CpG ODN stimulation [49,57,58]. Unlike human TLR9 [59,60], mouse TLR9 expression has been reported to be not restricted to pDCs [61]. In mice, immune cells of the myeloid lineage, monocytes, macrophages and myeloid DCs express TLR9 [61]. This makes it difficult to predict accurately the effect of TLR9 activation in humans by extrapolating from results obtained in mice, in which more types of immune cells express TLR9.

The immunostimulatory effects of CpG ODNs depend on the sequence, the type of backbone and the presence of motifs specific for a certain species. There are at least three classes of CpG ODNs with distinct structural and biological characteristics. The A-class of CpG ODN (also referred to as type D) strongly induce pDCs to secrete interferon-α (IFN-α), but only weakly stimulate B cell proliferation and pDC maturation [62]. The B-class ODNs (also referred to as type K) strongly induce B cell proliferation and pDC maturation, but are weaker inducers of IFN-α secretion [57,63]. The third class of CpG ODNs, the C-class, combines the immune effects of the A and B classes [64]. Moreover, structure –activity relationship (SAR) studies revealed species-specific differences in the optimal CpG motif. Mice and humans respond to different CpG motifs: the optimal CpG motif is GACGTT for mice but GTCGTT for humans [65] [46]. The CpG ODN used in this study is a B-type CpG ODN with a murine optimised sequence, the CpG ODN 1826. This is a 20-mer oligonucleotide: 5'-TCC ATG ACG TTC CTG ACG TT-3', which has a nuclease-resistant phosphorothioate backbone and which contains two copies of a CpG motif.

1.2.1.2. Immunostimulatory effects of CpG ODNs

The adjuvant activity of CpG ODNs is due to the several different effects that CpG ODNs have on innate and adaptive immune responses. First, CpG ODN induce potent B-cell activation and proliferation and immunoglobulin secretion [46]. As well, CpG ODNs improve antigen presentation, activating the antigen presenting cells to up-regulate MHC class II molecules and co-stimulatory molecules. The ability of CpG ODNs to stimulate mouse bone marrow-derived DC (BM-DCs) was investigated. It was shown that CpG

ODNs treatment induce maturation and activation of DCs to produce cytokines. This results in the up-regulation of MHC class II molecules and of co-stimulatory molecules such as CD40 and CD86 and in induction of the pro-inflammatory cytokines, such as IL-12, IL-6 and TNFα [66]. CpG ODNs activate also mouse macrophages to express activation markers and to secrete cytokines such IFN-α, TNF-α, IL-1β, IL-12, IFN-γ, IL-6 and IL-18 [67] . These cytokines are important for T cell and NK cell activation and the development of adaptive immune responses.

CpG ODNs were shown to be very potent adjuvants enhancing antigen-specific humoral and cellular responses to a wide variety of antigens such as model antigens as ovalbumin and to infectious disease antigens as the hepatitis B surface antigen (HbsAg) and influenza virus [66,68-70]. Mice vaccinated with protein antigens such as OVA or β-galactosidase (β-Gal) have higher IgG antibody titers (mainly IgG2a), CTL and IFNγ production when CpG ODNs are co-administered as an adjuvant. In addition to such antigen specific immune responses, systemically administered immunostimulatory CpG ODNs can induce non specific innate immune responses of a protective nature against several intracellular pathogens, including Listeria monocytogenes, Francisella tularensis, Leishmania major and malaria [71-74].

As many pathogens gain access to the host through a mucosal surface, the ability of CpG ODNs to boost mucosal immunity was also investigated. CpG ODNs are effective as a mucosal vaccine adjuvant, as mentioned above. Administering a combination of CpG ODNs plus inactivated influenza virus intranasally markedly increase influenza- specific antibody levels in the serum, saliva and genital tract of mice . Similarly, intranasal delivery of CpG ODNs plus HbsAg or β-Gal stimulates strong antigen specific IgA responses throughout the mucosal immune system and in the serum[75,76]. CpG ODNs provide effective mucosal adjuvant activity in models of *Chlamydia trachomatis* mouse pneumonitis and invasive pulmonary aspergillosis [77,78]. Beside vaccination, CpG ODNs, in the absence of any antigen, inhibit allergic lung inflammation and induce generic protection at mucosal surfaces in different animal models of infection. Multiple studies showed that CpG ODNs inhibit T helper (Th2) - mediated disease in the lung [79-82]. In a murine model of tuberculosis, CpG ODNs reduce growth of *Mycobacterium tuberculosis* and associated lung inflammation [83]. Pulmonary administration of CpG ODNs protect from *Cryptococcus neoformans* challenge in an IL-12-dependent manner and induce protective immune responses against *Klebsiella pneumoniae* [84,85]. Vaginal-mucosal administration and oral-mucosal administration of immunostimulatory CpG ODNs stimulate innate

immune responses in the murine female genital tract mucosa and in the gastrointestinal mucosa, respectively. A single vaginal dose of CpG ODNs induces rapid production of the Th1 associated cytokines in the murine female genital tract mucosa and elicits protective immunity against genital herpes infection; intragastric administration elicits local production of the CC chemokines RANTES, MIP-1α and MIP-1β and of the CXC chemokine IP-10 and confer protection against *H. pylori* infection in the gastric mucosa [86,87].

1.2.2. LTK63

1.2.2.1. LT wild type structure & function

The heat labile enterotoxin (LT) is an ADP-ribosylating enterotoxin belonging to the A/B family of microbial toxins that are made up by two structurally distinct components, an A subunit of 27 kDa, containing the enzymatic catalytic site, and the pentameric B subunit of 57 kDa that targets the toxin to the cell membrane. The A subunit contains two domains. The A1 domain possesss the ADP-ribosylating activity which is responsible for LT toxicity, while A2 links A1 to the pentameric B subunit. The LT protein exists in an inactive A/B pro-enzyme form that binds to the receptors on the cell surface via its pentameric B subunits. The main receptor of this toxin is the ganglioside GM1 [Gal(β1-3)GalNAc(β1-4)(NeuAc(α2-3)Gal(β1-4)Glc(β1-1)ceramide] that is ubiquitously expressed on the surface of most mammalian cells; but LT can also bind to other gangliosides such as GM2 and asialo-GM1, lactosylceramide, other glycosphingolipids and glycoprotein receptors that are found in the intestine of rabbits and humans, polyglicosilceramides (PCGs) and paragloboside[88]. Following the binding of LT to GM1 receptors, which seem to be localized on lipid rafts on the cell surface, the toxin is internalized into vesicles, transported to the Golgi and disassembled. In the Golgi, the cleavage of disulphide bond between the A and B subunits occurs. The A subunit translocates to the endoplasmic reticulum and then to the cytosol, where it interacts with ADP-ribosylation factors (ARFs), enhancing its ADP-ribosyltransferase activity. The A1 domain migrates to the plasma membrane, where it catalyses the ADP-ribosylation of G signaling proteins, including the alpha subunit of the Gs complex that controls adenylate cyclase activity, inducing a constitutive production of cAMP. The increase in the levels of cAMP results in the efflux

of ions from intestinal epithelial cells with consequent dehydration, the symptoms of diarrhea[88].

LT, as introduced before, is a potent mucosal adjuvant. It has been shown that LT is effective as a mucosal vaccine adjuvant and that the effect of LT on the immune system is a strong mucosal antibody response with antibody class switching to IgG and IgA, enhanced antigen presentation, stimulatory effects on T cell proliferation and cytokine production [89,90].

1.2.2.2. LT mutants

One of the major problems in the use of LT as a mucosal adjuvant in human vaccine formulations is the extremely high toxicity. A nasal LT-adjuvanted inactivated influenza vaccine had to be withdrawn from the market because of severe adverse reactions such as undesirable neurological side effects (Bell's palsy) linked to the presence of LT used as an adjuvant, most likely because of GM1 ganglioside binding of the B subunit of LT in neuronal tissues associated with the olfactory tract [91]. In order to circumvent the harmful drawbacks of the native LT toxin, site-directed mutagenesis was employed to generate LT mutants with significantly reduced toxicity but still active as mucosal adjuvants [92].

LT derived mutants are for example LTK63, with a serine to lysine substitution in position 63 of the A subunit, LTR72 with an alanine to arginine substitution in position 72 of the A subunit or LTB, containing only the B subunit of the wild type protein. LTK63 and LTB are fully non-toxic versions of the wild type protein, while LTR72 has a ~0.6% residual ADP-ribosyltransferase enzymatic activity as measured by toxicity assays *in vitro* (on Y1 cells) or *in vivo* (in rabbit ileal loop). The level of immunogenicity of LTK63 is comparable to that of the wild type toxin. LTK63 is also a much better immunogen than the LTB form, underscoring that inmmunogenicity is dependent on the presence of both the A and B subunits, but not on the enzymatic activity of LT [92,93]. Moreover, LTB/D33, a mutant of LTB lacking binding activity, is not immunogenic at all, demonstrating that the immunogenic response is also dependent on the binding of the toxin to GM1 receptors [88].

The LT derived mutant used in this study is LTK63, since it is a potent non-toxic mucosal adjuvant and there is supporting evidence that administration of LTK63 alone *in vivo* in mice can reduce both pathology and virus/bacterial load caused by either Influenza virus or *C. neoformans*, as described below.

1.2.2.3. The LT mutant LTK63 as an antigen

Administration of LTK63 elicits high levels of anti-LT IgG antibodies both in the serum and in the nasal washes of immunized mice and could therefore confer protection against challenge with LT [94-96]. Despite its very high immunogenicity, pre-existing immunity to LTK63 does not preclude it from being used as an adjuvant for a second antigen [97]. Indeed, antibody titers in serum and nasal washes against the antigens administered in a second vaccination show no difference compared to those obtained immunizing naïve mice with the same antigen. Furthermore, the same dose of adjuvant can be used to enhance the immune response to different antigens, such as MenC and HIV conjugate vaccines, being administered simultaneously [98,99].

Pre-existing immunity to LTK63 does not affect its ability to act as a mucosal adjuvant as demonstrated by a study performed by Ugozzoli et al. , where mice previously immunized i.n. with LTK63 and haemagglutin received a second immunization with LTK63 and an unrelated antigen, MenC [97]. In addition, consecutive LTK63 immunization has shown that exisiting antibodies against LT do not affect its immunogenicity [98,99].

1.2.2.4. The LT mutant LTK63 as an adjuvant

LTK63 has been successfully used as an adjuvant in animal models of mucosal vaccination. To date, LTK63 is the most powerful and non-toxic mucosal adjuvant [93]. For example, intranasal administration of LTK63 with pneumococcal glycoconjugate can confer protective immunity against invasive pneumococcal infection [100]. Similarly i.n. immunization of the LT mutants with SAG1, the major *T. gondii* surface antigen, confers protection against *Toxoplasma gondii*, resulting in lower cyst brain load [101]. Again, LTK63 induces protective antibodies when administered *in vivo* with CRM-MenC conjugate or with *Tetanus Toxoid* peptide [95]. LTK63 adjuvanted vaccines also confer protection against *H. Pylori*, RSV infection, Hib (*Haemophilus Influenzae* type B) and *B. Pertussis* respiratory challenge [97,102-104]. Recently, LTK63 has been tested as mucosal adjuvant for an intranasal influenza vaccine in a phase I clinical trial, demonstrating a good safety profile and mucosal adjuvanticity in humans [105].

The most intensely studied type of immune response to LTK63 is the antibody response. Intranasally administered LTK63 induces local and systemic antibody responses: antigen-specific IgG and IgA can be detected in serum and in nasal and lung lavages of immunized mice [95,98,101,104,106-109].

The antibody isotypes generated when LTK63 is used as an adjuvant depends on the type of antigen co-administered. For example mice immunized with LTK63 and tetanus toxoid (TT) generate mainly IgG1[99]. On the other hand, when LTK63 is administered with pneumococcal-tetanus toxoid glycoconjugates, *Toxoplasma gondii* SAG1 protein or *B. pertussis* antigens, the predominant antibodies are antigen-specific IgG2a [100,101,110]. The antibody isotype induced by LTK63 is also dependent on the dose of LTK63 used. Indeed, LTK63 with MenC antigen at low doses induces low levels of antigen-specific IgG1, while at higher doses both IgG1 and IgG2a isotypes are generated [94,109]. The antibodies produced reflect the induction of both a Th1 and Th2 mixed immune response [104].

The type of cytokines produced after LTK63 stimulation further supports a mixed Th1/Th2 response. When administered intranasally with acellular pertussis combination (DTPa) or acellular pertussis (Pa) vaccine for example, LTK63 is able to enhance the production of both Th1 (IFN-γ) and Th2 (IL-4 and IL-5) cytokines by antigen-stimulated spleen and lymph node cells. Increasing the dose of LTK63 enhances Th1 cytokine production [104] .

LTK63 used as an adjuvant is able to induce strong local and systemic T cell responses. For example LTK63 when administered with OVA induces OVA-specific T cell priming and strong T cell proliferation [92,104,111]. With tetanus toxoid, LTK63 can induce antigen-specific CD4+ T cells [96].

Several reports have shown that mucosal or intramuscular administration of LTK63 can elicit strong CD8+ cytotoxic T cell responses to co-administered antigens or peptides, such as HIV p55 gag protein and M2 protein of RSV [102,112].

In summary there is strong evidence that mucosal vaccination using LTK63 as adjuvant is very effective in triggering both humoral (IgA and IgG antibodies) and cellular (CD4 and CD8 T cells) immunity.

1.2.2.5. Generic protection induced by LTK63 in the lung

Recent studies have shown that intra-pulmonary administration of LTK63 modulates immunity and pathology to subsequent infection by completely un-related respiratory pathogens such as respiratory syncitial virus (RSV), Influenza virus or *Cryptococcus neoformans* [113]. This is called generic protection and has been described previously in the context of viral infections: A first infection by a virus alters the lung environment in a way that enhances the immune response to a subsequent, unrelated pathogen [114,115].

LTK63 reduces respiratory virus lung pathology when administered two weeks before infection. In the case of influenza virus, prior administration of LTK63 results in reduced weight loss and reduces cellular infiltration in the lung. In the case of challenge with RSV, LTK63 inhibits Th2-driven eosinophilia, tissue damage and weight loss. Similar results are obtained for *C. neoformans* infection, where pathogen burden is also reduced. LTK63 also increases CD44+ CD8+ T cells in RSV challenged mice and CD44+ CD4+ and CD8+ T cells in Influenza challenged mice. Proliferation of CD8+ T cells to influenza virus and RSV antigens is also augmented. In RSV challenged mice, LTK63 alters the cytokine balance by increasing the ratio of IFNγ/IL5 producing CD4+ T cell. The level of antigen-specific IgA is also increased in nasal washes by LTK63 after RSV and influenza infection. LTK63 induces a change in the lung microenvironment, both in terms of cytokine profile and antigen presentation. Indeed, LTK63 stimulates a mild Th1 environment, with an increase in IFNγ and TNFα production. LTK63 administration also matures lung APC by increasing the population of CD80+ and MHC class II macrophages and the population of activated B cells (expressing CD45R+, CD40+, CD80+ and MHC class II) [113].

The effect of LTK63 in lung immunomodulation is underlined by the retention of strong antibody responses, but diminished cellular inflammation and tissue damage following pathogen infection. These features make LTK63 a potential candidate for the generic prevention against airway infections.

1.3. Aim of the study

Although it is well documented that CpG ODNs and LTK63 are potent mucosal adjuvants and induce generic protection against airway pathogens, little is known about their mechanism of action after intrapulmonary administration in mice. Therefore, the aim of this thesis was to study the immunological events induced in the lung by these two adjuvants.

While the final outcome of CpG or LTK63 use is similar and consists in both cases in enhanced antibody titers to co-administered Ags or in a phase of increased protection against unrelated pathogens, it is likely that this is achieved through widely differing mechanisms. Thus, it is known that they act trough different receptors: CpG ODNs interact with TLR9 that is present in endocytic vesicles of some cell types, while LTK63 binds to the ganglioside GM1, that is ubiquitously expressed on the surface of most mammalian cells. The interaction of CpG ODNs with TLR-9 activates a well-defined molecular pathway, while LTK63 binding to GM1 triggers the internalization of LTK63 in the target cells with poorly defined signalling events downstream. It is clear that in contrast to the effects of wild-type LT, binding of LTK63 does not lead to the induction of ADP-ribosylation of G-proteins and activation of adenylate cyclase. In summary, while both CpG and LTK63 induce enhanced immune responses in the lung, the cellular targets, the signalling triggered in those target cells and the downstream events induced by these two adjuvants are partly not well understood and partly known to be different. Therefore, through the dissection and the comparison of the events leading to enhanced immune responses, I attempted to gain a better understanding of the mechanisms of action of both CpG ODN and of LTK63 when administered to the lung.

2. Material and Methods

2.1. Animals

BALB/c and C57BL/6 mice were purchased from Charles River Laboratories. Eight- to 12-week-old female mice were used for all experiments. Animals were housed and treated according to internal animal ethical committee and institutional guidelines.

2.2. Formulation of ODNs or LTK63 and immunization protocol

The CpG ODN used in this study was 1826 (TCC ATG ACG TTC CTG ACG TT), a 20-mer which has a nuclease-resistant phosphorothioate backbone and which contains two copies of a CpG motif known to have potent immunostimulatory effects on the murine immune system. The control ODN has the same sequence except the CpG motif (underlined) was inverted to GpC (TCC ATG AGC TTC CTG AGC TT). All ODNs were purchased from Invivo Gen. The ODNs were tested for endotoxin by using the Limulus amebocyte lysate assay (BioWhittaker). All dilutions were conducted with endotoxin-free PBS (Sigma).

Addition of 0.25% CHAPS and 200 mM arginine to the LTK63 preparation in PBS increased LTK63 stability at 4°C by preventing precipitation of the complex and dissociation of the A subunit from the B5 pentamer. Therefore, LTK63 was formulated in Buffer L (0.2 M arginine, 0.25% CHAPS, 20 mM NaH_2PO_4 in PBS (final pH 7.4)). All preparations of LTK63 used in this study were tested for GM1 binding.

PBS alone versus 10 μg of CpG in PBS, or Buffer L alone versus 5 μg of LTK63 in buffer L, respectively, were delivered intranasally by administration of 50 μl total volume (25 μl/nostril) to anesthetized BALB/c mice [116]. Anesthesia was performed by injecting i.p. 100 μl of solution containing 50 mg/kg ketamine plus 2.6 mg/kg xylazine.

2.3. Preparation of lung homogenates to determine intra organ cytokines

At various time intervals after intrapulmonary CpG ODN or LTK63 administration, mice were sacrificed and lungs were harvested. As controls, lungs were removed from naïve mice treated with buffer only or from mice that had been treated with a control GpC ODN.

Lungs were snap-frozen in liquid nitrogen and stored at –80°C until further analysis. The snap-frozen lungs were thawed, weighed and transferred to different tubes on ice containing 2 ml of tissue protein extraction reagent (T-PER) (PIERCE) containing Complete Mini Protease Inhibitor Cocktail tablets (Roche Diagnostics) at a proportion of 1 tablet/10 ml of T-PER. Lung tissue were homogenized at 4 °C with an Ultra-Turrax T25, and the homogenates were centrifuged at 10,000 × g for 10 minutes at 4 °C. The total protein concentrations were determined in the supernatants using a BCA protein assay kit (PIERCE). Lung tissue homogenates were diluted with T-PER reagent to a protein concentration of 2 mg/ml. Then samples were diluted with 75% standard diluent, provided in the Bio-Plex Mouse Cytokine 23-Plex kit, to a final protein concentration of 500 μg/ml.

2.4. Cytokine assays

After intrapulmonary CpG ODN or LTK63 administration, mice were sacrificed at different time intervals, and lungs and sera were taken. Alternatively, supernatants from cultures of AMs stimulated *in vitro* with CpG ODN and from cultures of lung $CD11c^+$cells isolated after *in vivo* LTK63 treatment, as described below, were collected.

Mouse lung homogenates, sera, AM and $CD11c^+$ cell culture supernatants were tested for multiple cytokines using the Bio-Plex Mouse Cytokine 23-Plex Panel (Bio-Rad) according to the manufacturer's instructions.

The panel included the following cytokines: interleukin 1-α (IL-1α), IL-1β, IL-2, IL-3, IL-4, IL-5, IL-6, IL-9, IL-10, IL-12 p40, IL-12 p70, IL-13, IL-17, eotaxin, granulocyte-colony-stimulating-factor (G-CSF), granulocyte-macrophage colony-stimulating-factor (GM-CSF), gamma-interferon (IFN-γ), KC, monocyte chemotactic protein-1 (MCP-1), macrophage inflammatory protein 1α (MIP-1α), macrophage inflammatory protein 1β (MIP-1β), RANTES, tumor necrosis factor alpha (TNF-α). Serial dilutions of the lyophilized standard were prepared in standard diluent: T-PER reagent (3:1) for cytokine measurement in lung homogenates; in serum standard diluent (1:4) for determination of cytokines in sera and in culture medium for cytokines measurement in AM culture supernatants and $CD11c^+$ cell culture supernatants. 50 μl of each diluted homogenate sample, 50 μl of diluted serum sample and 50 μl of culture supernatant sample were transferred to the wells containing differentially stained microbeads, each type of which is coated with antibodies recognizing different cytokines. Samples were incubated for 1 hour, washed, and incubated with biotinylated detection antibodies for 30 min. After washing,

streptavidin-phycoerytrin was added to each well and incubated for 10 min. After a final wash, the assay was read on a Bio-Plex array reader (Bio-Rad), and cytokine concentrations were calculated based on standard curve data using the Bio-Plex Manager Software (Bio-Rad).

2.5. Enzymatic digestion of lung and spleens for cellular assays

At different time points after intrapulmonary CpG ODN or LTK63 administration, mice were sacrificed and lungs and spleens were harvested. As controls, the same organs were removed from naïve mice and from mice that had been treated with a control GpC ODN.
Lungs were dissected from the trachea, main stem bronchi and surrounding tissue and cut into small pieces in cold HBSS (Invitrogen). The dissected tissue was then incubated in HBSS containing 5% FBS (Hyclone), 20 µg/ml Dnase I (Roche) and 200 U/ml collagenase type I (Gibco) for 45 min at 37 °C with constant gentle swirling. The digest mixture was then agitated, centrifuged and incubated in calcium and magnesium free HBSS containing 10 mM EDTA for 5 min at room temperature. After inhibition of collagenase activity with 10 mM EDTA in PBS, lung fragments were further disrupted by gently pushing the tissue through a 70 µm cell strainer (BD Biosciences), and the single cell suspension was subjected to RBC lysis. Cells were then washed, and the viability was determined by trypan blue dye exclusion.
Spleens were excised from sacrificed mice, suspended in in cold HBSS (Invitrogen) and minced. Briefly, the dissected tissue was digested in HBSS containing 5% FBS (Hyclone) with collagenase type I (Gibco) and DNase I (Roche), using the same concentration and digestion time indicated above for lung enzymatic digestion. Then the digested tissue was pressed through a 70 µm cell strainer (BD Biosciences), the single cell suspension was subjected to RBC lysis, and total viable cell count was determined.

2.6. Flow cytometric analysis

For flow cytometric analysis of lung and spleen cells, organs from four mice per group were taken at 12 hours and 1, 2, 4, 6, 8 and 14 days after CpG ODN or LTK63 treatment. In addition, organs were taken at 6 hours after CpG ODN treatment. The cells obtained by enzymatic digestion from lungs and spleens were preincubated with anti Fc block (anti CD16/CD32) to reduce nonspecific binding 10 min before addition of the Abs. The following anti mouse Abs: CD4-PE, CD8-biotin, DX5-FITC, B220-APC and CD3-PerCP-

Cy5.5 were used to define the lymphocyte subsets. In addition, cells were stained with anti-CD44-APC and anti-CD69-PerCP-Cy5.5 to determine the activation status of T and NK cells. DC subsets and the levels of costimulatory molecules were defined using anti-MHC-II-biot, anti-CD11c-APC, anti-CD11b-PerCP-Cy5-5-A, anti-B220-Alexa700, anti-CD80-FITC, anti-CD86-FITC, anti-CD40-FITC, anti-PDCA-1-PE. CD8 and I-A^d binding were identified by a secondary staining with Streptavidin-Pacific Blue. Anti-Ly6G-PE was used to identify granulocytes. Isotype monoclonal antibodies (PE-, Pacific Blue-, FITC-, APC-, Alexa-700 and PerCP-Cy5.5-conjugated) were used to determine the background of fluorescence. The incubations were conducted for 20 min in ice in the dark. All Abs were purchased from BD Pharmingen except the anti-plasmacytoid DC Ag-1 (PDCA-1), which was purchased from Miltenyi Biotec. Cell acquisition was performed on a FACS LSRII flow cytometer (BD Biosciences), and data were analyzed using the FACS Diva Software (BD Biosciences).

Within the lymphocyte gate (FSC^{low}/SSC^{low}), T cells were identified as $CD4^+CD3^+$ or $CD8^+CD3^+$, NK cells were identified as $CD3^-Dx5^+$, and B cells as $CD3^-Dx5^-B220^+$. T and NK cell activation was determined by cell surface expression of the activation markers CD69 and CD44.

Mature myeloid DCs were identified in the gate of $CD11c^+MHC\text{-}II^{high}$ cells (R2 cells) as CD11b expressing cells, which lack the expression of PDCA-1 and B220; whereas the mixed population of AMs and immature DCs was gated as $CD11c^+MHC\text{-}II^{int}$ cells (R1 cells).

Plasmacytoid DCs were identified as PDCA-1^+ $B220^+$ cell, which express CD11c and MHC-II at low levels and lacking the expression of CD11b.

Granulocytes were morphologically identified as $FSC^{medium}/SSC^{medium}$ cells and were identified as $Ly6G^+$ cells.

2.7. Isolation and stimulation of alveolar macrophages

Alveolar macrophages were isolated from bronchoalveolar lavage (BAL) of five naive BALB/c mice, and the cells were pooled. Bronchoalveolar cells consist of 99% AMs. Bronchoalveolar lavage is a technique used to sample the cellular or biochemical components of the conducting airways and lung alveoli. Mice were anaesthetized by injecting i.p. 100 μl of a solution containing 50 mg/kg ketamine plus 2.6 mg/kg xylazine, and BAL was carried out by placing a needle in the trachea and rinsing the downstream

compartment with PBS. BAL was obtained instilling three times 500 μl of cold PBS 1mM EDTA into the mouse lungs followed by gentle aspiration. Approximately 50-70% of the instilled volume was retrieved. BAL fluid from all mice was collected and was kept on ice until processed.

BAL fluid was centrifuged for 10 min at 1,200 rpm at 4°C, and subsequently, cells (AM 99% pure) were resuspended in culture medium. As culture medium, RPMI 1640 (Gibco) supplemented with 25 mM HEPES, 2 mM L-glutamine, 100 U/ml penicillin, 100 mg/ml streptomycin, 50 μM 2-ME and 10% heat-inactivated and filtered FBS (Hyclone), was used.

10^5 AMs/well were cultured for 2 h, and nonadherent cells were removed. After 18 hrs of culture with CpG (10 μg/ml, or 3 μg/ml), or control GpC 10 μg/ml, or LTK63 5 μg/ml or PBS, cell culture supernatants were collected to measure cytokine release.

2.8. Generation and culture of bone marrow-derived DCs (BM-DCs)

The method for generating bone marrow-derived DCs (BM-DCs) has been previously described [117].

Bone marrow cells were flushed from tibiae and femurs of 8 - to 12-wk-old BALB/c mice. At day 0, bone marrow leukocytes were seeded at 2×10^6 cells in 100 mm petri dishes in 10 ml of culture medium containing 200 U/ml GM-CSF (5×10^6 U/mg; Peprotech). On the third day, 10 ml of culture medium containing 200 U/ml GM-CSF were added to the plates. On the sixth day, half of the culture supernatant was collected, centrifuged, and the cell pellet resuspended in 10 ml of fresh culture medium containing 200 U/ml GM-CSF, and given back into the original plate. For the in vivo migration assay, the non adherent cells were collected by gentle pipetting on day 7 or 8. Before the labeling with CFSE (carboxyfluorescein succinimidyl ester) (Molecular Probes), an aliquot of BM-DCs was analyzed by FACS. For flow cytometric analysis, 5×10^5 BM-DCs were preincubated with anti Fc block (anti CD16/CD32) to reduce nonspecific binding 10 min before addition of the Abs. The antibodies anti-MHC-II-biot, anti-CD11c-APC and anti GR-1-Alexa700 were used (BD Pharmingen). I-A^d binding was identified by a secondary staining with Streptavidin-Pacific Blue. Isotype monoclonal antibodies (Pacific Blue-, APC- and Alexa700-conjugated) were used to determine the background of fluorescence. The incubations were conducted for 20 min in ice in the dark. All Abs were purchased from BD

Pharmingen. Cell acquisition was performed on a FACS LSRII flow cytometer (BD Biosciences), and data were analyzed using the FACS Diva Software (BD Biosciences).

2.9. In vivo migration assays

BM-DCs collected on day 7 or 8 of culture were labeled with CFSE (carboxyfluorescein succinimidyl ester) (Molecular probes) in accordance with the manufacturer's instructions. Briefly, cells were washed twice in prewarmed (37°C) PBS, and resuspended (10^7 cells/ml) in a 1 μM solution of CFSE for 10 min at room temperature. Following incubation, labeling was stopped by the addition of an equal volume of FCS (Hyclone) for 1 min and then, an equal volume of complete medium was added prior to washing. After washing, cells were incubated for another 30 minutes to ensure complete modifications of the probe. The cells were then washed three times in PBS, and 200 μl containing 10^7 labeled BM-DCs were injected into the tail vein of mice (n= 3) pretreated with LTK63 or buffer L 6 days before. After 24 hours, lungs and spleens were removed, and single cell suspensions were prepared by enzymatic digestion. Then, fluorescent injected DCs were enumerated in lung and spleen single cell suspensions by flow cytometric analysis, using the same antibodies used for the flow cytometric analysis of BM-DCs.

2.10. Isolation of lung dendritic cells

For functional experiments, lungs from four BALB/c mice treated for 8 days with LTK63 and from eight BALB/c mice treated for 8 days with Buffer L, respectively, were pooled to isolate lung $CD11c^+$ cells or $CD11c^+MHC\text{-}II^{high}$ DCs and $CD11c^{high}MHC\text{-}II^{int}$ cells.

Lung cell suspensions, obtained after enzymatic digestion as previously described, were subjected to RBC lysis. $CD11c^+$ cells were immunomagnetically isolated by positive selection with "CD11c (N418) microbeads" (Miltenyi Biotec), according to the manufacturer's instructions. Lung $CD11c^+$ cells, whose purity exceeded 95% as assessed by flow cytometry (data not shown), were used to stimulate allogeneic T cells from C57BL/6 mice.

Lung $CD11c^+MHC\text{-}II^{high}$ DCs and $CD11c^{high}MHC\text{-}II^{int}$ cells were isolated using flow cytometry cell sorting. Lung cells were stained with anti-MHC-II-FITC anti anti-CD11c-APC for 15 minutes at 4°C in dark condition at a cell concentration of 10^8 cells/ml with shaking. Cells were then washed, resuspended in 1 ml of PBS, filtered through a 30 μm

filter (Becton Dickinson), and sorted using a FACS Aria cell sorter (Becton Dickinson) in high-speed/purity mode. The $CD11c^{+}MHC\text{-}II^{high}$ DCs and $CD11c^{high}MHC\text{-}II^{int}$ cells were gated as $CD11c^{+}$ $MHC\text{-}II^{high}$ (R2) and $CD11c^{+}$ $MHC\text{-}II^{int}$ (R1), respectively. The $CD11c^{+}MHC\text{-}II^{high}$ DCs and $CD11c^{high}MHC\text{-}II^{int}$ cells obtained were ≥ 99% pure (data not shown).

2.11. Isolation of splenic T lymphocytes

Spleens from two naïve C57BL/6 mice were used for isolation of allogenic T cells.
A single cell suspension from spleens was prepared by mechanical disaggregation. Briefly, spleens were excised, suspended in complete medium and passed through a 70 μm cell strainer, and the single cell suspension was subjected to RBC lysis. T cells were immunomagnetically isolated using the mouse Pan T cell Isolation Kit (Miltenyi Biotec), according to the manufacturer's instructions. Splenic T cells, whose purity exceeded 95% as assessed by flow cytometry (data not shown), were used for proliferation assays.

2.12. Proliferation assays

Purifed lung $CD11c^{+}$ cells were plated in triplicate in 200 μl of culture medium with allogenic T cells at different ratios (1:4, 1:8, 1:16, 1:32, 1:64) in 96-well, flat-bottomed microwell plates at 37°C for 72 hours. Each culture was then pulsed with ^{3}(H)-thymidine (0.5 μCi/well, Amersham-Pharmacia) and harvested after 18 hours, when incorporated radioactivity was measured in a liquid scintillation counter and expressed as counts per minute. As controls, separate cultures of $CD11c^{+}$ cells alone and T lymphocytes alone were used. The results are expressed as the mean cpm of triplicate cultures ± SEM. Similar results were obtained in three separate experiments.
In addition, for cytokine profiling of stimulated T cells, the quantitation of IFN-γ, IL-2. IL-4, IL-5 and TNF-α was performed from the supernatants of 48 hour co-culture by using a custom kit for Th1/Th2 cytokines (Meso Scale Discovery), according to the manufacturer's instructions.
The proliferation assay was conducted also using as stimulator cells lung $CD11c^{+}MHC\text{-}II^{high}$ DCs and $CD11c^{high}MHC\text{-}II^{int}$ obtained from mice treated for 8 days with LTK63 and from mice treated for 8 days with Buffer L.

3. Results

3.1 CpG ODNs

3.1.1 Inflammatory cytokines rapidly increase in the lung after CpG administration.

CpG ODNs induce in TLR-9 expressing cells a signalling cascade which culminates in the up regulation of cytokine and chemokine gene expression [118]. In order to study at the protein level lung cytokine and chemokine expression, I determined at various time intervals after intrapulmonary CpG ODN administration the production of multiple cytokines by ELISA based multiplex analysis in lung homogenates.

As shown in Fig. 3.1.1, at early time points the proinflammatory cytokines IL-1α, IL-1β, IL-6 were induced by CpG ODN treatment reaching a peak at 6h (about 10-fold) and decreasing by 12h. The level of IL-12 (p40) increased within 3 h of CpG ODN treatment and peaked at 12 h (63-fold). G-CSF levels peaked at 12 h (50-fold). The levels of these cytokines rapidly decreased to baseline.

Inflammatory chemokines were induced by CpG ODNs in the lung (Fig.3.1.2). A rapid peak of MIP-1α was seen at 6h (5-fold) after CpG treatment and gradually reached baseline levels. The level of MIP-1β peaked at 12h (16-fold) and the level of RANTES peaked at 1 day (16-fold). A gradual decrease followed by sustained presence of both cytokines in treated mice compared to control mice was observed in the later time points examined. After intrapulmonary CpG ODN administration, KC protein expression reached a peak at 6h (22-fold), MCP-1 peaked at 12 h (17-fold) and both rapidly decreased to baseline levels. Levels of all cytokines tested were not elevated in naïve mice and in mice that had been treated with a control GpC ODN compared to PBS treated mice; two representative cytokines levels at one day of treatment are shown in Fig.3.1.3.

Table 3.1 shows the summary of cytokine proteins tested, CpG ODN induced cytokines with the time of peaking and their respective fold increase, unchanged cytokines and cytokines below detection threshold. Thus, higher IL-1α, IL-1β, IL-6, IL-12(p40), G-CSF, KC, MCP-1, MIP-1α, MIP-1β, RANTES production was observed in the lung of CpG ODN treated mice compared to control mice, peaking mainly at 6h-12 h. These effect is highly CpG specific: control GpC ODN intrapulmonary administration does not result in cytokine and chemokine secretion in the lung.

Fig. 3.1.1 CpG ODNs induce inflammatory cytokine release in lung tissue

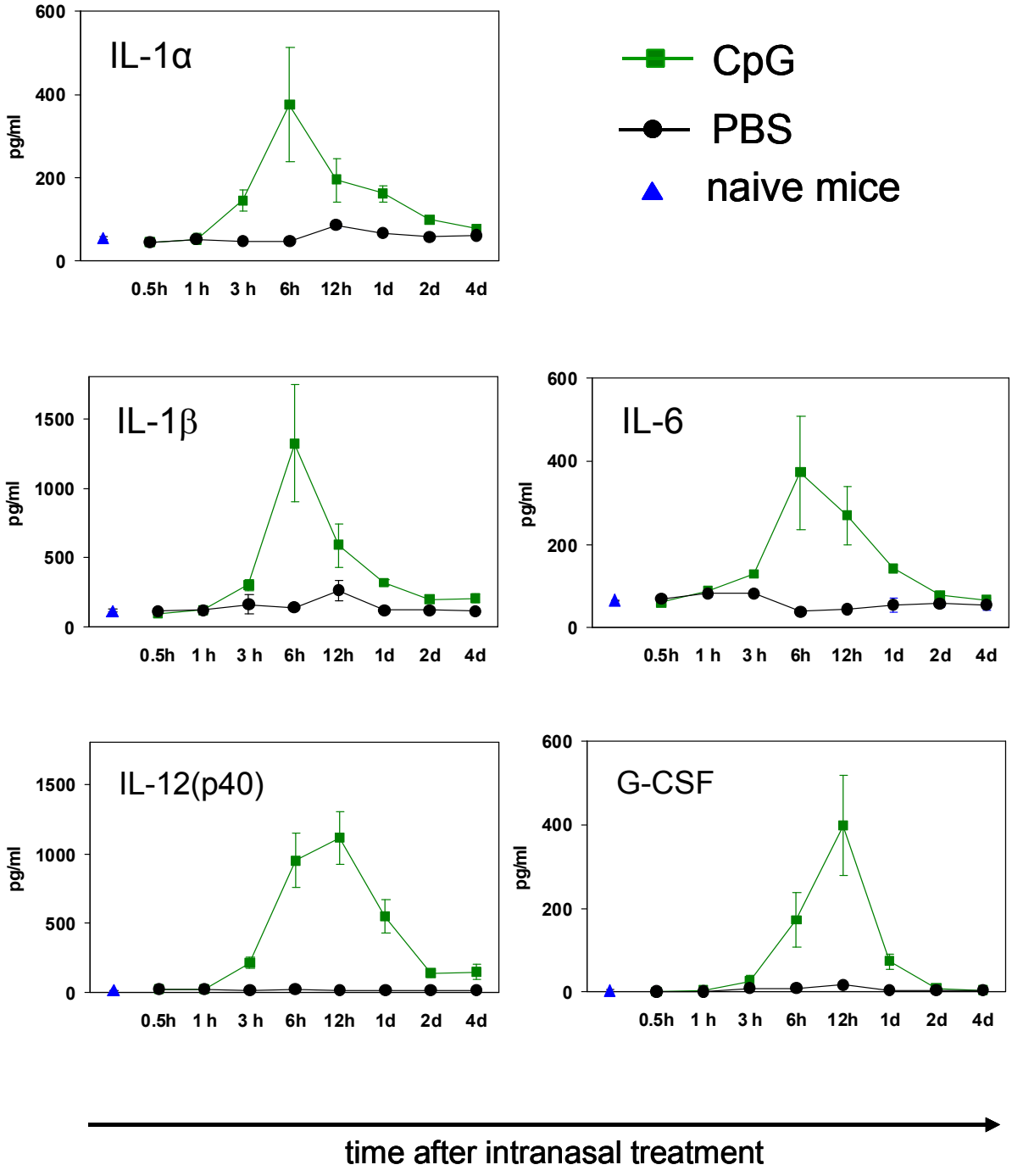

Fig. 3.1.1 Inflammatory cytokine production in lung tissue of CpG treated mice. Kinetics of inflammatory cytokines in lung tissue after CpG or PBS treatment (30 min-4 days) and in naïve BALB/c mice. Concentrations of indicated cytokines were determined by ELISA based multiplex analysis of lung homogenates. Data are expressed as means (pg/ml) + standard errors of the mean of three animals per group.

Fig. 3.1.2 CpG ODNs induce inflammatory chemokine production in the lung

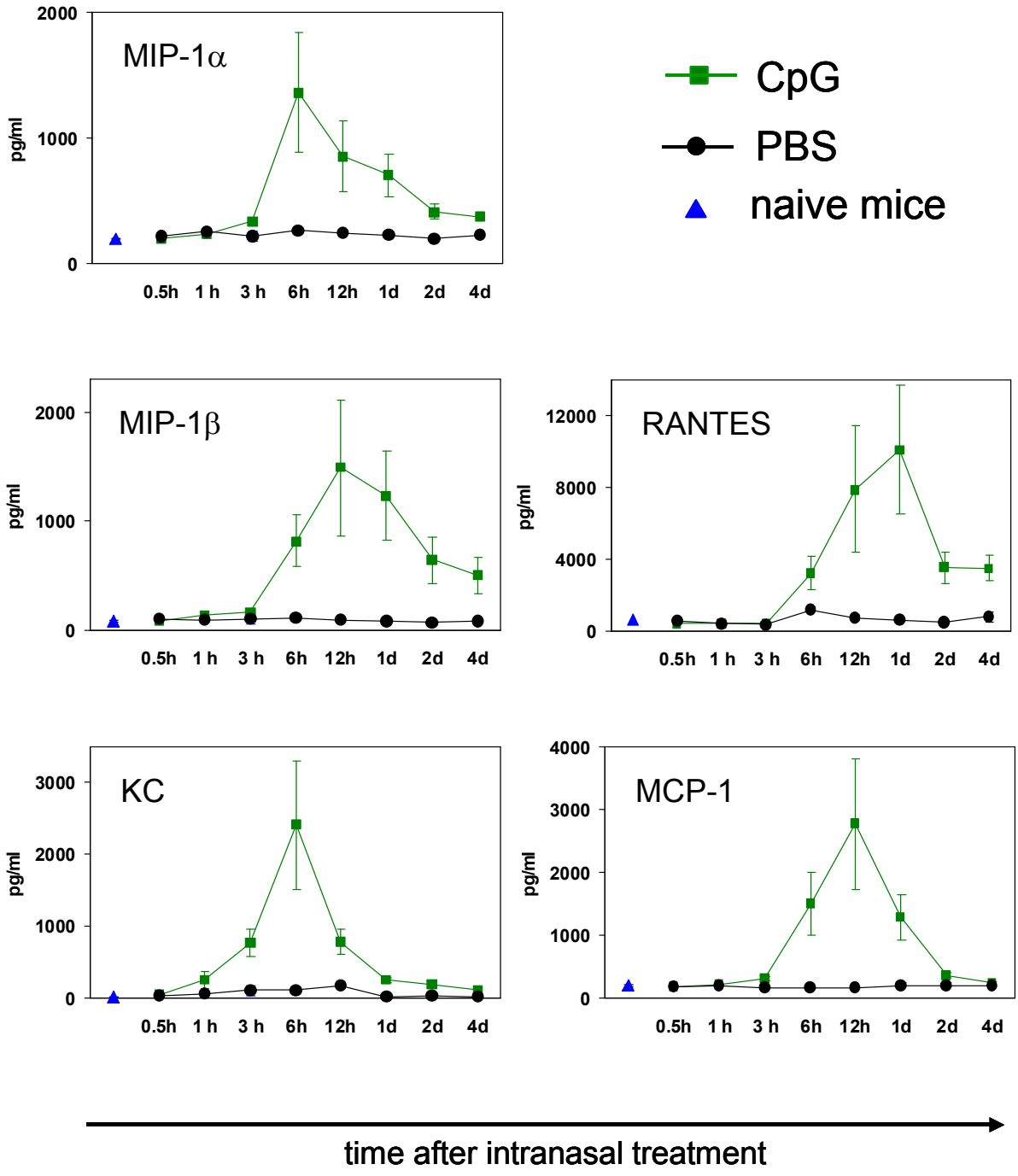

Fig. 3.1.2 Induction of inflammatory chemokines in the lung after CpG treatment. Time course of chemokine production in lung tissue of CpG treated and control mice (30 min-4 days) and in naïve BALB/c mice. Concentrations of indicated cytokines were determined by ELISA based multiplex analysis of lung homogenates. Results are represented as the mean (pg/ml) ± SEM. N = 3/treatment group.

Fig. 3.1.3 Representative cytokine levels at one day after CpG ODN administration

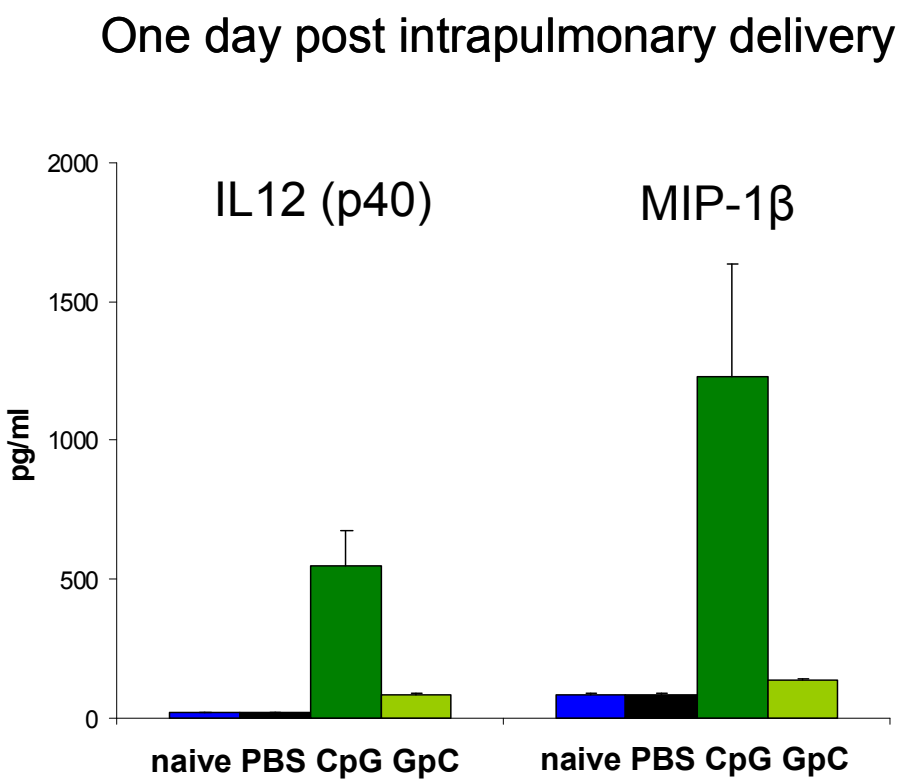

Fig. 3.1.3 Cytokine production in the lung of naïve BALB/c mice and after one day of CpG ODN, GpC control ODN and PBS treatment. Concentrations of indicated representative cytokines were determined by ELISA based multiplex analysis of lung homogenates. Results are represented as the mean (pg/ml) ± SEM. N = 3/treatment group.

Table 3.1.1. Summary of lung cytokine proteins tested

summary of cytokine proteins tested (lung)						
peaked at 6 h fold increase (6 h)	IL-1α (8)	IL-1β (9)	IL-6 (10)	KC (22)	MIP-1α (5)	
peaked at 12h fold increase (12 h)	IL12 p40 (63)	G-CSF (50)	MCP-1 (17)	MIP-1β (16)		
peaked at 1 d fold increase	RANTES (16)					
unchanged	IL-2	IL-9	IL-10	IL12 p70	IL-13	eotaxin
unchanged	GM-CSF	IFN-γ				
below detection threshold	IL-3	IL-4	IL5	IL-17		

Table 3.1.1. Multiplex analysis of cytokine protein expression in lung tissue
Summary of lung cytokine proteins tested: CpG ODN induced cytokines with the time of peaking and their respective fold increase, unchanged cytokines and cytokines below detection threshold.

3.1.2 *In vitro* CpG treatment induces cytokines release from alveolar macrophages

Alveolar macrophages (AMs) constitute the first line of phagocytic defence against infectious agents that evade the mechanical defense and gain acces to the gas-exchanging airways [5]. AM keep the airspaces quiet ingesting all types of inhaled particulates that reach the alveolar spaces without triggering inflammatory responses [1]. Building on the observation that alveolar macrophages rapidly internalize CpG ODNs into the cytosolic compartment after intranasal administration [80], I asked whether AMs will mediate the effect in lung cytokine environment observed *in vivo* after CpG ODN treatment. Therefore, I incubated AMs *in vitro* with or without CpG ODNs to evaluate cytokine release. As seen in fig. 3.1.4, AMs cultured for 18hrs with CpG ODNs up-regulated expression of IL-6, IL-12(p40), KC, MIP-1α, MIP-1β and RANTES, unlike cells culture with PBS, control GpC ODNs and LTK63. No changes were found for the other cytokines tested. These data indicate that CpG ODNs specifically activate *in vitro* AMs to release some inflammatory cytokines and chemokines and that AM activation could contribute to cytokine/chemokine microenvironment observed in *in vivo* after intrapulmonary CpG ODN administration.

Fig. 3.1.4 CpG ODNs treatment induces cytokine release from alveolar macrophages

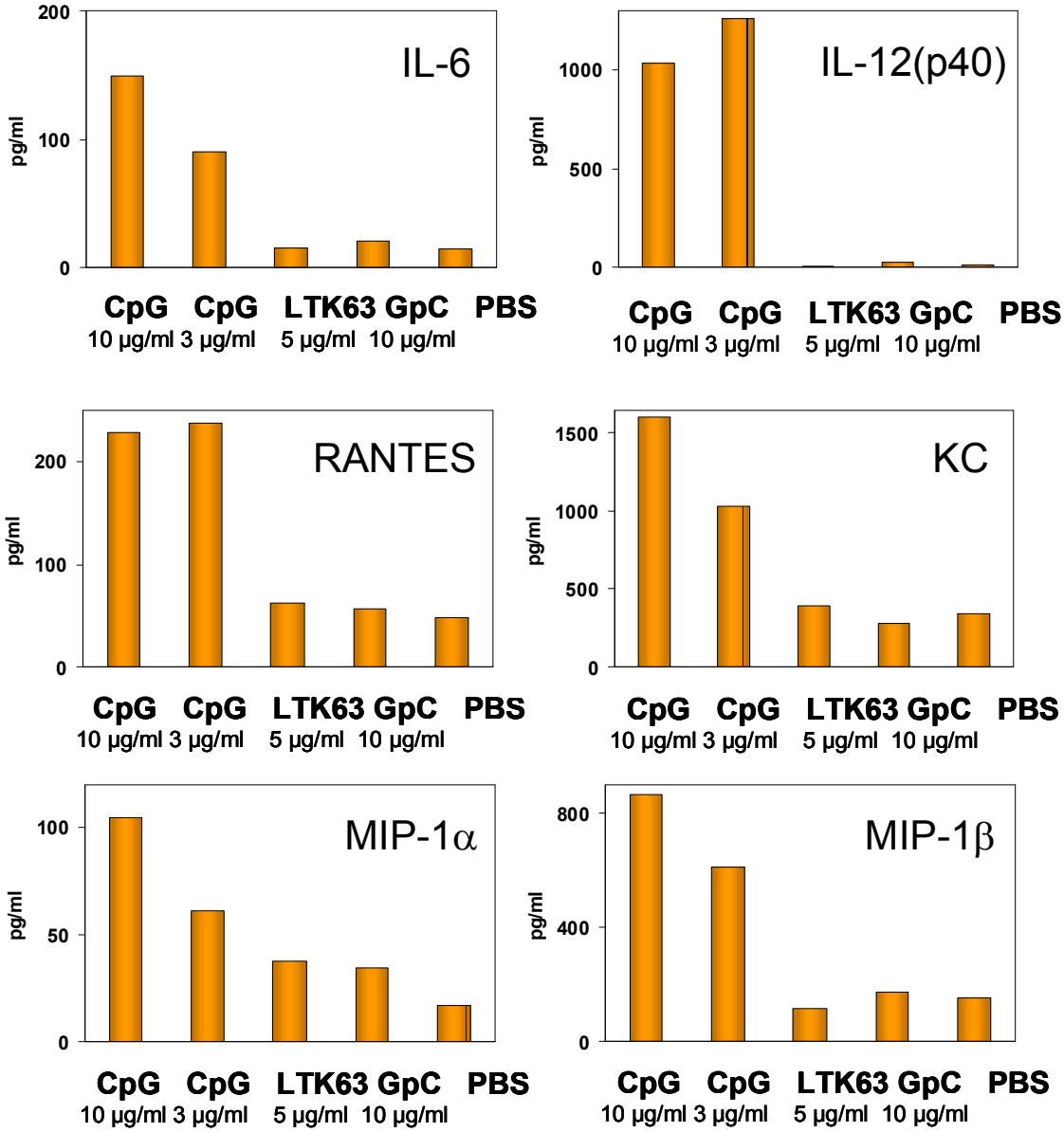

Cytokines unchanged : IL-1α; IL-1β ; IL-9; IL-10; IL-12 (p70); IL-13; eotaxin; G-CSF;MCP-1; TNF-α.

Cytokines below detection threshold: IL-2; IL-3; IL-4; IL-5; IL-17; GM-CSF; IFN-γ.

Fig. 3.1.4 CpG treatment induces cytokines release from alveolar macrophages. Alveolar macrophages from untreated BALB/c mice were cultured for 18 hrs with CpG (10 µg/ml, or 3 µg/ml); or control GpC 10 µg/ml , or LTK63 5 µg/ml or PBS. Cytokine release was measured in culture supernatants by cytokine multiplex analysis. Indicated cytokines were induced by CpG 10 µg/ml and CpG 3 µg/ml. Similar results were obtained from three experiments.

3.1.3 CpG ODNs augment both number and activation state of myeloid DCs

Lung DCs are ideally placed to sample inhaled agents at alveolar surface within and below the epithelium [26]. CpG ODNs improve antigen presentation, activating DCs to up-regulate MHC class II and costimulatory molecules [118]. Suzuki and coworkers demonstrated that mouse lung DCs express TLR-9 and respond directly to CpG stimulation *in vitro* [119]. In the present study was investigated if CpG administration *in vivo* will alter the pulmonary mDC number and expression of MHC-II and costimulatory molecules on the same cells in a time course ranging from 12 h to 14 days. No changes in total viable cells recovered from the lung were observed after CpG treatment, as shown in Fig. 3.1.5. At 4 days CpG ODN administration induced the increase of the absolute number of myeloid lung DCs expressing high level of MHC class II (fig. 3.1.6). I observed a rapid up-regulation of CD86 and CD80 expression by lung mature myeloid DCs at 1day to 4 days after CpG treatment, as assessed by percentage of cells expressing at high levels these costimulatory molecules , compared with lung mature myeloid DCs from control (fig. 3.1.7).

3.1.4 CpG treatment favors the increase of the number and activation of lung plasmacytoid DCs

Plasmacytoid DCs strongly express TLR-9 and are directly activated by CpG ODNs [118]. I assume that also lung plasmacytoid DCs express TLR-9 and I examined the number and phenotype of plasmacytoid DCs in a time course ranging from 12 h to 14 days following CpG or PBS administration. At 2 days after intrapulmonary CpG ODN administration the absolute number of plasmacytoid lung DCs, calculated on the basis of percentage of PDCA-1 positive cells, from CpG treated mice ($1.83 \times 10^5 \pm 0.07$) showed a 12-fold increase as compared with control mice ($0.15 \times 10^5 \pm 0.01$) as shown in fig.3.1.8. Rapidly after the treatment plasmacytoid lung DCs acquired an activated phenotype as determined by expression at high levels on cell surface of the costimulatory molecules CD86, CD80, CD40 and MHC-II (Fig.3.1.9).

Fig. 3.1.5 Lung cellularity after CpG ODN administration

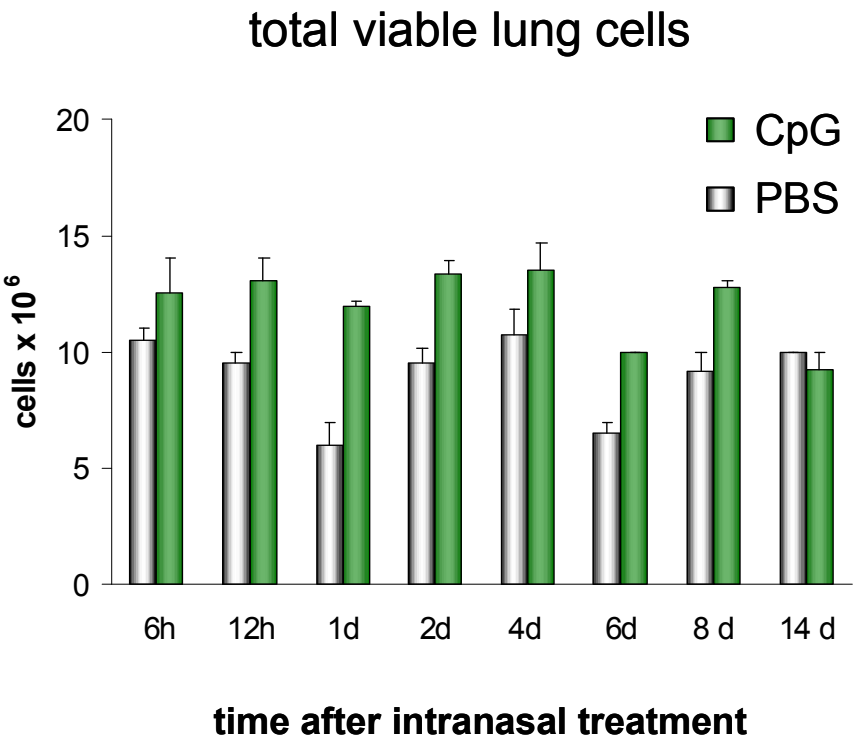

Fig. 3.1.5 Total viable lung cells obtained after enzymatic digestion, at different time points following administration of CpG or PBS. Total viable cells recovered from the lung were determined by trypan blue exclusion. Data are expressed as means of standard errors of the mean of four animals per group.

Fig. 3.1.6 CpG ODN augment number of mature lung myeloid DCs

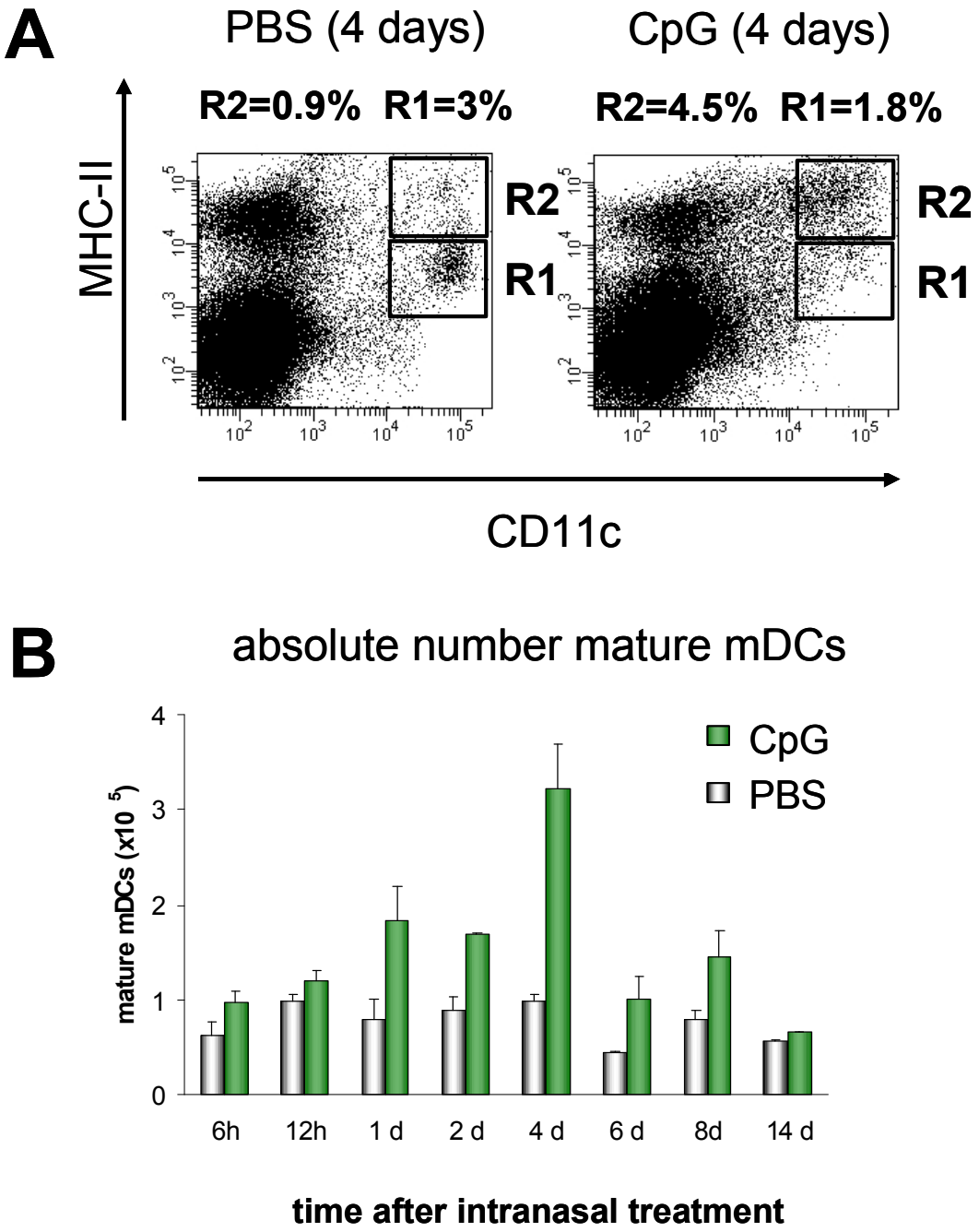

Fig. 3.1.6 Accumulation of mature lung myeloid DCs after CpG ODN administration. Example of FACS analysis of lung single cell suspensions after four days of CpG or PBS treatment: after gating of total live cells mature lung myeloid DCs are identified as $CD11c^{+}$ MHC-II^{high} DC (gate R2) population and macrophages and immature DCs are identified as $CD11c^{+}$ MHC-II^{low} DC (gate R1) population (A). Absolute numbers of R2 cells at different time points after intrapulmonary CpG treatment, calculated by multiplying the percentage of R2 cells by the total viable cell number (B). Data are expressed as means + standard errors of the mean of four animals per group.

Fig. 3.1.7 CpG ODN induce activation of mature lung myeloid DCs

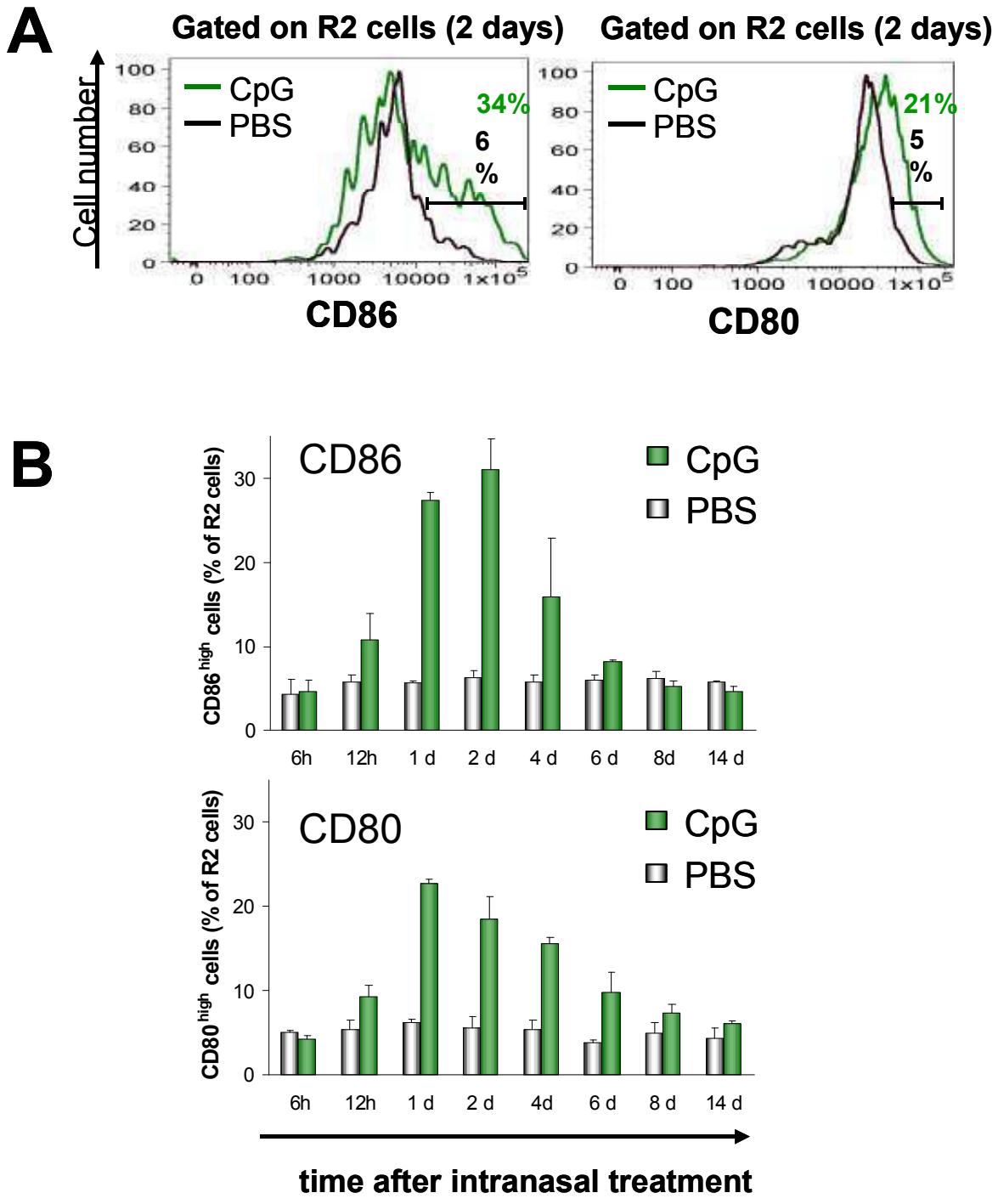

Fig. 3.1.7 Activation of mature lung myeloid DCs after CpG ODN administration. Levels of the costimulatory molecule CD86 and CD80 on mature lung myeloid DCs. Example of FACS analysis of lung single cell suspensions after two days of CpG or PBS treatment: surface CD86 and CD80 expression by R2 cells as select in fig. 3.1.5 (A); markers represent the limit defining the expression at high levels. Histograms show CD86 and CD80 expression at high levels on R2 cells after different periods of CpG or PBS treatment (B). Data are expressed as means + standard errors of the mean of four animals per group.

Fig. 3.1.8 CpG ODNs favor the increase of lung plasmacytoid DC number

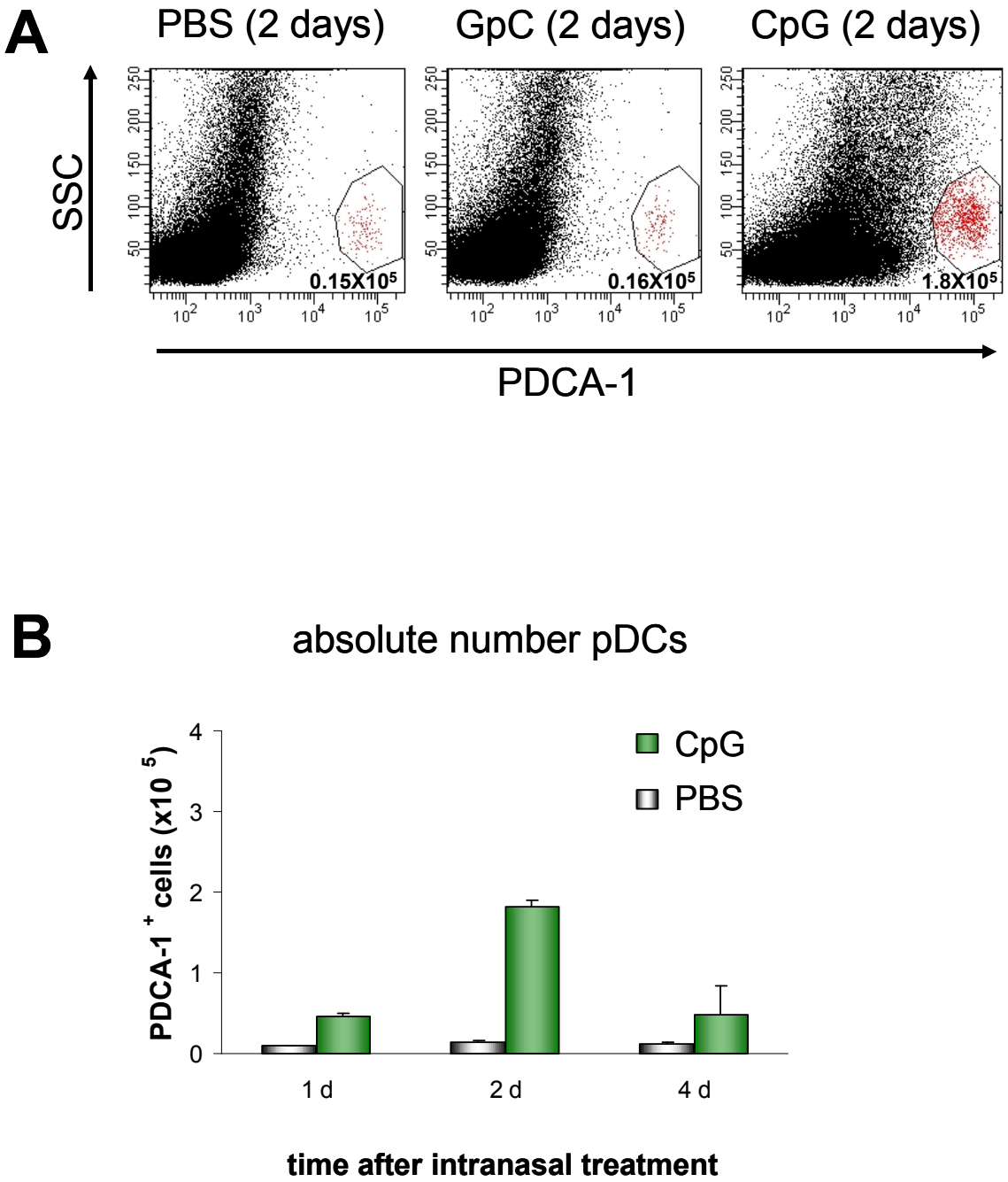

Fig. 3.1.8 CpG ODN treatment recruits lung plasmacytoid DCs. Example of FACS analysis of lung single cell suspensions after two days of CpG or PBS treatment: lung plasmacytoid DCs are identified as PDCA-1 positive cells (after gating of total live cells)(A). Absolute numbers of lung plasmacytoid DCs at different time points after intrapulmonary CpG treatment, calculated on the basis of percentage of PDCA-1 positive cells and total viable cell counts (B). Data are expressed as means + standard errors of the mean of four animals per group.

Fig. 3.1.9 CpG ODNs activate lung plasmacytoid DCs

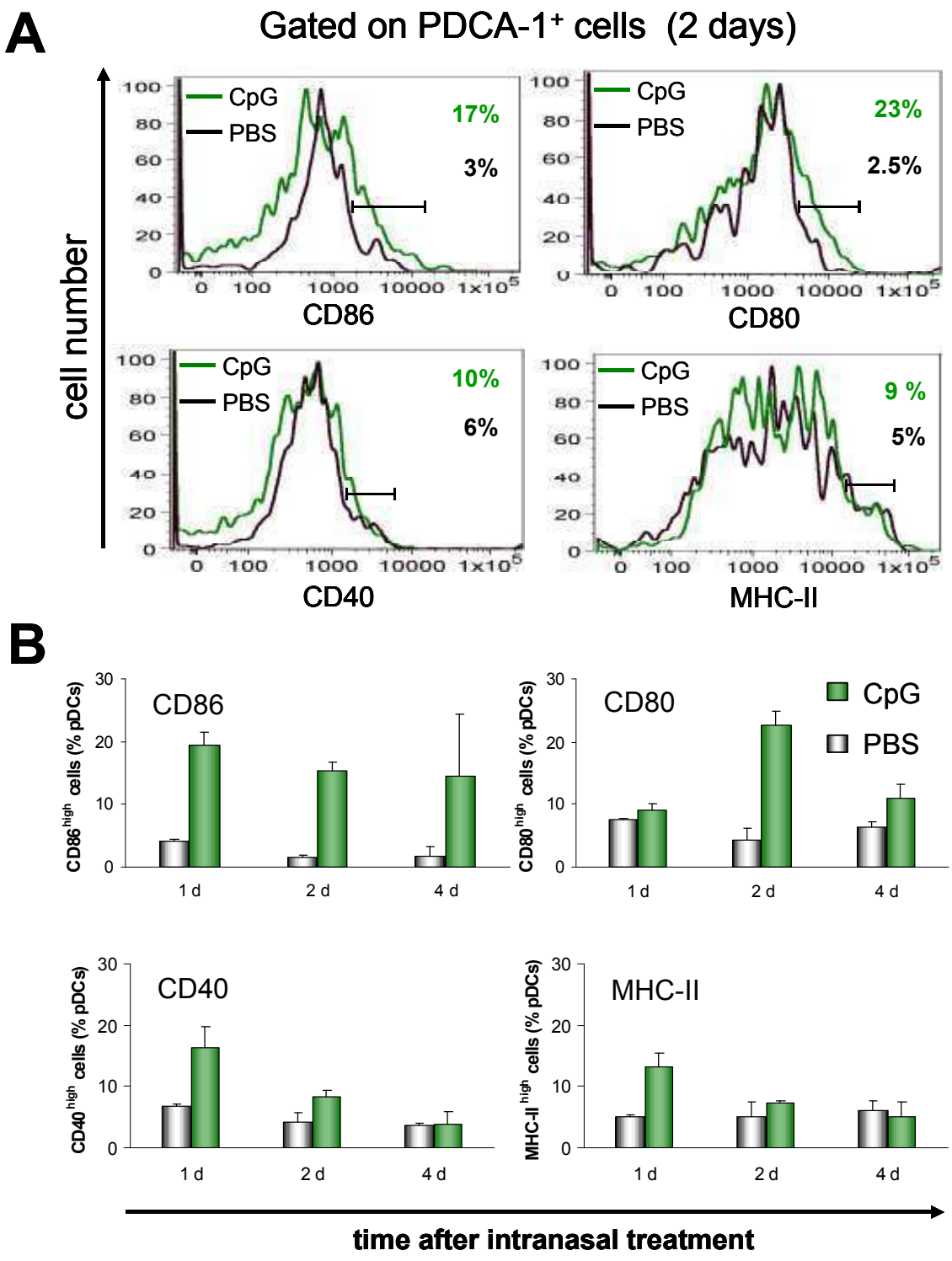

Fig. 3.1.9 CpG ODN treatment activates lung plasmacytoid DCs. FACS analysis of CD86, CD80, CD40 and MHC-II expression on PDCA-1 positive cells, as select in fig. 3.1.7, after two days of CpG or PBS treatment (A). The markers represent the limit defining the expression at high levels of the indicated surface molecules. Histograms show CD86, CD80, CD40 and MHC-II expression at high levels on PDCA-1 positive cells at 1, 2 and 4 days after CpG ODN treatment (B). Data are expressed as means + standard errors of the mean of four animals per group.

3.1.5 CpG ODNs activate T and NK cells in the lung but not in the spleen.

CpG ODNs generally have not been reported to have direct stimulatory effects on T cells and NK cells [118]. Because the above experiments showed a rapid induction of a inflammatory cytokine/chemokine microenvironment in the lung and DC activation after CpG ODN treatment, I investigated whether this was also reflected on lung T and NK cells. I determined *in vivo* the effect of intrapulmonary CpG ODN administration on lung T and NK cell activation in a time course ranging from 12 h to 14 days following CpG or PBS administration. As compared with control mice, CD8+ and CD4+ T cell subsets and NK cells found in the lung tissue at 1 to 2 days after CpG ODN administration, showed an activated phenotype as determined by cell surface expression of the activation markers CD69 and CD44 (Fig.3.1.10 and 3.1.11) . In contrast, no changes on T cells and NK cells were found in the spleen after CpG ODN treatment (Fig.3.1.12) .

Fig. 3.1.10 CpG ODNs induce T cell activation

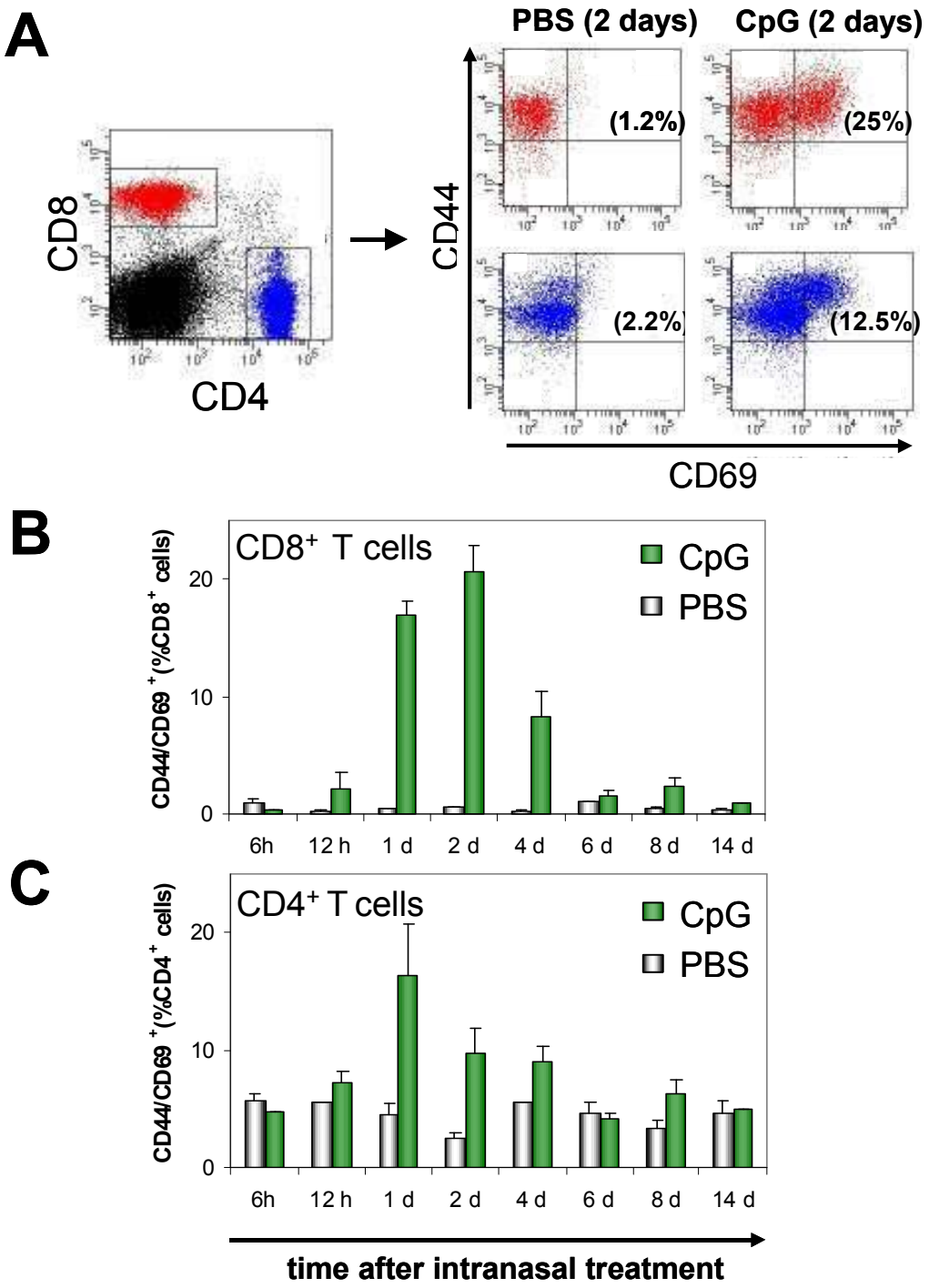

Fig. 3.1.10 Effect of CpG ODN administration on activation marker expression by lung T cells**.** Representative FACS analysis of lung T cells after 1 day of CpG or PBS treatment: after gating of total live cells $CD4^+$ T cells were defined as $CD3^+CD4^+$ and $CD8^+$ T cells as $CD3^+CD8^+$ and activation state of T cells were determined by measuring the percentage of cells positive for the activation markers CD44 and CD69 after gating for $CD3^+CD4^+$ and $CD3^+CD8^+$ cells as shown in A. The percentage of activated $CD4^+$ and $CD8^+$ T cells at different time points of CpG treatment (6h to 14d) was determined by measuring the percentage of CD44 and CD69 positive cells (B and C). Data are expressed as means + standard errors of the mean of four animals per group.

Fig. 3.1.11 CpG ODNs activate NK cells

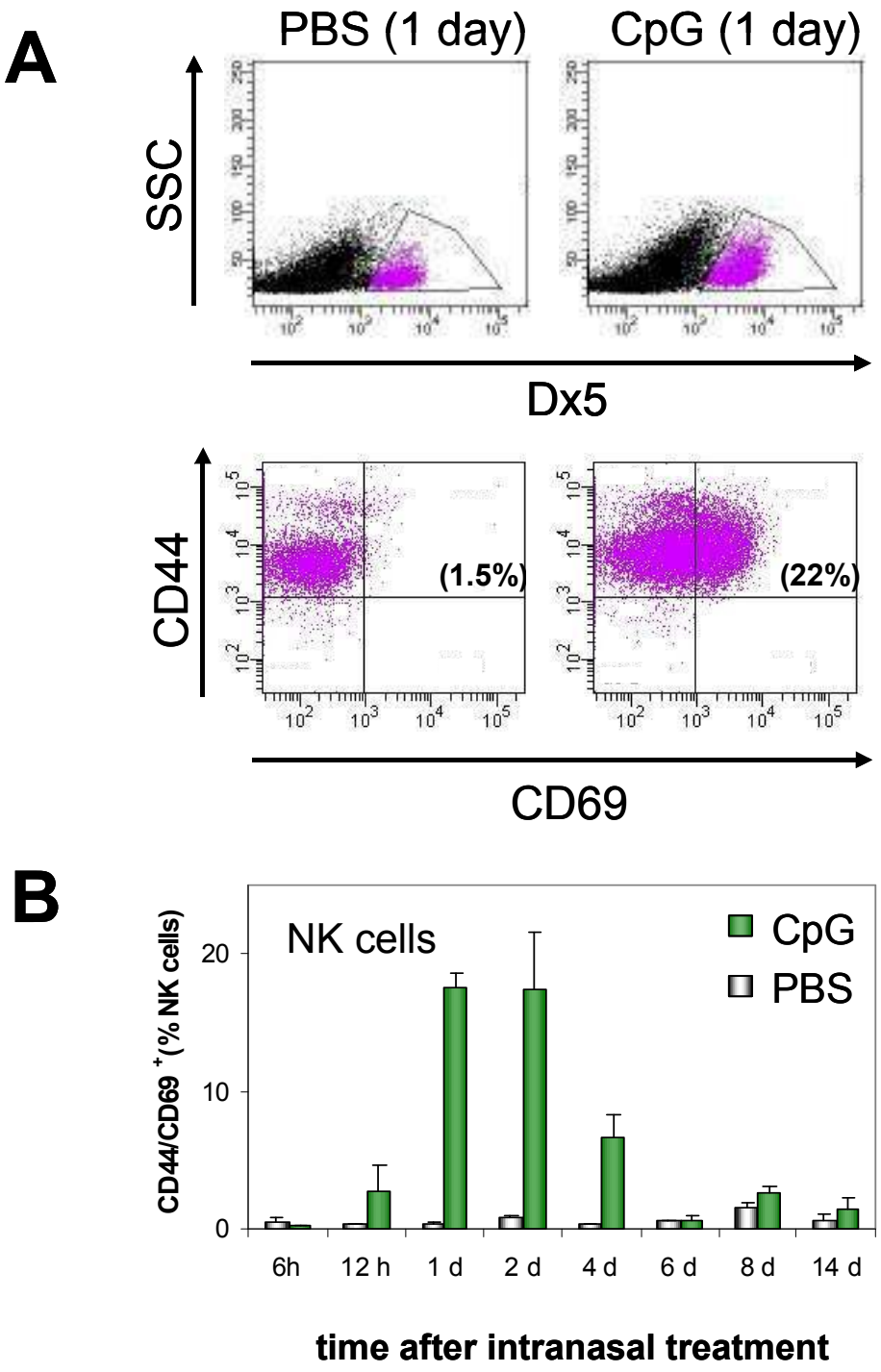

Fig. 3.1.11 Effect of CpG ODN administration on activation marker expression by NK cells. FACS Analysis of lung NK cells after CpG or PBS treatment (1 day). NK cells were identified as Dx5+ $CD3^-$ cells after gating of total live cells. Activation state of NK cells was determined by measuring the percentage of cells positive for the activation markers CD44 and CD69 after gating for $CD3^-$ $Dx5^+$ cells as shown in A.
In B histogram shows activated NK cells after different periods of treatment. Data are expressed as means + standard errors of the mean of four animals per group.

Fig. 3.1.12 Activation marker expression by splenic T and NK cells

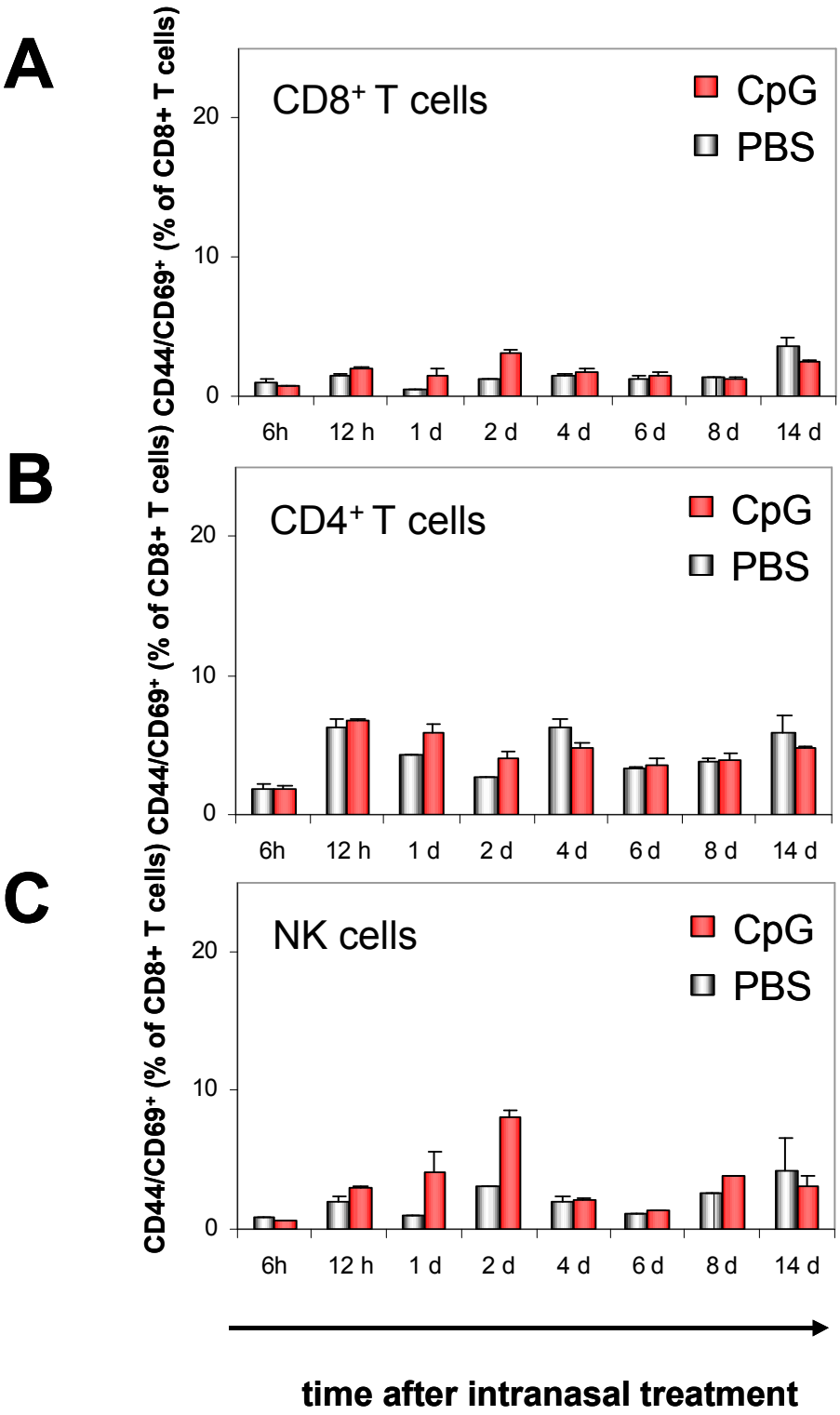

Fig. 3.1.12 CpG ODN administration and activation marker expression by splenic T and NK cells. Splenic $CD4^+$ and $C8^+$ T cells and NK cells positive for the activation markers CD44 and CD69 in a time course ranging from 6 h to 14 days following CpG or PBS administration.

3.1.6 Kinetics of serum cytokines response to intrapulmonary CpG treatment.

CpG ODN intrapulmonary administration induced local cytokine and chemokine protein expression in the lung as reported in previous results. No systemic effect of CpG ODN intrapulmonary administration was observed at cellular level in splenic DCs (data not shown), T cells and NK cells. I asked whether a systemic effect of CpG ODN intrapulmonary administration will be observed in mouse serum cytokines, so I determined at various time intervals the production of multiple cytokines in mouse serum, by ELISA based multiplex analysis. Serum concentrations of representative cytokines at different time points after intrapulmonary treatment are shown in Fig. 3.1.13. IL-12(p40) protein expression increased within 6h of CpG ODN treatment and peaked at 12 h (6-fold) and IL-6 protein expression peaked at 6h (19-fold).

The level of G-CSF in serum dramatically increased only at 12 h time point (46-fold) after treatment and the level of KC increased only at 6h (36-fold). I observed a slightly increase of MIP-1β (5-fold at peaking time) level and MCP-1 level (10-fold at peaking time) in sera and a rapid decline to baseline levels for both chemokines at 1 day after CpG ODN treatment. A rapid peak of RANTES in sera was seen at 12h (5-fold) after CpG treatment, but was not observed a sustained production in treated mice compared to control mice. The summary of serum cytokine proteins tested, peaking time points and fold increase for CpG ODN up-regulated cytokines, unchanged cytokines and cytokines out of range below are reported in table 3.2.

Fig. 3.1.13 Kinetics of representative serum cytokines after CpG ODN administration

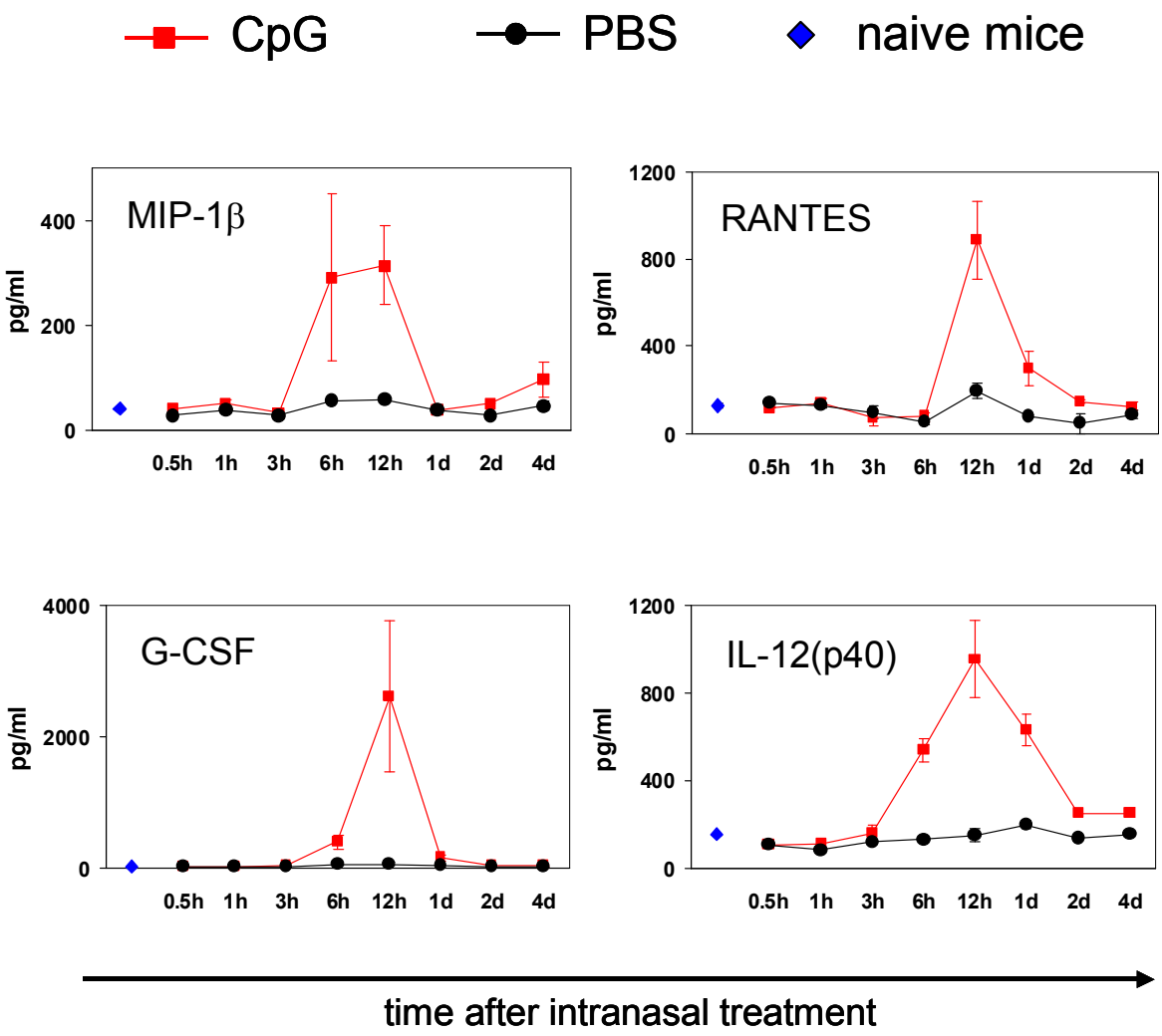

Fig. 3.1.13 Kinetics of serum cytokines in CpG treated and control mice (30 min -4 days) and in naïve BALB/c mice. Concentrations of indicated representative cytokines were determined by ELISA based multiplex analysis of lung homogenates. Results are represented as the mean (pg/ml) ± SEM. N = 3/treatment group.

Table 3.1.2. Summary of serum cytokine proteins tested

summary of cytokine proteins tested (serum)						
peaked at 6 h fold increase (6 h)	IL-6 (19)	KC (36.3)	MIP-1β (5.5)			
peaked at 12h fold increase (12 h)	IL12 p40 (6.36)	G-CSF (46.5)	MCP-1 (10)	RANTES (5)	IL12 p70 (3)	
unchanged	IL-1α	IL-1β	IL-2	IL-9	IL-10	IL-13
unchanged	IL-17	eotaxin	GM-CSF	IFN-γ	MIP-1α	TNF-α
below detection threshold	IL-3	IL-4	IL5			

Table 3.1.2. Multiplex analysis of cytokine protein expression in serum.
Summary of serum cytokine proteins tested, CpG ODN induced cytokines with the time of peaking and their respective fold increase, unchanged cytokines and cytokines below detection threshold.

3. Results

3.2. LTK63

3.2.1. LTK63 treatment increases immune cell numbers in the lung of mice

I investigated the effect of a non-toxic heat-labile enterotoxin (LTK63) from *Escherichia coli* in the lungs of mice. BALB/c mice were treated intrapulmonarily with 5 μg of LTK63 or Buffer L, and lungs were sampled over 14 days. In agreement with a previous report I found that LTK63 promotes a profound increase in the number of total immune cells in the lung [113]. After treatment, total viable cell counts showed that cellular infiltration was greatest on day 8 (mean cell count ± SE: LTK63, $26.75 \pm 5.76 \times 10^6$; Buffer L: $8.25 \pm 1.31 \times 10^6$; n=4) and that a slight increase of cellularity was also present at 2 days (mean cell count ± SE: LTK63, $9.77 \pm 2.31 \times 10^6$; Buffer L: $6.57 \pm 1.7 \times 10^6$; n=4) (Fig. 3.2.1; A). After 14 days of LTK63 treatment cellularity was decreased but did not reach baseline. In addition, at the same time points increased lung weight was observed after intrapulmonary LTK63 administration and weight reached baseline level at 14 days (Fig. 3.2.1; B).

Fig. 3.2.1 LTK63 increases lung cellularity and weight

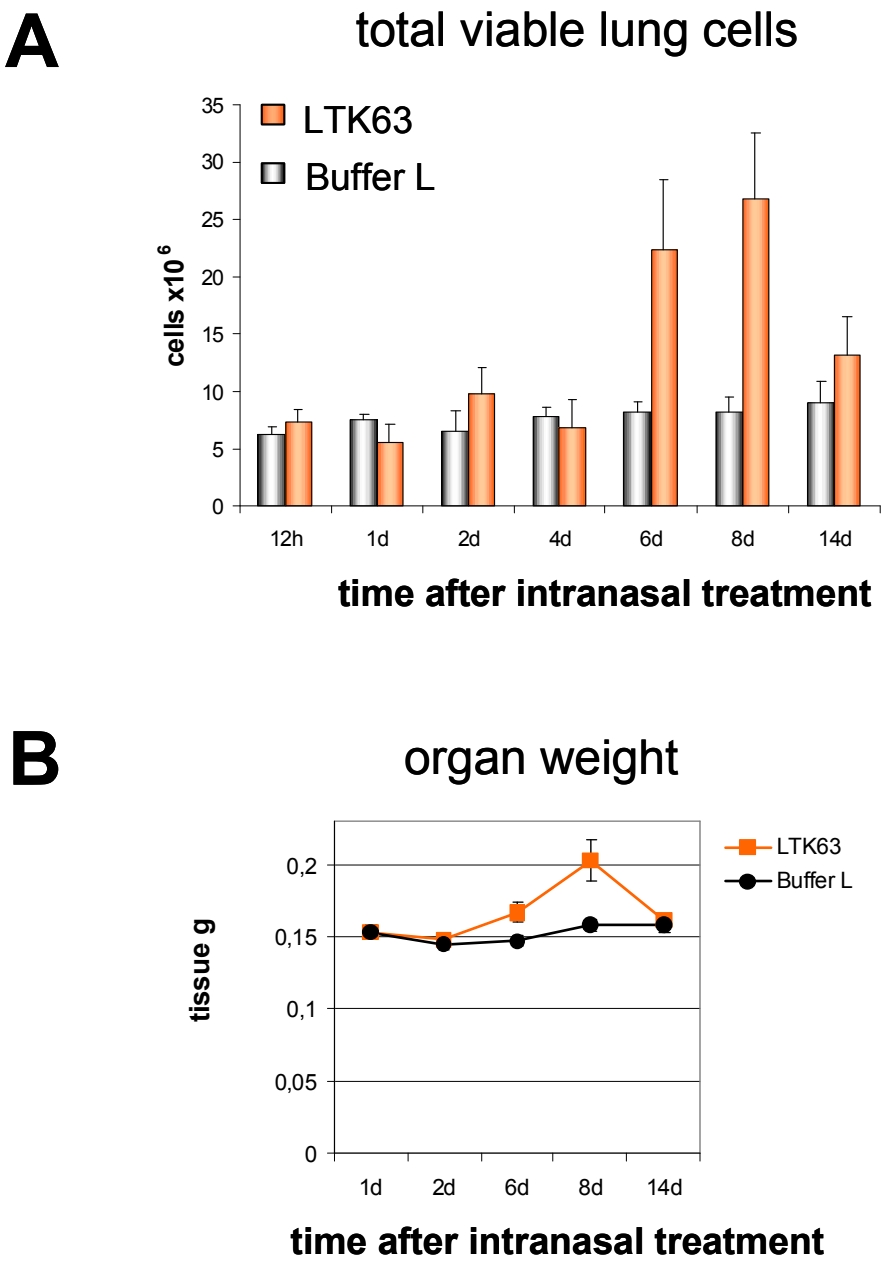

Fig. 3.2.1 LTK63 enhances the cellularity and the weight of the lung. Balb/c mice were anaesthetised and treated intrapulmonary with 5 µg of LTK63 in buffer L or buffer L for different periods of time (12h-14d). Total number of viable lung cells obtained after enzymatic digestion at different time points following administration of LTK63 or buffer L (A). Cellularity of the lung was enumerated by trypan blue exclusion of cells recovered from the lungs. Data are expressed as means + standard errors of the mean of four animals per group. At 1, 2, 6, 8 and 14 days after LTK63 or buffer L treatment lungs were removed and weighted (B). Lung weight (tissue g) is expressed as mean + standard error of the mean of five animals per group.

3.2.2 LTK63 treatment favors the expansion of myeloid and plasmacytoid lung DCs

Lung immune cells have the task of differentiating dangerous antigens from innocuous antigens, and a key role in mounting effective immunity to pathogens as well as in modulating the activity of immune responses is played by DCs. Lung DCs are ideally placed to sample inhaled agents at alveolar surface within and below the epithelium [26]. Therefore, I asked which could be the effect of intrapulmonary LTK63 treatment on number and phenotype of lung DC subsets at different time points (12h-14days). Characterization of lung DC subsets by flow cytometry and comparative phenotypic analysis of DCs in single cell suspensions from lung of 8 day LTK63 or buffer L treated mice is shown in Fig. 3.2.2. $CD11c^{+}MHC\text{-}II^{high}$ cells (R2 cells) (Fig. 3.2.2 A) were B220 negative, and CD11b positive and CD11b negative (Fig. 3.2.2 C,D). The CD11b positive subset have been defined as the myeloid DC subset and was preferentially expanded in the lung of 8 days LTK63 treated mice over the CD11b negative lymphoid subset. Cells expressing PDCA-1 and B220 (fig.3.2.2 B, C), low levels of CD11c and MHC-II and lacking the expression of CD11b (fig.3.2.2 A, D) have been defined as plasmacytoid DC subset. As depicted in fig. 3.2.3 (A), the absolute number of myeloid lung DCs (R2 cells) increased at 2 days and reached the greatest increase at 8 days after LTK63 treatment and decreased by 14 days. At 8 days myeloid DCs from LTK63 treated mice ($1.83 \pm 0.37 \times 10^6$) showed a 25-fold increase as compared with buffer L treated mice ($0.07 \pm 0.007 \times 10^6$). In contrast, no changes in the absolute number of R1 cells, a population comprised of alveolar macrophages and immature DCs, were observed (fig. 3.2.3 B). After 8 days of treatment I observed a slight increase of CD86 expression on R2 cells and no change in CD86 level on R1 cells as shown in the histograms in fig. 3.2.3 C. I examined then number and phenotype of lung plasmacytoid DCs in a time course ranging from 2 to 14 days following LTK63 or buffer L administration. In addition, at 8 days after intrapulmonary LTK63 administration, I observed a profound increase of the absolute number of plasmacytoid lung DCs, calculated on the basis of percentage of PDCA-1 positive cells. Plasmacytoid lung DCs from LTK63 treated mice ($5.2 \times 10^5 \pm 0.05$) showed a 32-fold increase as compared with control mice ($0.16 \times 10^5 \pm 0.001$) as shown in fig.3.2.4 A. Up-regulation of CD86 expression by plasmacytoid DCs was seen at 8 days after the treatment, as assesed by percentage of cells expressing CD86 at high levels, compared with the same cells from control animals (fig. 3.2.4 B).

Fig. 3.2.2 Comparative phenotypic analysis of lung DC subsets

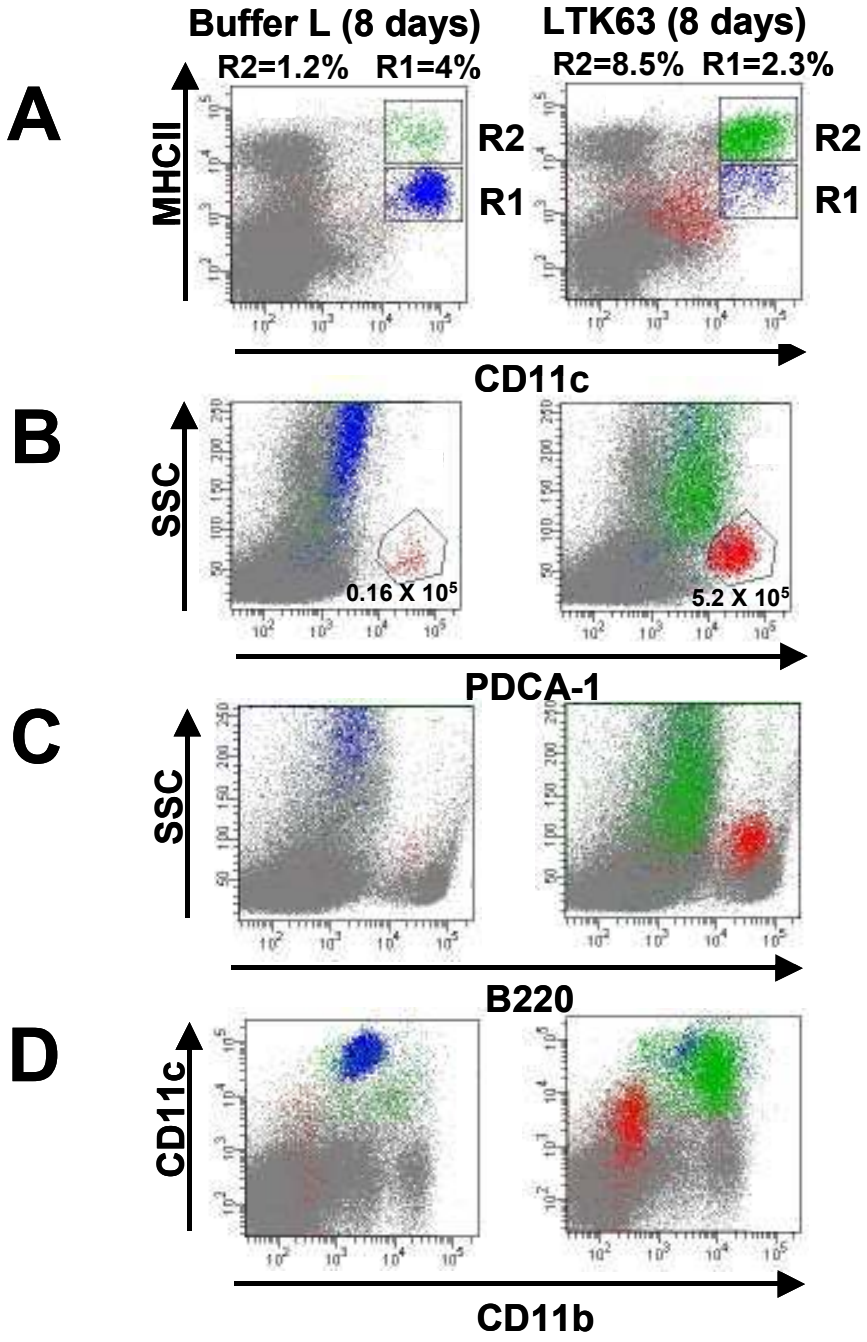

Fig. 3.2.2 FACS-based detection of DC subsets in the lungs of LTK63 or buffer L treated mice. Single cell suspensions from enzymatically digested lungs were stained with CD11c-APC, CD11b PerCP-Cy5.5, B220 PE-Cy7, PDCA-1-PE and I-A^d -biotin and analyzed by flow cytometry. Dot plots on the right show representative samples of lung cells obtained after 8 days of LTK63 treatment while dot plots on the left show samples obtained after buffer L treatment. Dot plots in A indicate flow cytometry gating criteria of lung cells expressing CD11c and MHC-II at intermediate (R1, blue cells) and at high levels (R2, green cells). In B plasmacytoid DCs were identified as PDCA-1 positive cells (red cells). Expression of CD11b and absence of B220 expression on $CD11c^{+}MHC\text{-}II^{high}$ green cells (gate R2) and expression of B220 and absence of CD11b expression on PDCA-1 positive red cells was shown in dot plots (C,D). Data are representative of four independent experiments.

Fig. 3.2.3 LTK63 increases the number of myeloid lung DCs

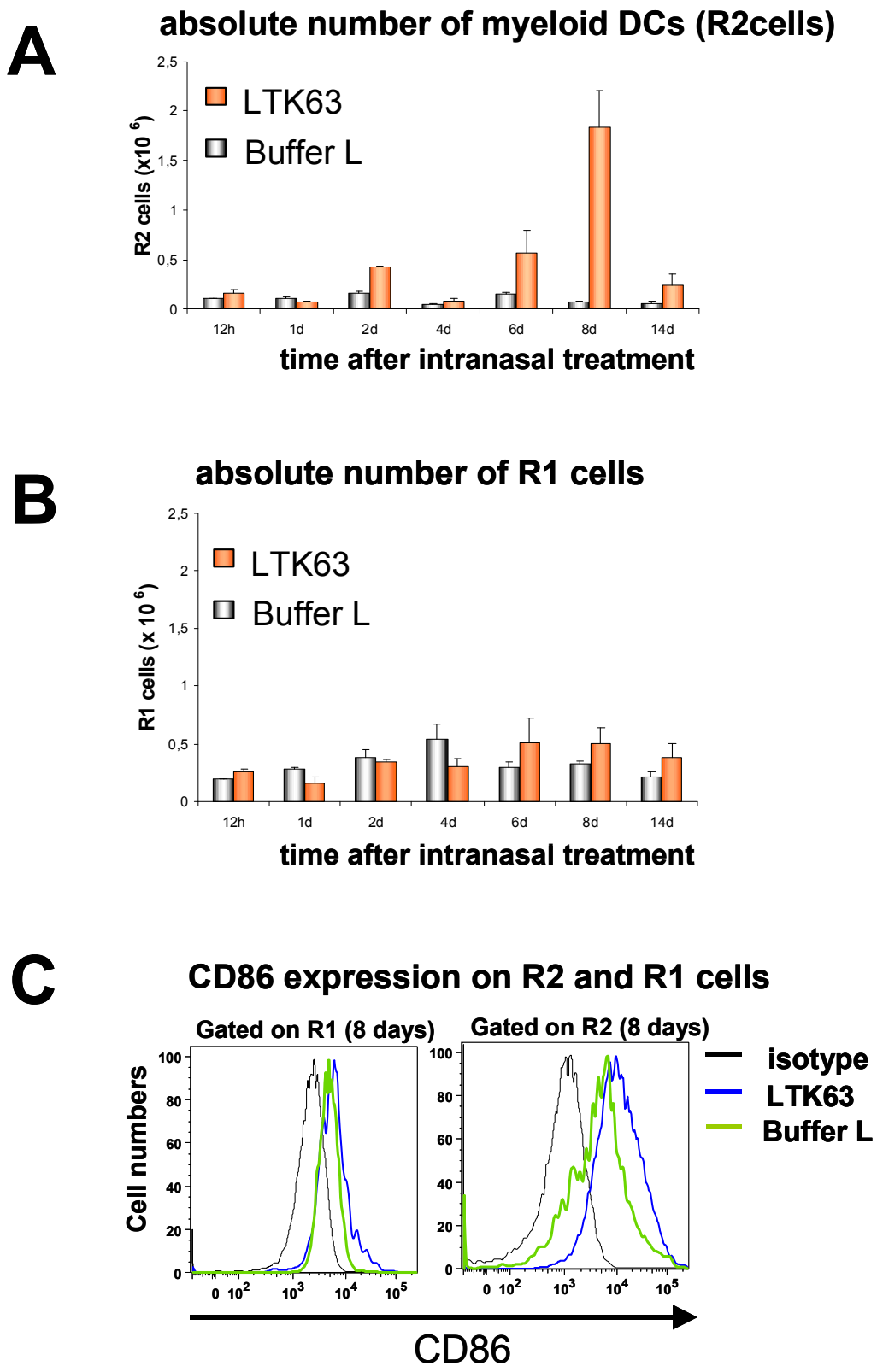

Fig. 3.2.3 LTK63 increases the number of myeloid lung DCs. Absolute number of myeloid DCs (R2) and R1 cells per lung, calculated by multiplying percentage by total viable cell number, at different time points after intrapulmonary treatment are shown in A and B. Data are expressed as means + standard errors of the mean of four animals per group. Histograms show the levels of the costimulatory molecule CD86 on myeloid DCs (R2) and R1 cells after 8 days of treatment (C).

Fig. 3.2.4 LTK63 treatment favours the increase of the number of activated lung plasmacytoid DCs

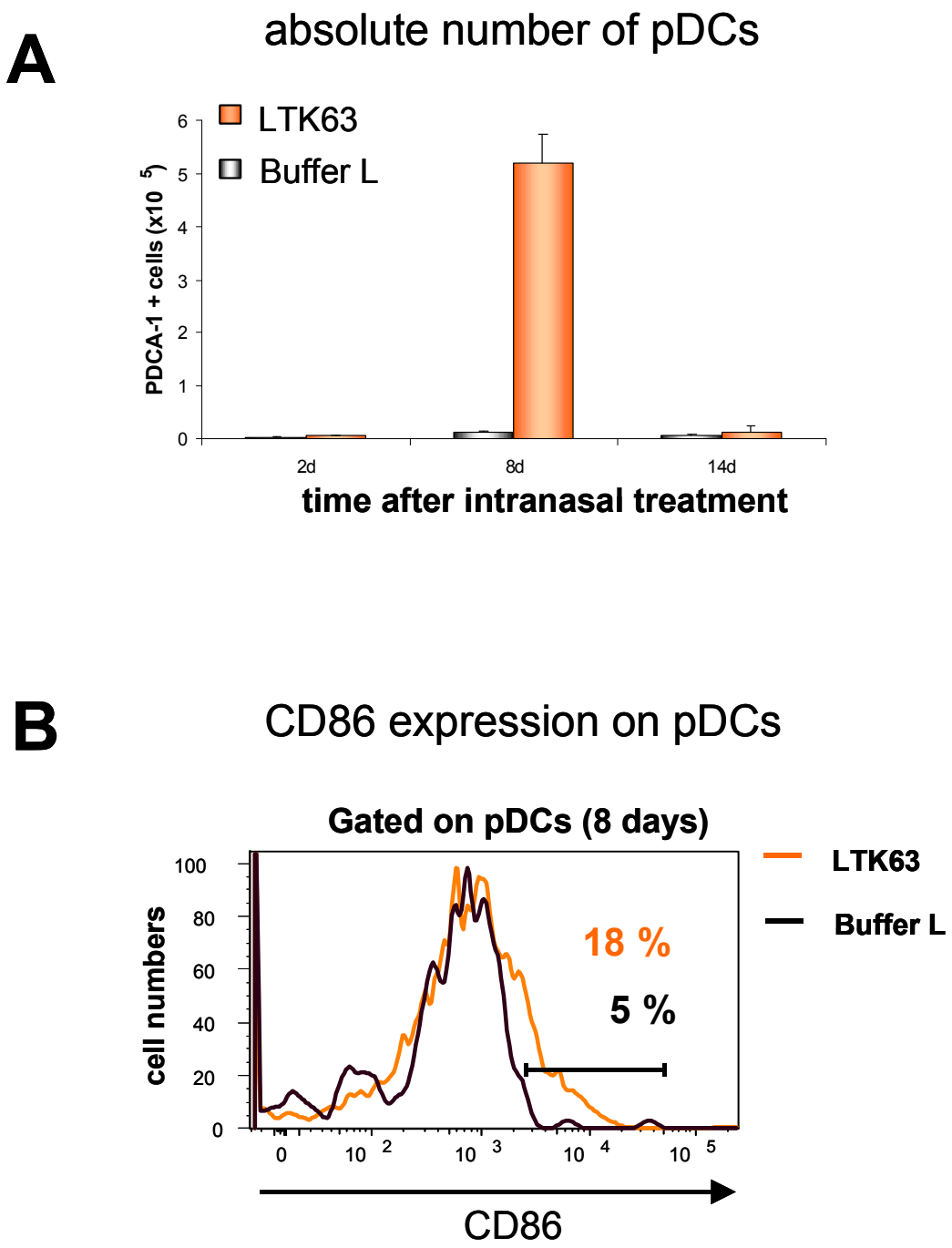

Fig. 3.2.4 LTK63 treatment favours the increase of the number of activated lung plasmacytoid DCs. Absolute number of plasmacytoid DCs at different time points after intrapulmonary LTK63 treatment, calculated on the basis of percentage of PDCA-1 positive cells and total viable cell counts (A). Data are expressed as means + standard errors of the mean of four animals per group. Histogram show CD86 expression on PDCA-1 positive cells in a representative sample of lung cells obtained after 8 days of LTK63 or CHAPS buffer treatment (B).

3.2.3 Biphasic expansion of granulocytes in the lung after LTK63 treatment

Pulmonary vasculature contains a particularly rich supply of granulocytes which are recruited into alveolar spaces to enhance phagocytic defence in response to various inflammatory stimuli, including microbial-derived compounds and tissue released mediators [2]. To investigate whether granulocytes could play a role in the local response to intrapulmonary LTK63 administration, I determined at different time points after the treatment the absolute number of granulocytes, calculated on the basis of percentage of Ly6G positive cells and total viable cell count. As shown in Fig.3.2.5, LTK63 treatment induced a rapid increase in the absolute numbers of granulocytes peaking at 2 days (mean granulocyte absolute number ± SE: LTK63, $1.67 \pm 0.32 \times 10^6$; Buffer L: $0.57 \pm 0.05 \times 10^6$; n=2), and this was followed by a second peak at 8 days (mean granulocyte absolute number ± SE: LTK63, $1.42 \pm 0.26 \times 10^6$; Buffer L: $0.38 \pm 0.003 \times 10^6$; n=2).

Fig. 3.2.5 LTK63 treatment induces biphasic expansion of granulocytes

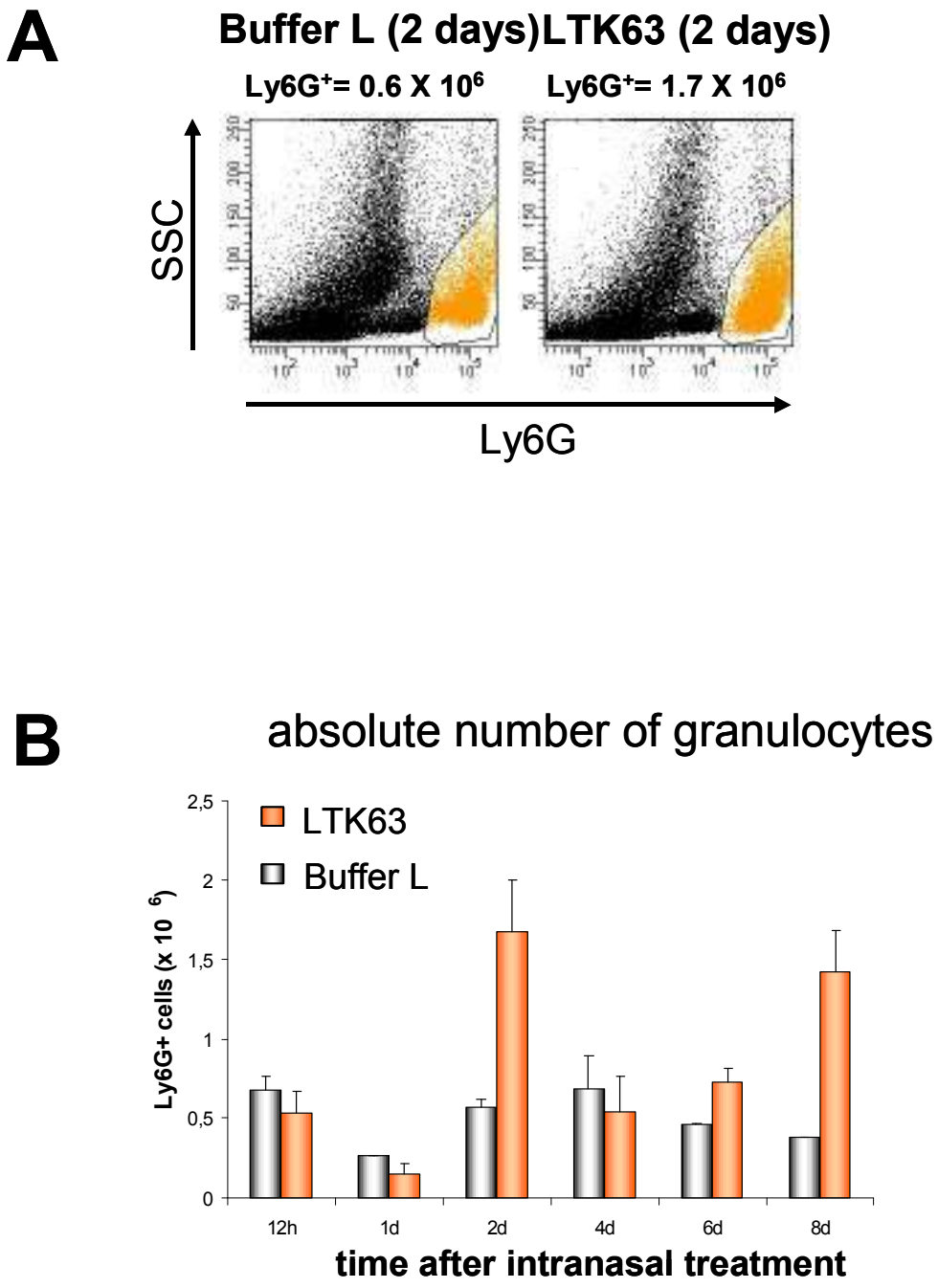

Fig. 3.2.5 Increased number of granulocytes. Absolute number of $Ly6G^+$ cells per lung, calculated by multiplying percentage by total viable cell number, at different time points after intrapulmonary treatment. Data are expressed as means + standard errors of the mean of two animals per group.

3.2.4 LTK63 treatment leads to enhanced recruitment of CFSE$^+$ BM-DCs and granulocytes into the lung

DCs can populate the lung throught different mechanisms: chemokine-driven recruitment of differentiated DCs from the circulation; recruitment of DC precursors, which then differentiate into DCs after exposure to local cytokines, and, albeit less documented, proliferation of intrapulmonary DC progenitors and transdifferentiation of pulmonary macrophages into DCs [26]. To investigate whether LTK63 treatment does increase DC recruitment from the bloodstream into the lung, CFSE-labelled BM-DCs were intravenously injected into control mice and in mice treated 8 days before with LTK63. After 24 hrs, injected cells were enumerated in lung and spleen single cell suspensions (schematic picture in Fig. 3.2.6 A). After eight days of culture, BM-DCs were contained 71% DCs or their progenitors (CD11c$^+$ cells) and 25% granulocyte contamination (GR1$^+$, CD11c- cells). Migration of BM-DCs to the lung and to the spleen upon i.v. injection was previously observed [120]. As shown in Fig. 3.2.6. (B,C), I detected more lung CFSE$^+$ CD11c$^+$ DCs in mice pretreated with LTK63 compared with mice pretreated with control buffer. Similar numbers of DCs were observed in the spleens collected from LTK63 or buffer L treated mice. In addition, in both groups of mice, injected DCs showed a higher ability to home to the lung as compared with their ability to home to the spleen.

Previously I have described granulocyte accumulation in the lung at 2 and 8 days after LTK63 treatment (fig. 3.2.5). Therefore, I asked whether 8 day LTK63 treatment leads to higher pulmonary recruitment of granulocytes. As depicted in Fig. 3.2.7 A, CFSE-labelled BM-DCs were i.v. injected into mice pretreated with LTK63 or buffer L (6 days before) and after 24 hrs injected cells were enumerated in lung and spleen. BM-DC cultures maintained for seven days contained 55% DCs or DC progenitors (CD11c$^+$ cells) and 38% granulocyte contamination (GR-1$^+$, CD11c$^-$ cells). GR-1 labelling was utilized in combination with CFSE to identify injected granulocytes.

In both organs I observed increased number of lung CFSE$^+$ GR-1$^+$ granulocytes in mice pretreated with LTK63 compared with mice pretreated with control buffer. Contrary to DCs, injected granulocytes showed higher accumulation in the spleen.

Fig. 3.2.6 LTK63 increases BM-DCs accumulation in the lung following i.v. injection

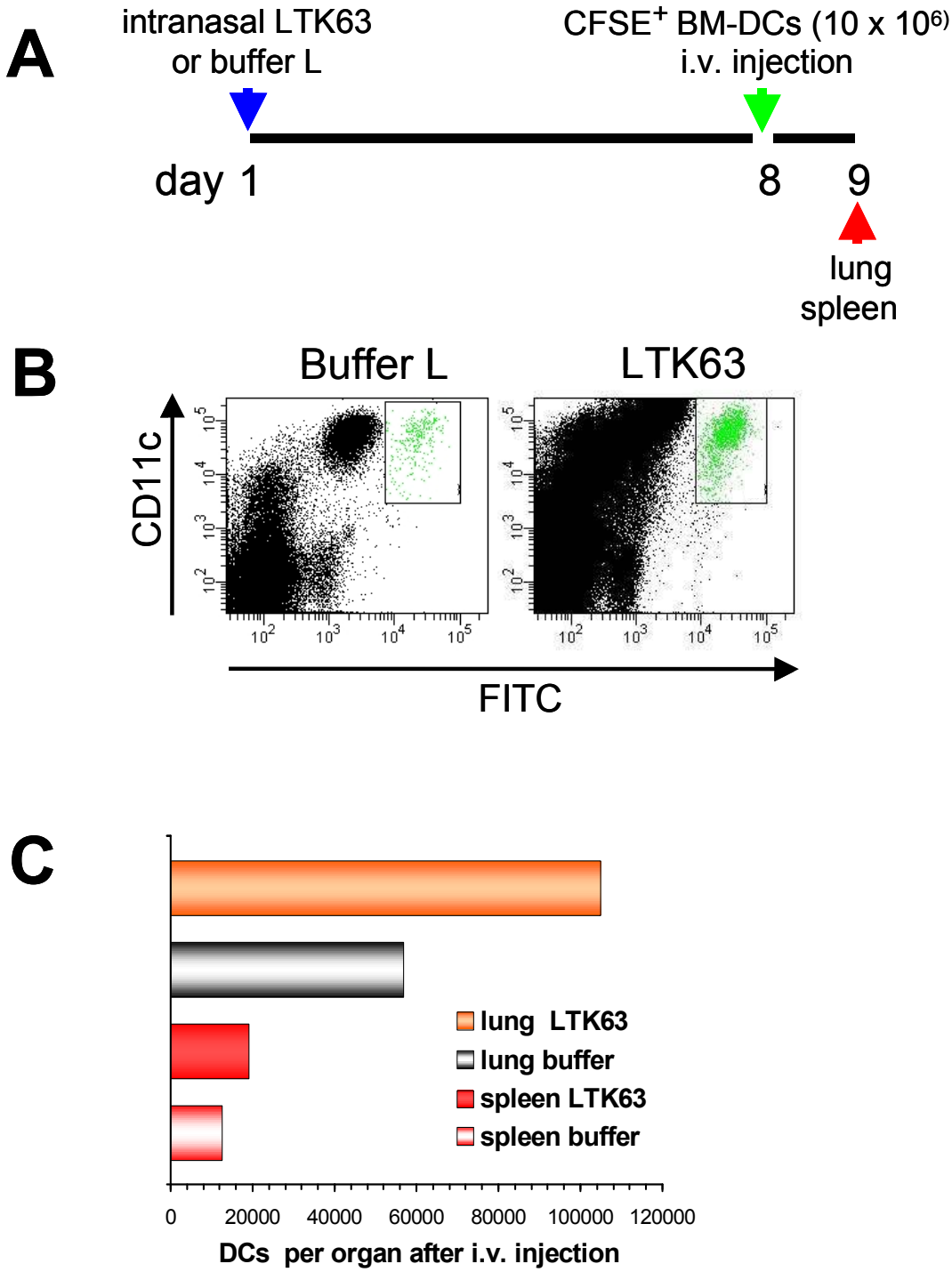

Fig. 3.2.6 DC accumulate in the lung following i.v. injection. BM-DCs were labelled with CFSE and 10×10^6 cells were injected i.v. into mice after 8 days of LTK63 or buffer L treatment. BM-DCs were generated for eight days and contained 71% DC or their progenitors (CD11c+) and 25% granulocyte contamination (GR1+, CD11c- cells). After 24 hr, lungs and spleens were removed and a single cell suspension produced as depicted in schematic picture in A. Representative FACS analysis of lung single cell suspensions. CD11c labelling was utilized in combination with CFSE to identify injected DCs in mice pretreated with LTK63 or buffer L (B).DC i.v. injected were enumerated by flow cytometry and the results expressed as DC per organ (C). Results are representative of three experiments

Fig. 3.2.7 LTK63 increases granulocytes accumulation following i.v. injection

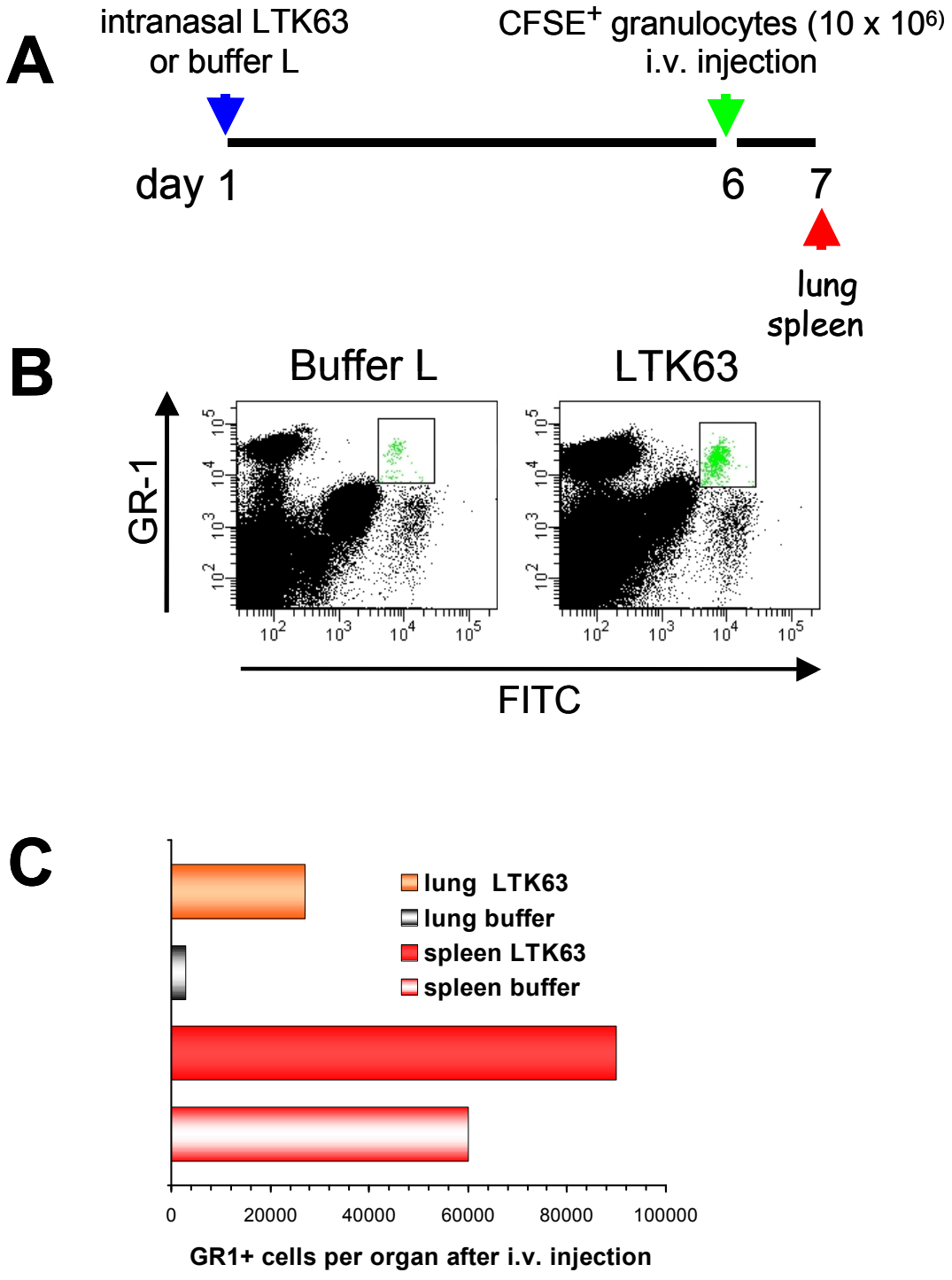

Fig. 3.2.7 Granulocyte accumulate in the lung and spleen following i.v. injection. BM-DCs were labelled with CFSE and 10×10^6 cells were injected i.v. into mice after 6 days of LTK63 or buffer L treatment. BM-DCs were generated for seven days and contained 55% DC or their progenitors (CD11c+ cells) and 38% granulocyte contamination (GR1+, CD11c- cells). After 24 hr, lungs and spleens were removed and a single cell suspension produced as depicted in A. Representative FACS analysis of lung single cell suspensions. GR-1 labelling was utilized in combination with CFSE to identify injected granulocytes in the organs of mice pretreated with LTK63 or buffer L (B). Granulocyte number were analysed by flow cytometry and the results expressed as granulocytes per organ (C). Similar results were obtained from three experiments.

3.2.5 Kinetics of lung cytokine response to intrapulmonary LTK63 administration

Cytokines and chemokines orchestrate the cellular response of the lung and I asked which lung cytokine environment is induced by LTK63. Also: the recruitment of different cell populations is likely to be mediated by chemokines. Therefore, I studied at the protein level lung cytokine and chemokine expression at various time intervals after intrapulmonary administration of LTK63. The production of multiple cytokines was determined in lung homogenates by ELISA based multiplex analysis. A rapid peak of G-CSF (11-fold increase) was observed at 1 day, and this was followed by a second peak at 6 days in treated mice compared to control mice. IL-1β and KC increased within 1 d of LTK63 treatment, peaked at 6 days and reached baseline level at 14 days. IL-12(p40), MIP-1α, MIP-1β and RANTES showed a late peak at 6 and 8 days before declining toward baseline by day 14 (Fig. 3.2.8; Fig. 3.2.9).

Table 3.2.1 shows the summary of cytokine proteins tested, LTK63 induced cytokines with the time of peaking and their respective fold increase, cytokines whose levels did not change upon treatment, and cytokines that remained below detection threshold. Thus, at early time points G-CSF, IL-1β and KC were induced by LTK63 treatment. At later time points (6-8 days) I observed a trend for higher production of IL-1α, IL-1β, IL-12(p40), KC, MIP-1α, MIP-1β, RANTES in the lungs of LTK63 treated mice compared to control mice.

Fig. 3.2.8 LTK63 induces cytokines in the lung

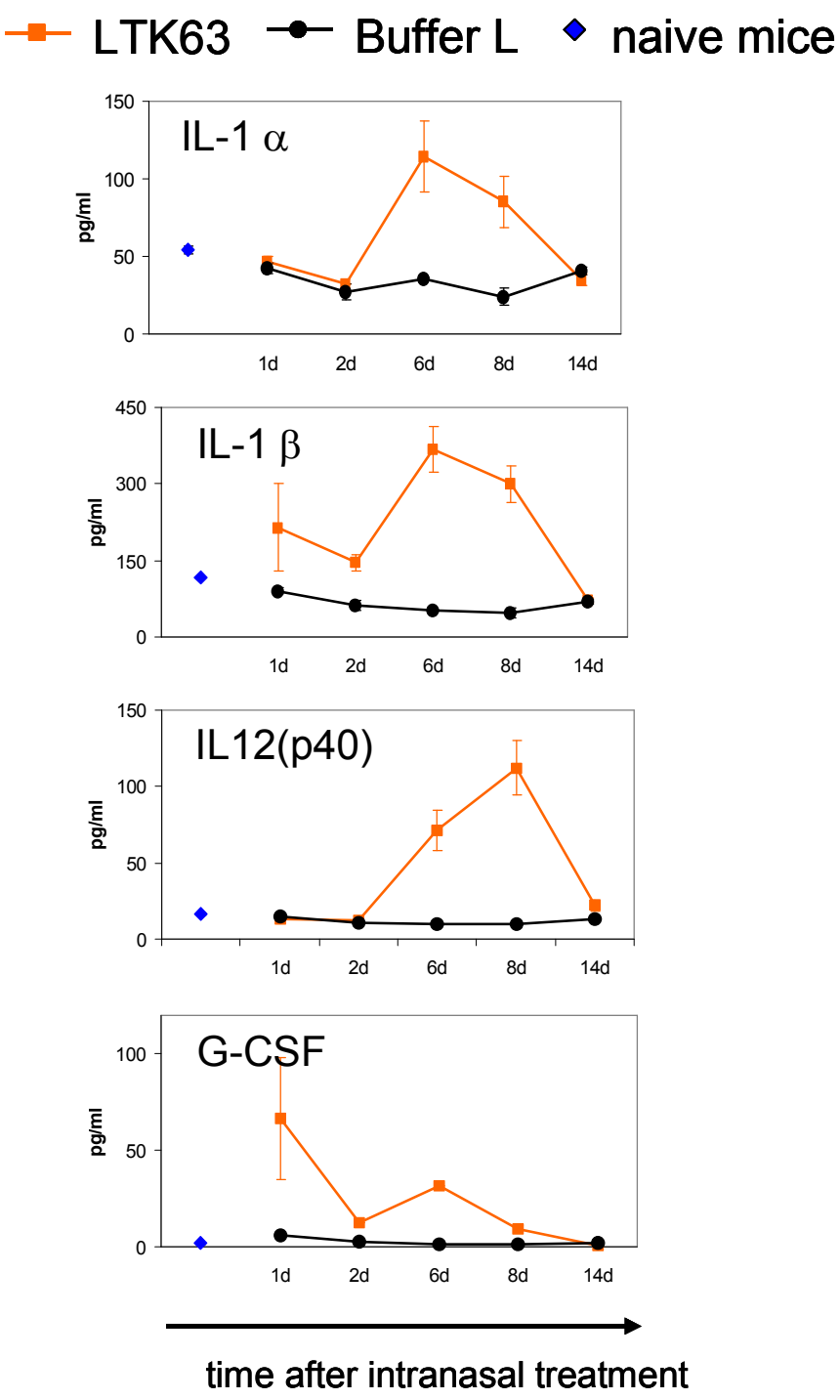

Fig. 3.2.8 Kinetics of inflammatory cytokines in lung tissue after LTK63 or buffer L treatment (1 day-14 days) and in naïve BALB/c mice. Concentrations of indicated cytokines were determined by ELISA based multiplex analysis of lung homogenates. Data are expressed as means (pg/ml) + standard errors of the mean of three animals per group.

Fig. 3.2.9 LTK63 induces chemokines in the lung

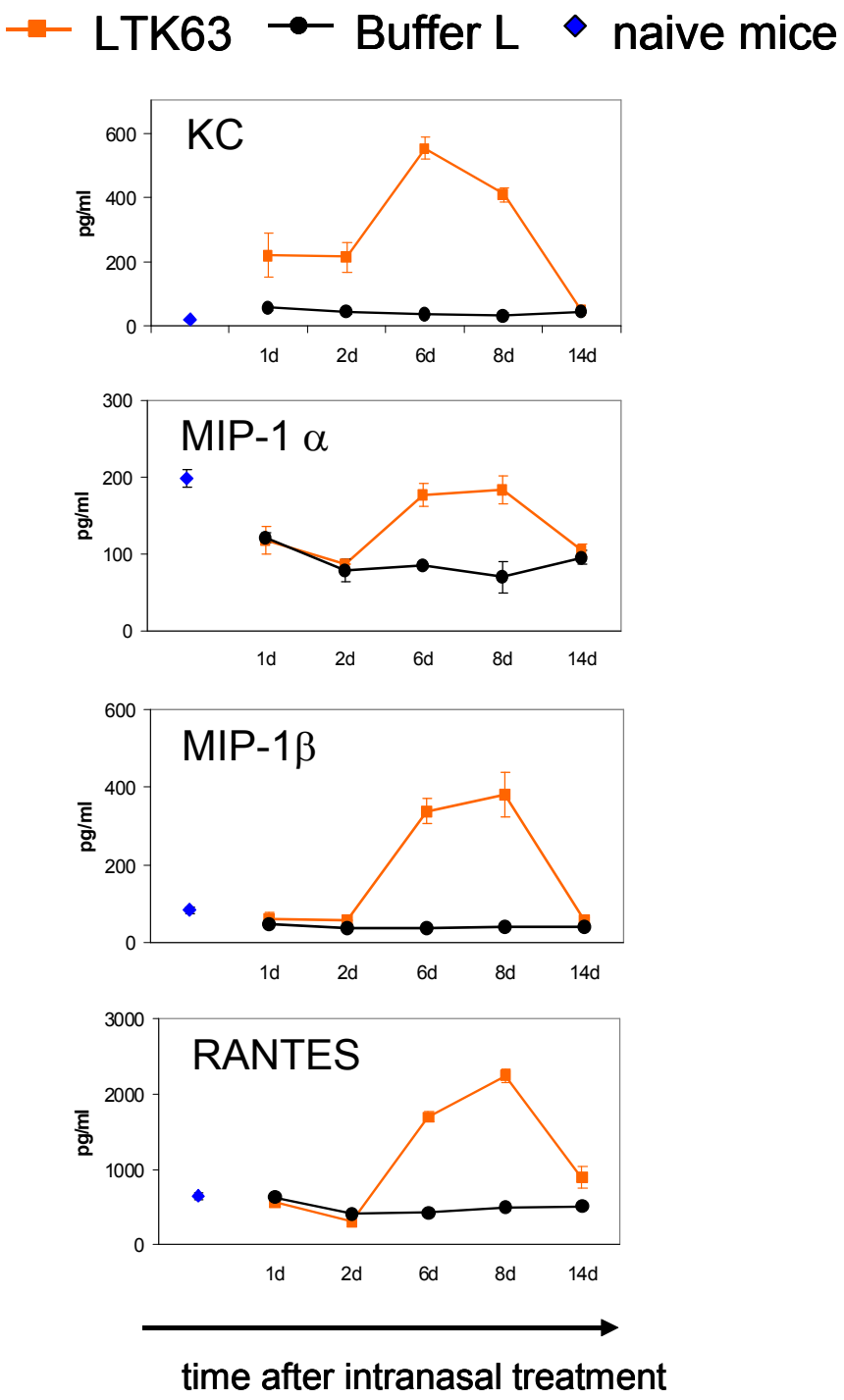

Fig. 3.2.9 Time course of chemokine production in lung tissue of LTK63 treated and control mice (1 day-14 days) and in naïve BALB/c mice. Concentrations of indicated cytokines were determined by ELISA based multiplex analysis of lung homogenates. Results are represented as the mean (pg/ml) ± SEM. N = 3/treatment group.

Table 3.2.2. Summary of lung cytokine proteins tested

summary of cytokine proteins tested (lung)						
peaked at 8 days fold increase (8 d)	IL12 p40 (11)	MIP-1α (3)	MIP-1β (10)	RANTES (5)		
peaked at 6 days fold increase (6 d)	IL-1α (3)	IL-1β (7)	KC (16)			
peaked at 1 day fold increase (1 d)	G-CSF (11)					
unchanged	IL-2	IL-5	IL-6	IL-9	IL-10	IL12 p70
unchanged	IL-13	IL-17	eotaxin	IFN-γ	MCP-1	TNF-α
below detection threshold	IL-3	IL-4	GM-CSF			

Table 3.2.1. Multiplex analysis of cytokine protein expression in lung tissue.
Summary of lung cytokine proteins tested: LTK63 induced cytokines with the time of peaking and their respective fold increase, unchanged cytokines and cytokines below detection threshold.

3.2.6 Cytokine release from lung CD11c$^+$ cells

To investigate which cytokines are produced by CD11c$^+$ cells in the lung after LTK63 treatment, I tested *ex vivo* cytokine secretion profiles of these cells. Cytokine levels were determined by multiplex analysis in the supernatant of CD11c$^+$ cells freshly isolated from the lungs of mice treated for 8 days with LTK63 or Buffer L (and subsequently culture at10^6 cells/ml for 48 h). CD11c$^+$ cells isolated from lungs of 8 days LTK63 treated mice secreted 2800 pg/ml MCP-1 by 48 h compared with 300 pg/ml for CD11c$^+$ cells from control mice. CD11c$^+$ cells from treated mice produced higher IL-1α, IL-12 (p40) and IL-6 compared with the same cells from control mice. A slight increase of IL-10 levels were also observed in CD11c$^+$ cells from treated mice.

IL-1β, IL-9, IL-12 (p70), IL-13, eotaxin, G-CSF, KC, MIP-1α, MIP-1β, RANTES and TNF-α release was similar for CD11c$^+$ cells isolated from treated and control mice. Levels of IL-2; IL-3; IL-4; IL-5; IFN-γ; IL-17 and GM-CSF were below the level of detection from both CD11c$^+$ cells from LTK63 and buffer L treated mice.

3.2.7 LTK63 induces T cell activation in the lung

LTK63 treatment triggers the expansion in the lungs of CD8$^+$ T cells, CD4$^+$ T cells, B cells, NK cells at 6-8 days of treatment (Fig. 3.2.11 A, B, C, D). Both CD4$^+$ and CD8$^+$ T cells increased in number at 6 and 8 days after LTK63 treatment; but the proportion between these two subsets remained constant throughout the analysis. These results are in agreement with a previous report [113].

In addition, I examined whether these cells were activated: the effect *in vivo* of intrapulmonary LTK63 administration on lung T and NK cell activation was determined in a time course ranging from 12 h to 14 days. As compared with control mice, CD8$^+$ and CD4$^+$ T cell subsets found in the lung tissue at 6 to 8 days after LTK63 administration, showed an activated phenotype as determined by cell surface expression of the activation markers CD69 (Fig.3.2.12 A, B). In contrast, NK cells appeared to be less activated after LTK63 treatment (Fig. 3.2.12 C). Thus, intrapulmonary administration of LTK63 leads to primary lung T cell activation.

Fig. 3.2.10 LTK63 induces cytokine release by CD11c+ cells

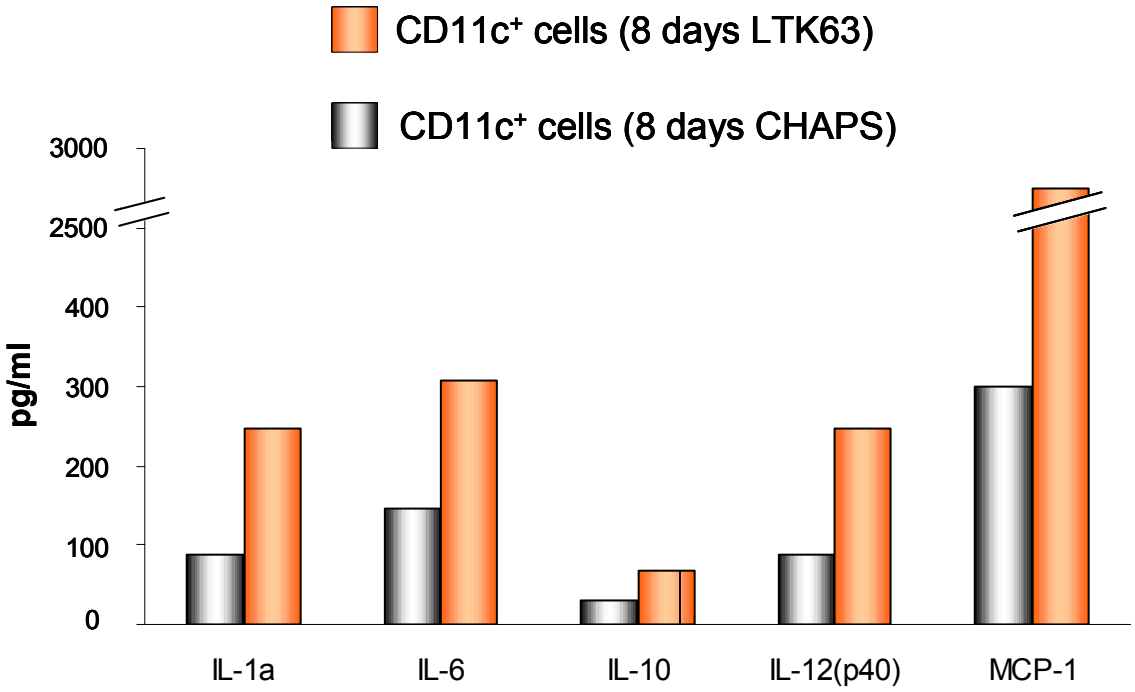

Cytokines unchanged :IL-1β ; IL-9; IL-12 (p70); IL-13; eotaxin; G-CSF; KC; MIP-1α; MIP-1β; RANTES; TNF-α.

Cytokines below detection threshold: IL-2; IL-3; IL-4; IL-5; IFN-γ; IL-17; GM-CSF.

Fig. 3.2.10 LTK63 induces cytokine release from lung CD11c positive cells isolated 8 days after the treatment. CD11c positive cells were isolated from 8 days LTK63 or buffer L treated mice and cultured for 48 h. Concentrations of indicated cytokines were determined by ELISA based multiplex analysis in culture supernatants. Similar results were obtained from three experiments

Fig. 3.2.11 LTK63 induces T cell, B cell and NK cell accumulation

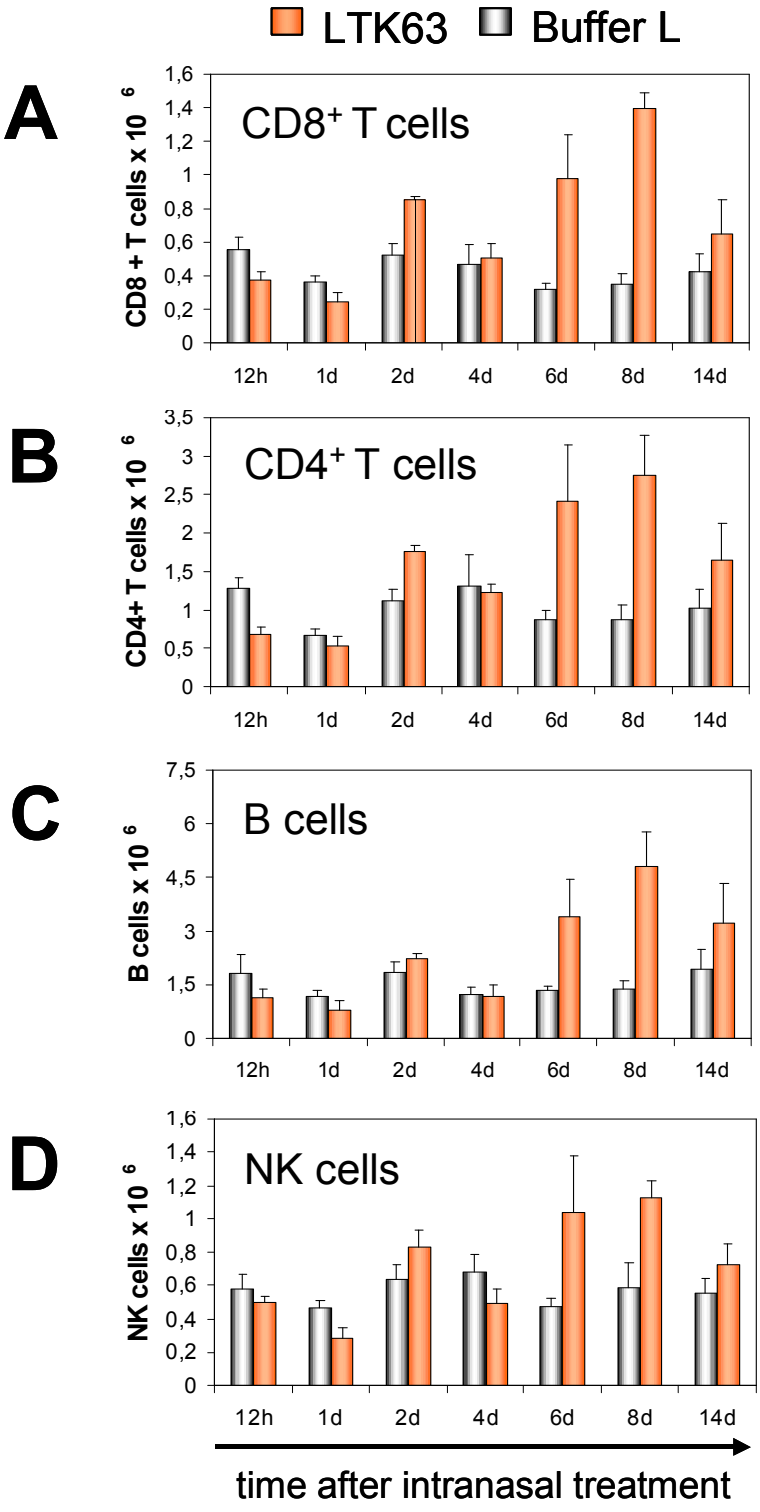

Fig. 3.2.11 LTK63 increases the number of lymphocyte and NK cells. The absolute number of CD4+ T cells (A), CD8+ T cells (B), B cells (C) and NK cells (D) was obtained by multiplying the frequency of each cell type by total viable cell number measured by trypan blue exclusion. Data are expressed as means + standard errors of the mean of four animals per group.

Fig. 3.2.12 LTK63 induces T cell activation

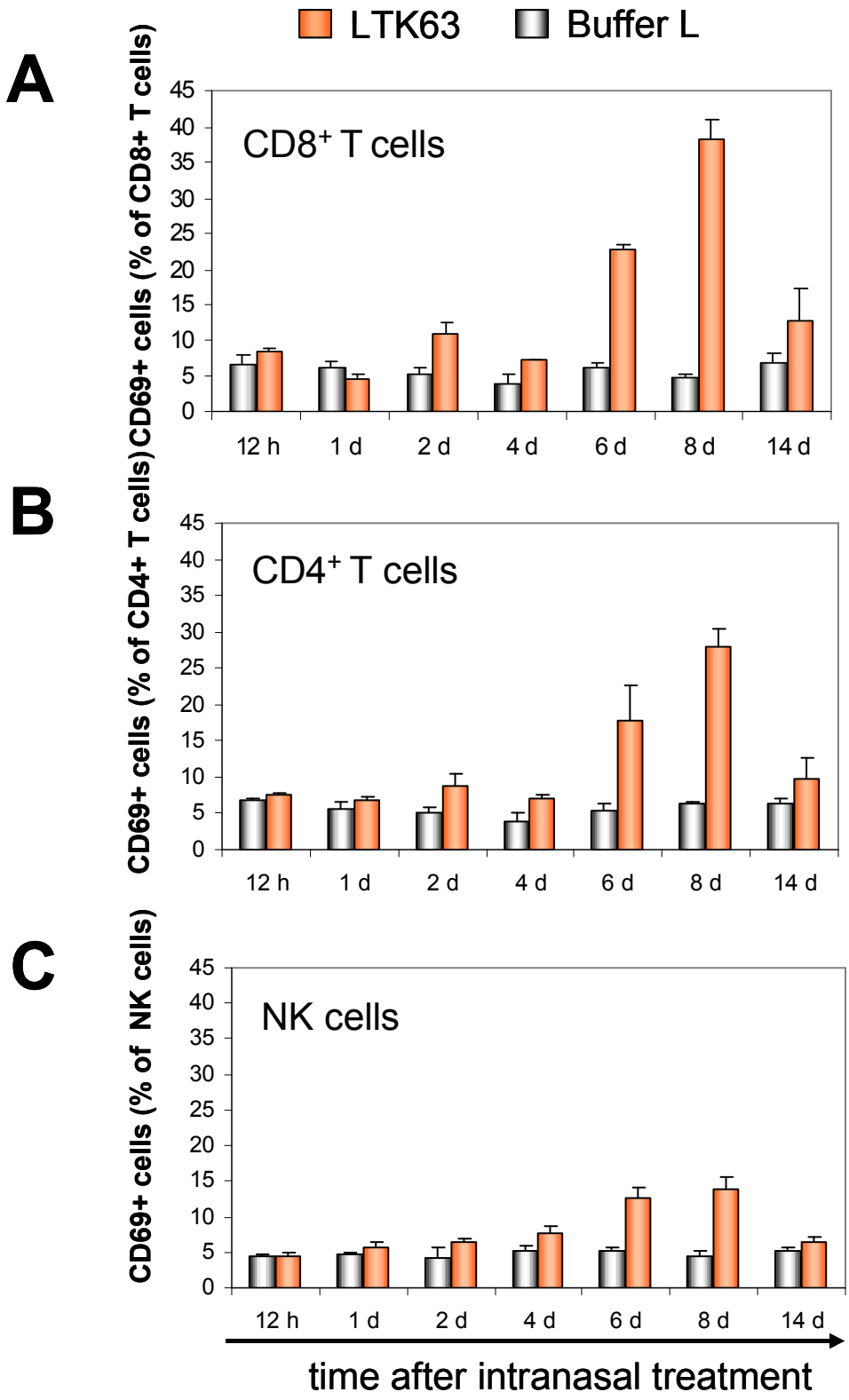

Fig. 3.2.12 Effect of LTK63 administration on T and NK cells activation. The percentage of activated $CD4^+$ and $CD8^+$ T cells (A, B) and NK cells (C) at different time points of LTK63 treatment (6h to 14d) was determined by measuring the percentage of CD69 positive cells. Data are expressed as means + standard errors of the mean of four animals per group.

3.2.8 CD11c$^+$ cells from LTK63 treated mice are more potent stimulators of allogenic T cells

To test the functional consequences of LTK63 treatment on lung DCs, I examined whether this treatment leads to a more efficient T cells priming by lung DCs. First, I studied the function of total lung CD11c positive cells. Allogeneic splenic T cells from C57BL/6 mice were stimulated for 3 days with lung CD11c positive cells from control Balb/c mice and from mice treated with LTK63 for 8 days. Allogeneic T cells co-cultured with CD11c$^+$ cells isolated from the lungs of LTK63 treated mice showed higher proliferation and Th1 cytokine production (Fig.3.2.13). Functionally, the mixed population of total CD11c$^+$ cells isolated from the lungs of LTK63 treated mice were more efficient than those from buffer-treated mice at stimulating allogeneic T cell responses.

3.2.9 Ability of CD11c$^+$MHC-II^{high} DCs and CD11c^{high}MHC-II^{int} sorted cells to activate allogenic T cells

Purified lung CD11c$^+$MHC-II^{high} DCs, but not CD11c^{high}MHC-II^{int} cells, were found capable of supporting a mixed leukocyte reaction [121,122]. I asked whether the previously observed enhanced ability of total lung CD11c$^+$ cells to induce T cell proliferation could be due to functional differences between control and LTK63 treated lung CD11c$^+$MHC-II^{high} DCs. The cells were stained with CD11c and MHC-II, and sort gates were set to isolate populations of R2 and R1 cells (see Fig. 3.2.14 A). FACS sorted CD11c$^+$MHC-II^{high} cells from lungs of 8 days LTK63 treated mice showed a higher allostimulatory activity than CD11c^{high}MHC-II^{int} cells obtained from the same mice. The number of CD11c^{high}MHC-II ^{high} cells from lungs of buffer-treated mice was extremely limited and mixed leukocyte reaction was carried out with concentrations of less stimulating cells. On a per cell basis, CD11c$^+$MHC-II^{high} DCs from LTK63 treated or control mice were similar in their ability to activate allogeneic T cells as shown in Fig 3.2.14 B,C. Thus, CD11c$^+$MHC-II^{high} cells from 8 days treated mice are expanded but functionally are the same as CD11c$^+$MHC-II^{high} cells from control mice.

Fig. 3.2.13 CD11c+ cells from LTK63 treated mice are more potent stimulators of

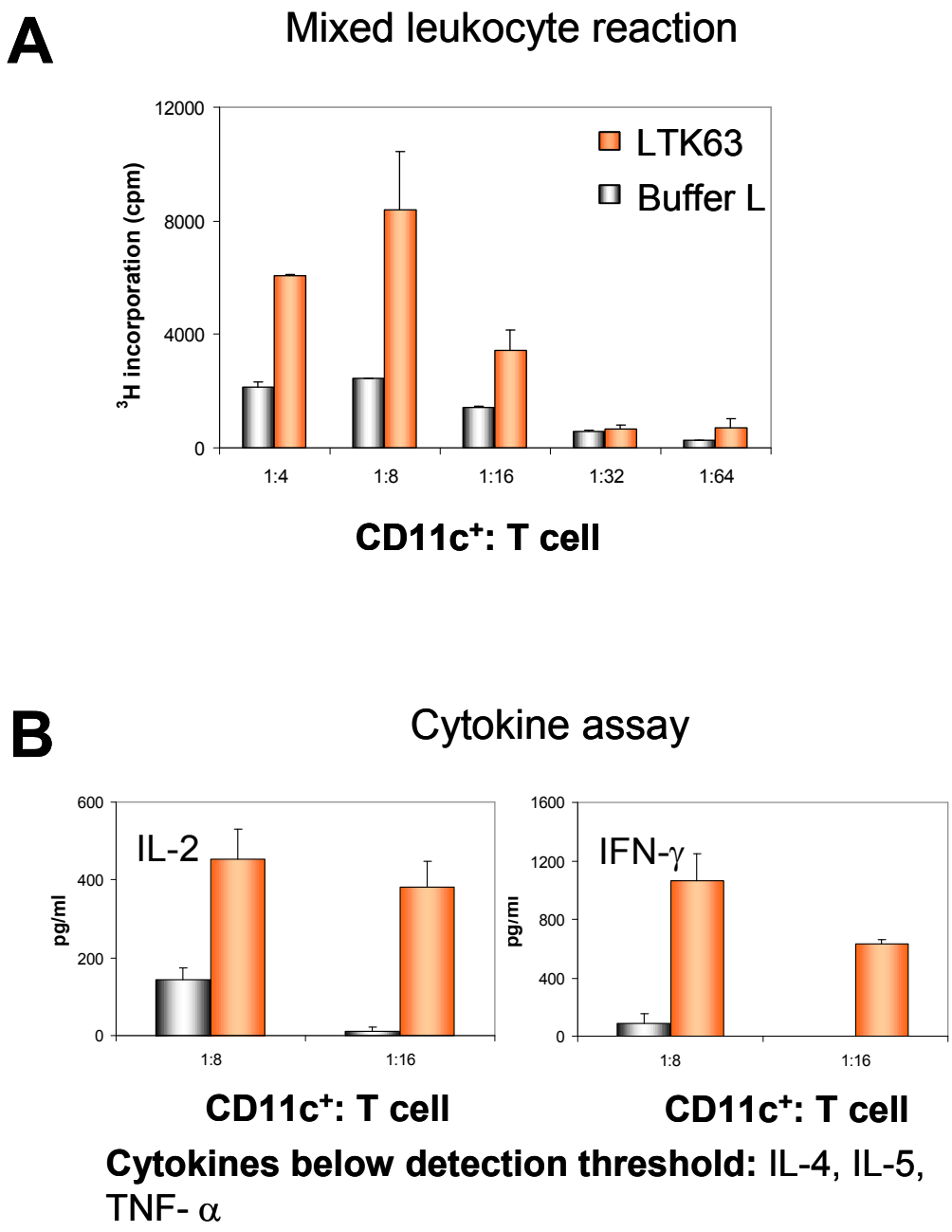

Fig. 3.2.13 CD11c$^+$ cells from treated mice are more potent stimulators of allogenic T cell proliferation than those from control mice. Mixed leukocyte reaction was carried out using as stimulator cells lung CD11c$^+$ cells isolated from pooled lungs of Balb/c mice treated 8 days with LTK63 or buffer L. Splenic allogeneic T cells (2 x 10^5/well) from C57BL/6 mice were stimulated for 3 days with various concentrations of lung CD11c$^+$ cells, and thymidine incorporation was measured during the last 18 hrs. The data shown in A are represented as the mean cpm of triplicate cultures ± SEM. Similar results were obtained in three separate experiments.
At 2 day co-culture supernatants were collected and assayed by MESOSCALE for Th1/Th2 cytokines (IFN-γ , IL-2. IL-4; IL-5 and TNF-α). In B graphs show the mean IFN-γ and IL-2 production and SEM of triplicate wells and results are representative of three experiments conducted in the same manner.

Fig. 3.2.14 Allogeneic T cell stimulation induced by R2 and R1 cells

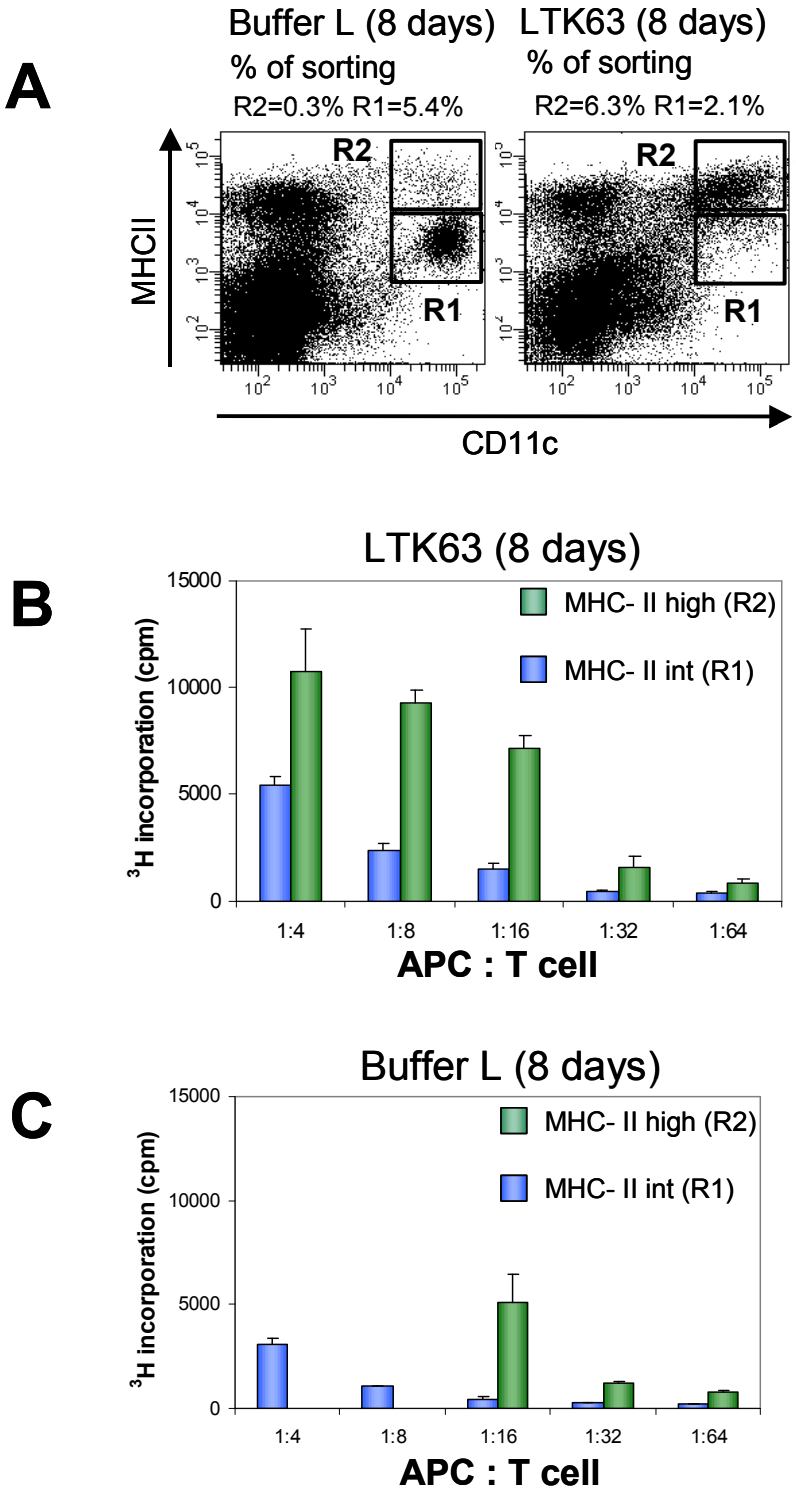

Fig. 3.2.14 Allostimulatory activity of $CD11c^{+}MHC\text{-}II^{high}$ and $CD11c^{high}MHC\text{-}II^{int}$ cells.
Cell sorting of enzymatically digested pooled lungs of 8 days LTK63 or buffer L treated mice (A). FACS sorted $CD11c^{+}MHC\text{-}II^{high}$ and $CD11c^{high}MHC\text{-}II^{int}$ cells from both groups of mice were used to stimulate allogeneic T cells from C57BL/6 mice for 3 days. Proliferation was measured by thymidine uptake during the last 18 hrs culture. Results are represented as the mean cpm of triplicate cultures ± SEM, as shown in B and C. Similar results were obtained in three separate experiments.

3.2.10 Kinetics of serum cytokines response to intrapulmonary LTK63 administration.

No systemic effect of intrapulmonary LTK63 administration was observed at cellular level in splenic DCs, T cells and NK cells (data not shown). I asked whether I could measure a systemic cytokine response to LTK63 in my experimental conditions. Therefore, I studied at the protein level serum cytokine and chemokine expression at various time intervals after LTK63 intrapulmonary administration. The production of multiple cytokines was determined in lung homogenates by ELISA based multiplex analysis. The level of IL-6 dramatically increased (315-fold) only at the 14 day time point, and at 16 days, it declined to baseline levels. IL-3, G-CSF peaked at 14 days (18 and 27 fold increase) and reached baseline level at 14 days. IL-10, IL-12(p40), MCP-1 and RANTES levels were slightly increased at 14 days and rapidly decreased to baseline. TNF-α peaked at 14 days (31 fold increase) and then gradually decreased; the same kinetic was observed for IL-1β and MIP-1β (Fig. 3.2.15).

Table 3.2.2 shows the summary of cytokine proteins tested, LTK63 induced cytokines with the time of peaking and their respective fold increase, unchanged cytokines and cytokines below detection threshold.) Thus, I observed a trend for a single and delayed peak at 14 days of IL-1β, IL-3, IL-6, IL-10, IL-12(p40), TNF-α, G-CSF, MCP-1, MIP-1β, RANTES levels in the lungs of LTK63 treated mice compared to control mice.

Fig. 3.2.15 LTK63 induce serum cytokines

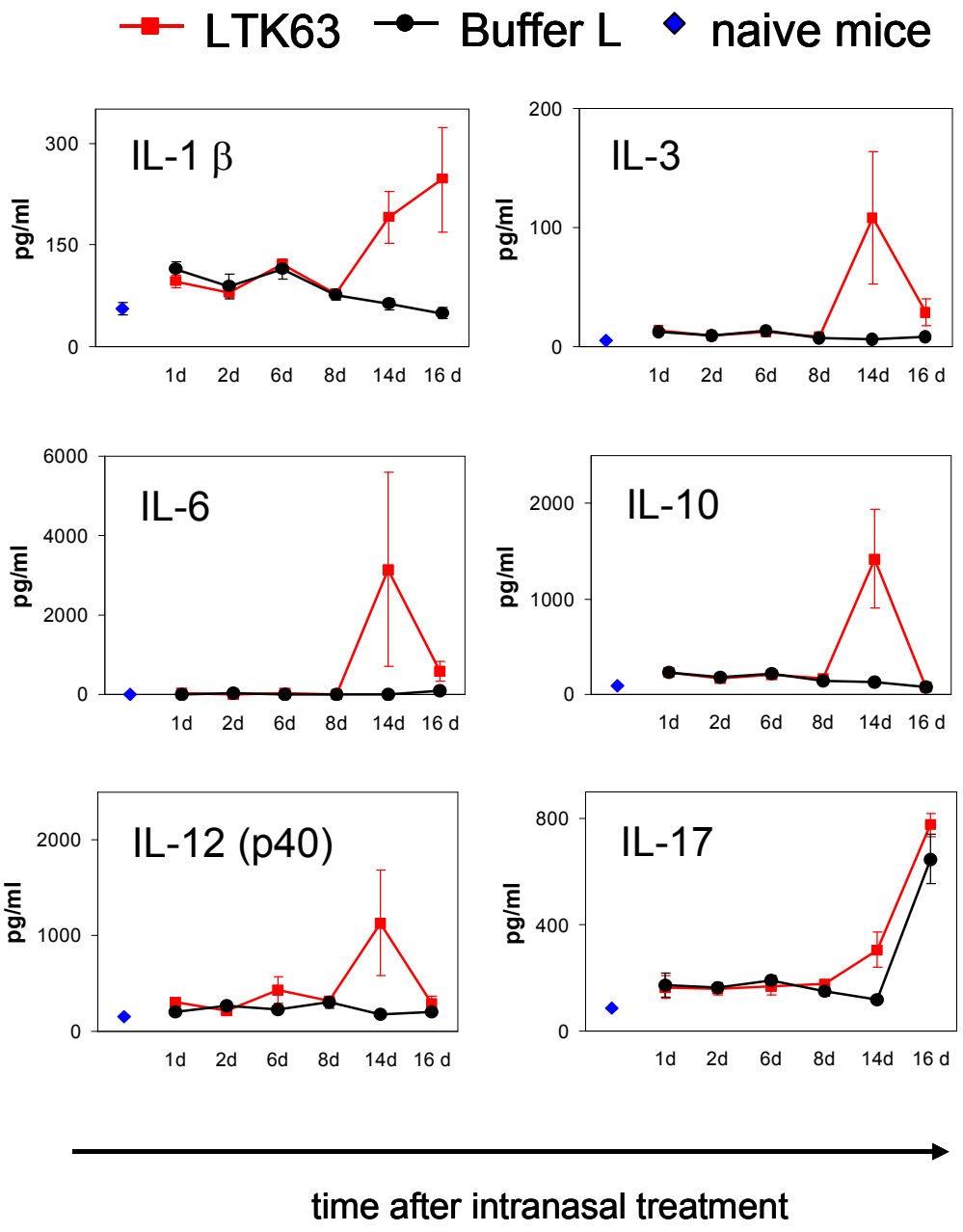

Fig. 3.2.15 Time course of cytokine production in serum of LTK63 treated and control mice (1 day-14 days) and in naïve BALB/c mice. Concentrations of indicated cytokines were determined by ELISA based multiplex analysis of lung homogenates. Results are represented as the mean (pg/ml) ± SEM. N = 5 /treatment group.

Fig. 3.2.16 LTK63 induce serum cytokines

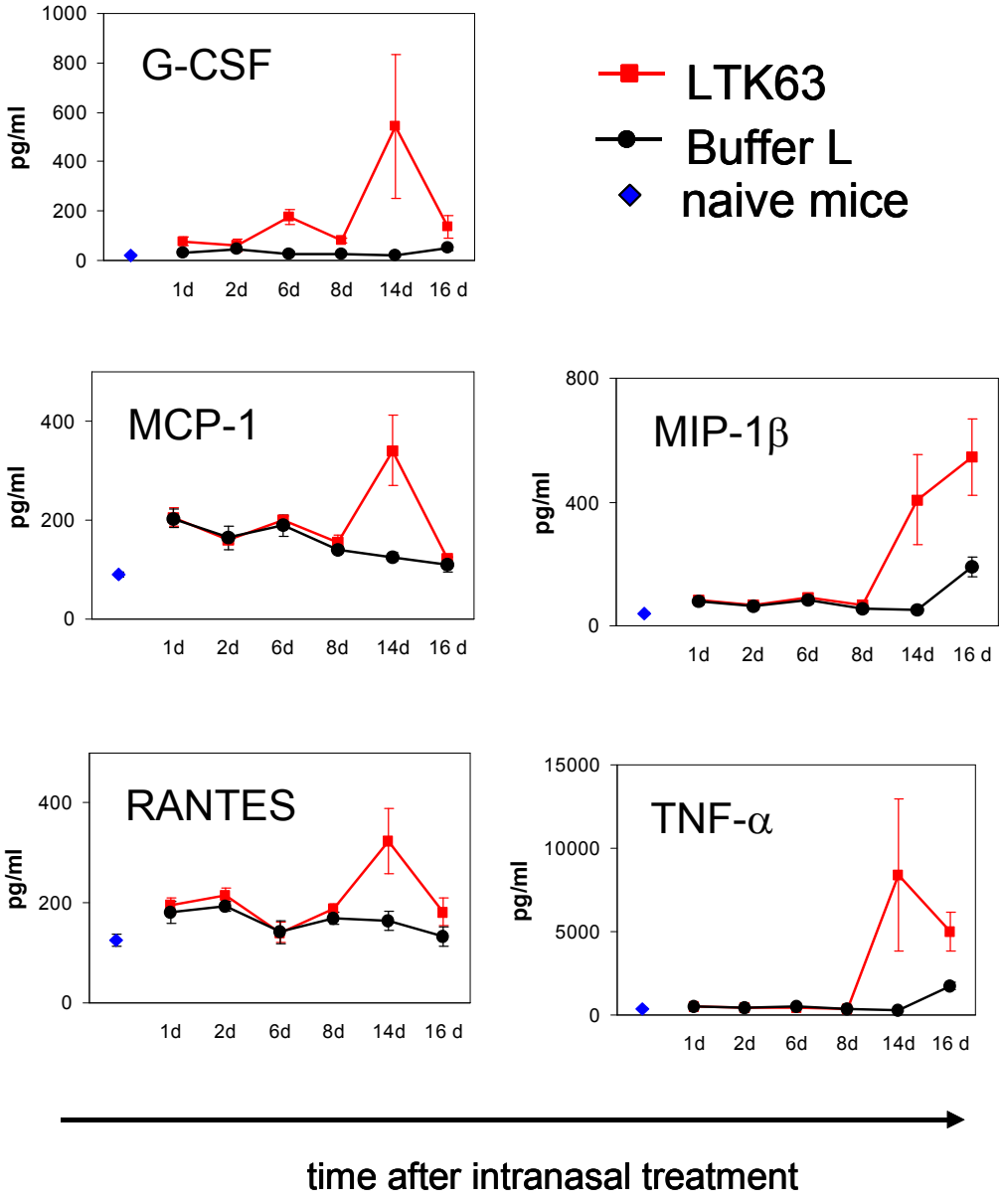

Fig. 3.2.16 Time course of cytokine production in serum of LTK63 treated and control mice (1 day-14 days) and in naïve BALB/c mice. Concentrations of indicated cytokines were determined by ELISA based multiplex analysis of lung homogenates. Results are represented as the mean (pg/ml) ± SEM. N = 5 /treatment group.

Table 3.2.2. Summary of serum cytokine proteins tested

summary of cytokine proteins tested (serum)						
peaked at 14 days fold increase	IL-3 (18)	IL-6 (315)	IL-10 (11)	IL12 p40 (6)	G-CSF (27)	MCP-1 (3)
peaked at 14 days fold increase	MIP-1β (8)	RANTES (2)	TNF-α (31)			
peaked at 16 days fold increase	IL-1β (5)					
unchanged	IL-1α	IL-2	IL-5	IL-9	IL12 p70	IL-13
unchanged	eotaxin	GM-CSF	IFN-γ	KC	MIP-1α	
below detection threshold	IL-4					

Table 3.2.2 Multiplex analysis of serum cytokine protein expression.
Summary of serum cytokine proteins tested: LTK63 induced cytokines with the time of peaking and their respective fold increase, unchanged cytokines and cytokines below detection threshold.

4. Discussion

4.1. CpG ODNs

CpG ODNs promote Th1 immune responses and have adjuvant activity in the induction of antigen-specific immune responses to co-administered antigens [123]. CpG ODNs were shown to be very potent adjuvants for inducing humoral and cellular responses to model antigens as ovalbumin and to infectious disease antigens such as the hepatitis B surface antigen (HbsAg) and influenza virus [68-70].

Mice vaccinated with protein antigens such as OVA or β-Gal had higher IgG antibody titers (mainly IgG2a), CTL and IFNγ production when CpG was co-administered as an adjuvant. Similarly, after intranasal vaccination of mice with inactivated influenza virus plus CpG, flu-specific antibody titers, including neutralizing antibodies in the sera, saliva and genital tract, increase. In addition to adjuvant activity, systemically administered CpG ODNs can induce nonspecific innate immune responses of a protective nature in a number of experimental infections [71-74].

However, the use of CpG ODNs at mucosal sites, in particular the lung, is less studied. CpG ODNs are effective as a mucosal vaccine adjuvant in mouse models of *Chlamydia trachomatis* pneumonitis and invasive pulmonary aspergillosis [77,78]. CpG ODNs induce protective immunity after pulmonary administration; reduce growth of *Mycobacterium tuberculosis* and the associated lung inflammation [83]; protect from *Cryptococcus neoformans* challenge in an IL-12-dependent manner [84] and induce protective immune responses against *Klebsiella pneumonia* [85].

In the present study, the immunological events induced by intrapulmonary CpG ODN administration in mice were investigated. Lung and serum were monitored from 3 hours to 14 days after intrapulmonary CpG ODN administration by combining different approaches: multiplex analysis of cytokine protein expression and flow cytometric analysis of immune cell populations. In addition, *in vitro* AM sensitivity to CpG ODNs was tested. After CpG ODN treatment, a rapid cytokine production, activation of pDCs, mDCs, CD4 T cells, CD8 T cells and NK cells and recruitment of DCs into the lung, were observed and are discussed in detail below.

4.1.1. Early cytokine response after intrapulmonary CpG ODN treatment

The earliest response detected after intrapulmonary CpG ODN administration is production of higher levels of cytokines in the lung. Higher levels of IL-1α, IL-1β, IL-6, IL-12 (p40) GCS-F, KC, MCP-1, MIP-1α, MIP-1β and RANTES, as assessed by multiplex analysis in lung homogenates, are released in the lung rapidly after treatment. CpG ODN treatment does not induce higher IFN-α production in the lung (data not shown), and this is in line with the fact that we use the B-class CpG ODN called 1826. In fact, B-class CpG ODNs are strong B cell stimulators and weaker inducers of IFN-α.

It is known that up regulation of cytokine and chemokine expression is induced directly in TLR-9 expressing cells by CpG ODN [118]. The following studies of TLR-9 expression in the lung help identify which may be the principal cells producing cytokines after CpG treatment. Constitutive expression levels of TLR9 have been detected in human and mouse lung endothelial cells and in the mouse macrophage cell line RAW264.7. [124]. Mouse AMs, obtained by whole lung lavage, show negligible expression of TLR9, although mouse peritoneal macrophages and bone-marrow derived macrophages have been shown to express TLR9 and be responsive to CpG [119]. TLR-9 is expressed in human airway epithelial cells [10] and strongly in mouse B cells [119]. Unlike human TLR9 [59,60], mouse TLR9 expression has been reported to be not restricted to pDCs [61]. Expression of TLR-9 in mouse lung mDCs and lung $CD11c^+$ was observed [119,125] but this is in conflict with one report demonstrating that TLR-9 is absent in lung draining LN mDCs and pDCs [125].

I hypothesized that AMs may be the primary cells responding to CpG ODNs, because they constitute the first line of defence in the alveolar space and Choudhury and coworkers demonstrated that CpG ODNs were internalized into the cytosolic compartment of AMs after intranasal administration [80]. AM responses to CpG ODNs were tested *in vitro,* and results showed that CpG ODNs stimulate AMs to release IL-6, IL-12 (p40), KC, MIP-1α, MIP-1β and RANTES. Inconsistent with these results, Suzuki and coworkers [119] reported that AMs do not respond releasing cytokines to CpG ODN. We are currently not able to explain this discrepancy. As our experimental protocol for isolation is similar to that of Suzuki et al but also includes an adhesion step, our cells should be if anything more enriched in AMs than theirs. Alternatively, the use of different CpGs may explain the difference, even though in both cases, B-type CpGs were used. Thus, IL-6, IL-12 (p40), KC, MIP-1α, MIP-1β and RANTES induced in the lung after intrapulmonary CpG ODN administration are likely produced by AM as suggested by our *in vitro* experiments.

However, the remaining cytokines IL-1α, IL-1β, G-CSF and MCP-1 are induced in the lung after CpG treatment and are not released by AM *in vitro,* and the question is which are the cells responsible for the production of these cytokines. Production of these cytokines by lung cells after CpG stimulation was not previously investigated, and these cytokines are not released by AM *in vitro*. It is known that AMs produce these cytokines after pathogen encounter, and this evidence suggests that *in vivo* AM could release also these cytokines after CpG treatment. Therefore, one possibility is that AMs *in vivo* produce more cytokines than those detected *in vitro;* alternatively other cells may be involved in production of these cytokines.

One approach to identify the possible source of cytokines after CpG intrapulmonary administration was to consider published studies where the cytokine production by lung cells after *in vitro* CpG stimulation was investigated. Human airway epithelial cells recognize CpG DNA by TLR-9, leading to NF-κB activation and production of IL-6, IL-8 and β2-defensin in the airways [10]. A previous report showed that after CpG ODN stimulation *in vitro,* lung DCs produce large amounts of cytokines, including IL-12 p40, IL-6 and TNF-α, whereas lung B cells secrete only IL-6 [119]. One plausible hypothesis is that increased levels of IL-8, IL-6 and IL-12 p40 observed after CpG ODN treatment are not released only by AMs. IL-8 could be released also by airway epithelial cells; IL-6 by airway epithelial cells, lung B cells and DCs and IL-12 p40 by DCs. Therefore, I conclude that the appearance of these cytokines is likely due mainly to AMs, with the contribution of other types of lung cells, which could lead to the inflammatory environment observed early in the lung after intrapulmonary CpG administration.

As we try to understand the sequence of events in the lung after CpG administration, an obvious issue is the effects of the cytokines induced by the treatment. A number of previous studies investigate the effects of cytokine production after different stimuli. IL-8 and G-CSF, produced by AMs, initiate a localized inflammatory response by recruiting neutrophils into the airway lumen in response to invading pathogens [2]. MCP-1 and RANTES produced by AMs recruit activated monocytes and lymphocytes into the lung[1] . Early release of MIP-1α, MIP-1β and RANTES is involved in attracting immature DCs and NK cells into the tissue after TLR activation of macrophages and DCs [126]. The production of IL-12p40 after Mycobacterium tuberculosis infection is associated with the ability of DCs to migrate to the lymph node and initiate T cell response [127].

One plausible hypothesis is that increased levels of cytokines induced by CpG treatment cause activation of pDCs, myeloid DCs (mDCs), CD4 T cells, CD8 T cells and NK cells, and the accumulation of DCs in the lung, which will be discussed further below.

Most but not all of the lung cytokines induced by CpG intrapulmonary administration are also found systemically in the serum. At early time points, higher levels of IL-6, IL-12 p40, IL-12 p70 GCS-F, KC, MCP-1, MIP-1β and RANTES were measured in serum by multiplex analysis.

Increased levels of cytokines such as IL-1α, IL-1β and MIP-1α are observed in the lung but not in serum. These results indicate that higher levels of IL-1α, IL-1β, MIP-1α, measured in the lung are not due to the presence of blood contaminations in lung homogenates. In addition, in serum from CpG treated mice a narrow peak of RANTES and MIP-1β is seen compared to the sustained production of both cytokines observed in the lung from the same mice. These and the other serum cytokines, which show increased cytokine levels at later time points in serum compared to their appearance in the organ, are all possibly due to spill over from the lung. While we cannot conclusively exclude that the appearance of these cytokines are due to a systemic effect of CpG ODN intrapulmonary administration, it is plausible that lung-produced cytokines are found also in serum, since cytokines work through a gradient from the tissue towards the blood vessels and into the blood.

4.1.2. Immune cell activation after intrapulmonary CpG ODN administration

As mentioned before, in our experimental system, intrapulmonary administration of CpG ODN induces activation of pDCs, myeloid DCs (mDCs), CD4 T cells, CD8 T cells and NK cells as well as DC recruitment into the lung.

We found that CpG ODN treatment rapidly activates *in vivo* lung mDCs as assessed by the percentage of cells expressing CD86 and CD80 at high levels (12h-4d). The question here is if this is a direct or indirect effect of the treatment. As mentioned above, mouse lung mDCs express TLR9, and Suzuki and coworkers demonstrated that *in vitro* stimulation with CpG ODN enhances the expression of CD80, CD86 and CD40 on mouse lung mDCs [119,125]. Therefore, we suggest that also after intrapulmonary administration *in vivo*, CpG ODN directly activate mDCs, most likely through TLR9 recognition, inducing the increased expression of costimulatory molecules and also the production of cytokines.

We also observed that early after intrapulmonary CpG administration, lung pDCs are activated as determined by expression at high levels on cell surface of the costimulatory molecules CD86, CD80, CD40 and MHC-II (1d-4d).

TLR9 expression on mouse lung pDCs was not previously investigated although mouse pDCs have been shown to express TLR9 like human pDCs. In humans, pDCs strongly express TLR9 and it is clearly demonstrated that they are directly activated by CpG ODN, which induce in these cells increased expression of co-stimulatory molecules, secretion of Th1 promoting cytokines and chemokines, upregulation of the chemokine receptor CCR7, and resistance to apoptosis [118]. Since pDCs from other mouse organs have been show to be directly activated by CpG ODNs [128,129], I conclude that, as suggested for lung mDCs, most likely also lung pDCs express TLR9 and are directly activated by CpG ODNs.

Moreover, we found that CpG ODNs induce the accumulation of both mature mDCs and pDCs at 4 days and 2 days after the treatment, respectively. Several possibilities exist that might explain the observed accumulation of lung DCs. The increased number of MHC-II^{high} mDCs observed 4 days after CpG treatment could be due to MHC-II up-regulation on resident immature DCs, or on recruited differentiated DCs or, alternatively, on DCs derived from newly recruited monocytes or DC progenitors, from resident intrapulmonary DC progenitors or from transdifferentiation of pulmonary macrophages into DCs [26] . Among these hypotheses, it is likely that MHC-II^{high} mDCs accumulation is driven by the chemokine production induced in the lung after CpG treatment. As introduced before, MIP-1α, MIP-1β and RANTES attract immature DCs into the lung, and MCP-1 drives monocyte recruitment. Therefore, mDC and pDC accumulation may be driven by recruitment in response to the sustained production of MCP-1 MIP-1α, MIP-1β and RANTES in the lung after intrapulmonary CpG administration. However, up-regulation of MHC-II is a consequence of activation, and sice I have observed mDC activation by CpG, part of the numerical increase of CD11c^{+}MHC-II^{high} mDCs will be due to activation and subsequent upregulation of MHC-II on the immature mDCs present in the CD11c^{+}MHC-II^{low} population.

Another observation was that 1-4days after CpG treatment, lung CD8+ and CD4+ T cell subsets are activated as determined by cell surface expression of the activation markers CD69 and CD44. The mechanism by which CpG ODNs induce T cell activation is unclear. CpG ODNs have not been reported to have direct stimulatory effects on T cells [118]. One plausibile hypotesis is that CpG ODNs induce in an indirect way T cell activation through up-regulation of lung inflammatory cytokines. The activation marker upregulation on

CD8+ and CD4+ T cells, which is independent of specific T-cell-receptor (TCR) stimulation, could be mediated by this bystander mechanism, as described previously [130]. Further research, using T cells isolated from lung of naïve mice and stimulated in vitro with the cytokines induced *in vivo* by CpG ODN treatment, will demonstrate whether the cytokine cocktail induced in our experimental conditions is able to activate T cells directly. In conclusion, we favour the hypothesis that intrapulmonary administration of CpG ODNs activates lung CD8+ and CD4+ T cells through a bystander mechanism.

Lung NK cells are also activated after CpG treatment (1-4d), as determined by activation marker upregulation. This led to the question how NK cells are activated by CpG ODN. It has not been reported that CpG ODN have a direct effect on NK cells [118]. The same type of research, previously described to investigate whether cytokine induced *in vivo* by CpG mediate T cell activation, will help to explain how CpG ODNs activate NK cells. As hypothesized for T cells, the NK cell activation is likely mediated by cytokines induced after CpG ODN treatment or by other soluble factors.

4.1.3. Adjuvant role

CpG ODNs act through a well-defined molecular pathway, and our results suggest that after intrapulmonary administration, CpG ODNs directly activate lung DCs, both mDCs and pDCs, as assessed by expression of costimulatory molecules, and activate AMs, as measured by cytokine release after *in vitro* CpG treatment. The molecular and cellular events observed in the lung after CpG ODN administration are similar to that observed for other adjuvants that interact with Toll-like receptors such as imiquimod [131,132]. The adjuvant activity of CpG ODN after intrapulmonary administration could be explained by several effects of the treatment, previously discussed, on lung innate immunity. The results indicate that administration of CpG ODNs improve antigen presentation in the lung causing up-regulation of costimulatory molecules and MHC-II molecules on lung DCs. CpG ODNs enhance innate immunity in the lung eliciting local production of chemokines. CpG ODN induce inflammatory cytokines, likely secreted by lung DCs and Ams directly activated by CpG ODN, which in turn can induce effector functions of T and NK cells.

These observations indicate that the activation of DCs and AMs in the lung is a key event for the enhancement of innate immunity and for the development of antigen-specific adaptive immunity when CpG ODN are co-administered with an antigen.

4.1.4. Generic protection

Studies in mice have demonstrated that the immune defences activated by CpG ODN, given by different ways of administration, can protect against a wide range of viral, bacterial and even some parasitic pathogens. In particular, it was reported that intra-pulmonary CpG ODN administration induces protective immune responses for *Mycobacterium tuberculosis*, *Cryptococcus neoformans*, and *Klebsiella pneumonia* [83-85]. Little is known about the mechanisms of protection at mucosal surfaces, particulary in the lung.

The results obtained by this study help to explain how CpG ODNs induce protective immunity after intrapulmonary administration. Protection elicited by CpG ODN could be explained by several mechanisms: improvement of antigen presentation by activated DCs, both mDCs and pDCs; induction of inflammatory cytokines which are likely involved in T and NK cell activation; up-regulation of chemokines responsible for recruitment of innate immune cell which are the first defense line against the pathogen, and effector responses of T and NK cells. Our observations indicate that CpG ODNs induce in the lung an early robust innate immune response that increases host defence to pathogens while facilitating the development of antigen-specific adaptive immunity and cellular effector response.

4.2. LTK63

Several reports show that LTK63 is strongly immunogenic [92], and the most intensely studied type of immune response to LTK63 is the antibody response.

Many studies report the use of LTK63 as an adjuvant in different animal models. For example, coadministration of LTK63 with candidate vaccines via the respiratory tract improves the efficacy of the group C meningococcal conjugate vaccine [109] and enhances immunity to SAG1 Ag of *Toxoplasma gondii* [101]. Recently, LTK63 has been tested as mucosal adjuvant for an intranasal influenza vaccine in a phase I clinical trial, demonstrating a good safety profile and mucosal adjuvanticity in humans [105].

In addition to that, intranasal LTK63 administration induces generic protection from respiratory syncytial virus (RSV), influenza virus, or Cryptococcus neoformans challenge performed two weeks after the treatment [113].

Thus, it is clear that LTK63 is immunogenic and functions efficiently as adjuvant, but the mechanism of action in both adjuvanticity and in generic protection is largely unknown.

In the present study, *ex vivo* molecular and cellular events associated with intrapulmonary LTK63 administration in the whole mouse lung were investigated. Lungs were monitored from 12 hours to 14 days by combining different approaches: flow cytometric analysis of lung cell populations, multiplex analysis of cytokine and chemokine protein expression in the lung and serum, and at 8 days after the treatment, DC recruitment was studied by *in vivo* migration assays and DC function by MLR. In the course of this study, two phases of activation after LTK63 treatment, as outlined below, were identifie

4.2.1. Early phase of LTK63 response

During the first phase, which extends from 1 to 2 days after intrapulmonary LTK63 administration, cytokines were found up-regulated, and granulocyte and mDC accumulation in the lung was observed. This led to the question which could be the direct target cells of LTK63, and which cells are the possible source of the cytokines detected.

One day after intrapulmonary administration, LTK63 induces local release of G-CSF, KC (the functional homologue of human IL-8) and IL-1β as measured in lung homogenates.

The earliest detectable cellular response to intrapulmonary LTK63 treatment is the accumulation of granulocytes and myeloid lung DCs at 2 days. Moreover, LTK63 induces 2 days after administration a slight increase of T cell numbers, which may be an early

antigen-independent recruitment. AM isolated by BAL are not activated to release cytokines after *in vitro* LTK63 treatment (data not shown). At early time points, lung DCs are not activated after *in vivo* LTK63 treatment. A previous report showed that intrapulmonary LTK63 administration for 2 days does not induce activation of B cells and interstitial macrophages as assessed by the expression of activation markers [113]. In previous reports *in vitro,* the effect of LTK63 in several mouse and human systems was tested: LTK63 did not elicit detectable activation on DCs, macrophages and B lymphoma cells [113].
In order to determine by which cells in the lung these cytokines may be produced the following publications were considered.
After infectious and inflammatory stimuli, airway epithelial cells produce IL-1β, IL-6, IL-8, RANTES, GM-CSF, and TGF-β, in addition to other proinflammatory cytokines [8]. Engagement of pattern recognition receptors stimulates epithelial cells to produce CXC and CC chemokines and enhances the production of antimicrobial defensins [1,9]. For example, airway epithelial cells recognize unmethylated bacterial DNA and produce IL-6, IL-8 and β2-defensin [1,10]. In response to invading pathogens, alveolar macrophages produce proinflammatory cytokines, notably IL-8 and G-CSF [2]. AMs also have an important role in producing CC chemokines, and IL-1 alone can be used as a mucosal adjuvant.
A further approach to identify the possible source of these cytokines was the comparison of the LTK63 induced cytokines with cytokines described after different stimuli.
The first consideration is that alveolar macrophages produce IL-8 and G-CSF after invading pathogen encounter, but *in vitro* LTK63 does not activate these cells, and therefore, it is likely that AMs do not release these cytokines *in vivo* after LTK63 treatment.
The second consideration is that epithelial cells produce IL-8 and IL-1β after stimulation as above reported, and it is plausible that LTK63 recognition by epithelial cells leads to secretion of G-CSF, KC and IL-1β. Further research with mouse epithelial cell lines will be needed to elucidate whether epithelial cells express recognition receptors for LTK63 and which cytokines are produced by these cells after the stimulation.
Which is the effect of the cytokines induced by LTK63? After stimulation as described above, chemokines produced by epithelial cells or alveolar macrophages initiate a localized inflammatory response by recruiting neutrophils into the airway lumen [1]. In line with the known effect of cytokines induced by LTK63, granulocyte accumulation in the lung was observed.

G-CSF and KC induction in the lung after 1 day of treatment likely induce the recruitment of granulocytes observed at 2 days after LTK63 administration. The increased number of MHC-II^{high} mDCs observed 2 days after the treatment could be due to MHC-II up-regulation on resident immature DCs, or on recruited differentiated DCs or on DCs derived from newly recruited monocyte. Future work using chemotaxis assay will help to determine the chemotactic capacity of LTK63 induced cytokines to attract freshly isolated lung DCs, and transfer of DCs *in vivo* to elucidate how the number of MHC-II^{high} mDCs increases 2 days after LTK63 administration. In addition, the use of labeled monocytes in *in vivo* migration assays will directly demonstrate whether monocytes differentiate into DCs with a MHC-II^{high} phenotype.
In addition, one possibilty is that a response is induced in the lung earlier than the first time point of observation, namely 12 hours post LTK63 application.

4.2.2. Late phase of LTK63 response

As introduced before, the LTK63 response develops in two phases. The second phase, which is observed at 6-8 days after the treatment, is characterized as follows.
mDCs and pDCs accumulate after 6-8 days of LTK63 treatment in the lung. DC subsets were identified by phenotypic analysis as shown in Fig. 3.2.2. At the same time points, CD8+ and CD4+ T cell, granulocyte, NK cell and B cell numbers increase. LTK63 treatment induces in the lung the release of several cytokines: IL-1α, IL-1β, IL-12(p40), G-CSF, KC, MIP-1α, MIP-1β and RANTES . In order to understand which cells are a possible source of these cytokines, total lung CD11c$^+$ cells were isolated from lungs of 8 days treated and untreated mice to evaluate the *ex vivo* cytokine release by these cells.
CD11c$^+$ cells isolated from lungs 8 days after LTK63 treatment secrete *ex vivo* higher levels of IL-12, IL-1α, IL-10, IL-6 and MCP-1 compared with the same cells from control mice. This experiment suggests that the IL-12 and IL-1α induced by LTK63 treatment *in vivo* in the lung are produced by CD11c$^+$ cells. In contrast, IL-10, IL-6 and MCP-1 are produced at higher levels by CD11c$^+$ cells *ex vivo*, but no increased levels of these cytokines were observed in lung homogenates, likely because there is a rapid uptake of these cytokines by target cells and/or these cytokine levels are below detection limit. Increased levels of several other cytokines were found in lung homogenates and are not produced by CD11c$^+$, and the question is which are the cells responsible of their production. G-CSF, KC and IL-1β which are not produced at higher levels by CD11c$^+$

cells, were shown to be released by macrophages and epithelial cells early after pathogen encounter, as mentioned above, but there are no indications in the literature about which cells are responsible of the production of these cytokines in the late phase of the response to LTK63. One possibility is that G-CSF, KC and IL-1β are released by epithelial cells, as suggested above for the early phase of LTK63 response. MIP-1α, MIP-1β and RANTES are not produced at higher levels by $CD11c^+$ cells *ex vivo* in our experimental system. While it is published that these chemokines can be released by resident tissue DCs and macrophages after TLR activation, the time course of release observed in response to TLR agonists differs greatly from that seen in our experiments [126]. Therefore, I conclude that it is unlikely that the appearance of these cytokines is due to direct activation of DCs or macrophages.

A time course that resembles more closely the kinetics we find with LTK63 is the release of these cytokines by activated lymphocytes during secondary immune responses [126]. It is possible that MIP-1α, MIP-1β and RANTES are produced by activated lymphocytes since this chemokine release is not an early event and because at 6-8 days after LTK63 treatment, lung CD8+ and CD4+ T cell subsets are activated as assessed by CD69 expression. Lymphocytes probably were activated early in response to LTK63, and at 6-8 days after the treatment they are recruited to the lung.

Cytokine production induced late after intrapulmonary LTK63 administration is likely due mainly to $CD11c^+$ cells, activated lymphocytes and epithelial cells. Which is the role of this cytokines in the late response to LTK63?

The production of IL-12p40 by DCs is associated with activation of these cells, the ability to migrate to the lymph node and to initiate T cell response [127]. As mentioned for the early phase of lung LTK63 response, higher levels of G-CSF, KC and IL-1β induce granulocyte recruitment. MIP-1α, MIP-1β and RANTES recruit innate and adaptive immune cells into sites of inflammation [126].

One plausible hypothesis is that increased levels of cytokines induced by LTK63 lead to the recruitment of leukocytes and DC activation observed at 6-8 days in the lung, as discussed below.

LTK63 treatment induce both mDC and pDC accumulation. Several possibilities exist that might explain the observed expansion of lung DCs. Even in the absence of inflammation, DCs or their precursors are constantly recruited from the blood into the lung, where resident populations are renewed. Holt and coworkers were the first to demonstrate that respiratory tract DCs are continuosly replenished [25]. Inflammatory stimuli have a profound

impact on these steady state dynamics through different mechanisms: chemokine-driven recruitment of differentiated DCs from the circulation; recruitment of DC precursors, which then differentiate into DCs after exposure to local cytokines, and, albeit less documented, proliferation of intrapulmonary DC progenitors and transdifferentiation of pulmonary macrophages into DCs [26]. In addition, pDCs may differentiate into mDCs as observed upon virus stimulation [133]. Among these hypothesis, I was not able to test all, but I could investigate the effect of LTK63 on recruitment of differentiated mDCs using an *in vivo* migration assay and $CFSE^+$BM-DCs as a model of a mixed population of mature and immature DCs. Increased numbers of CFSE labeled BM-DCs migrate to the lung of mice 8 days after LTK63 treatment, compared to steady state migration observed in control mice, but the number of recruited cells is low compared to 25-fold increase of mDCs observed at 8 days after *in vivo* treatment. One possibility to explain this discrepancy is that the migration assay does not reproduce exactly *in vivo* conditions, likely also due to the slightly different nature of BM-DCs compared to mDCs in vivo; or other mechanisms, for example pDC or macrophage differentiation into mDCs, might contribute to the profound increase of the absolute number of lung mDCs after *in vivo* treatment. Further research using monocyte migration assays, generation of DCs by total lung cells isolated from control and LTK63 treated mice, and macrophage and pDC depletion experiments will help to explain mDC accumulation at 6-8 days after LTK63 administration. Several technical problems are associated with these experiments; for example the known difficulty in identifying macrophages and DCs. Therefore, I conclude that late lung mDC accumulation is in part due to differentiated DC recruitment as suggested by previous described experiments and that likely the recruitment is driven by increased MIP-1α, MIP-1β and RANTES production observed in lung homogenates at these time points.

Both DC subsets, identified as shown in Fig.3.2.2 (A), accumulate 6-8 days after LTK63 treatment and some of these are activated as assessed by the percentage of cells expressing CD86 at high levels. A higher percentage of DCs in LTK63 treated mice express CD86, known to be expressed on mature DCs and to enhance T cell costimulation. The percentage of DCs expressing CD80 was similar to that in control mice.

In order to see how LTK63 improves the immune response, the question was if DCs are not only increased in number but also more potent stimulators of allogenic T cells. Functionally, the mixed population of total $CD11c^+$ cells isolated from the lungs of 8 days LTK63 treated mice are more efficient than those from buffer-treated mice at stimulating allogeneic T cell responses. The mixed $CD11c^+$ cell population includes pDCs, which are

activated and expanded 8 days after the treatment. In contrast to the tolerogenic function of immature pDCs in baseline conditions, activated pDCs increase their T cell stimulatory ability, although less efficiently than mDCs, and become immunostimulatory cells [134].
Purified lung $CD11c^{+}MHC\text{-}II^{high}$ cells, defined as mDCs and called R2 cells in Fig. 3.2.2, but not $CD11c^{high}MHC\text{-}II^{int}$ cells, defined as a mixed population of AM and immature DCs and identified as R1 cells in Fig. 3.2.2 (A), were found capable of supporting a mixed leukocyte reaction [121,122]. In order to investigate functional differences between LTK63 treated and control mDCs, MLR experiments were done with cells sorted by FACS.
$CD11c^{+}MHC\text{-}II^{high}$ mDCs isolated from lungs of 8 days LTK63 treated mice show a profound numerical increase but functionally are as capable as cells from control mice. On a per cell basis, these cells are functionally equal, but the numerical increase of the $CD11c^{+}MHC\text{-}II^{high}$ mDC subset in the lungs of treated mice translates into an overall greater potential for T cell activation. In addition, it is likely that activated pDCs supply help for T cell stimulation.

4.2.3. LTK63 specific adaptive immune response

One plausible hypothesis is that CD4+ and CD8+ T cells recruited to the lung are derived from the lymphoid compartment and have proliferated in response to LTK63. Recently, my group demonstrated that T cells are required for recruitment of innate and adaptive immune cells seen 8 days after LTK63 treatment in the lung as assessed by comparative analysis of BAL cellular composition at 8 days in Fox Chase CB-17 SCID mice, Fox Chase CB-17 wild type mice, BALB/c nude mice and BALB/c wild type mice [135]. T cell re-homing to the lung is probably antigen (LTK63) driven, and recruited activated T cells are the key cells for localization and amplification of the immune response by releasing chemokines to recruit innate and adaptive immune cells. DCs are known to be the primary cells responsible for activating naïve T and B cells, and it is likely that in low respiratory tract draining LN, LTK63 specific T and B cell responses are induced by DCs. After proliferation and differentiation, activated naïve T cells leave the LN and become effector or memory T cells within 4 days. Moreover, activated T cells move towards the germinal centres where B cells are located to induce maturation of antigen-specific immunoglobulin secreting B cells. Effector T cells recirculated to the lungs as cytokine-producing effector T cells and memory T cells recirculate to non-draining lymph nodes and the spleen. Lung DCs prime T cell and B cell responses not only by providing antigenic and costimulatory

signals to lymphocytes but also by imprinting in them the ability to home back into the lung and perhaps to other mucosal sites by upregulating chemokine and homing receptors [4,11].

It is likely that the increased number of immunostimulatory mDCs and pDCs 8 days after LTK63 treatment is important for stimulation of recruited effector T cells, which in contrast to naïve T cells can be stimulated by local airway DCs, and can mediate effector functions.

It was shown that intra-pulmonary administration of LTK63 modulates the pathology caused by a subsequent (two weeks after the treatment) and completely un-related respiratory pathogen, such as respiratory syncitial virus (RSV), Influenza virus or *Cryptococcus neoformans*. Heterologous protection elicited by LTK63 can be explained by lung immune modulation induced 6-8 days after the treatment. We can hypothesize that LTK63 provides heterologous protection to pathogen challenge by multiple mechanisms: increased number of activated lung DCs which could efficiently present pathogen antigens; induction of inflammatory lung environment and up-regulation of chemokines which are a chemotactic stimulus for innate and adaptive cells that might be involved in the first defence against the pathogen and induction of adaptive immunity; bystander T cell activation and cross reactivity of memory T cells. In addition, another event that might contribute to pathogen killing is the presence at 14 days in the BAL of a relatively large number of B cells, described recently by my group, that might produce cross-reactive Abs.

It was described that, similarly to LTK63 treatment, previous mouse respiratory infection with influenza or choriomeningitis virus can confer heterologous protection against secondary infection caused by unrelated virus such RSV and vaccinia virus [114,115]. Late accumulation of activated T cells induced by LTK63 is similar to T cell recruitment described during influenza infection in previous reports [136,137]. These observations suggest that LTK63 might induce heterologous immunity by mimicking an airway infection. Moreover, increase in CD11c+ cells observed 6-8 days after LTK63 treatment is similar to CD11c+ cell increase observed in the lung concomitant with the resolution phase of viral respiratory infection [138,139].

These observations indicate that LTK63 induces an local immune response, which is too slow to consist merely of an innate component. It is presumed that at early stages, lung DCs are responsible for LTK63 presentation to T cells in low respiratory tract draining LN, bridging the gap between early events and late events observed in the lung after intrapulmonary treatment. It is very likely that cellular events observed in the lung 6-8

days after LTK63 administration are due in part to LTK63 specific immune responses, and that effector T cells are the main force driving the recruitment of innate and adaptive immune cells in the lung. Clearly, the mechanism of action of LTK63 differs from many other adjuvants that interact with Toll-like receptors or other pattern recognition receptors and from adjuvant common action model. Although LTK63 is an adjuvant, LTK63 is also a large and complex protein antigen; thus, a unique combination of antigen and adjuvant. It is presumed that early events previously discussed explain in which local inflammatory environment LTK63 is recognized as an antigen and could work as an adjuvant when co-administered with an antigen.

5. References

1. Martin TR, Frevert CW. Innate immunity in the lungs. Proc Am Thorac Soc. 2005;2:403-411.

2. Zhang P, Summer WR, Bagby GJ, Nelson S. Innate immunity and pulmonary host defense. Immunol Rev. 2000;173:39-51.

3. Lehrer RI. Primate defensins. Nat Rev Microbiol. 2004;2:727-738.

4. Iwasaki A. Mucosal dendritic cells. Annu Rev Immunol. 2007;25:381-418.

5. Sibille Y, Reynolds HY. Macrophages and polymorphonuclear neutrophils in lung defense and injury. Am Rev Respir Dis. 1990;141:471-501.

6. Reynolds HY. Immunologic system in the respiratory tract. Physiol Rev. 1991;71:1117-1133.

7. Underhill DM, Ozinsky A, Hajjar AM, et al. The Toll-like receptor 2 is recruited to macrophage phagosomes and discriminates between pathogens. Nature. 1999;401:811-815.

8. Diamond G, Legarda D, Ryan LK. The innate immune response of the respiratory epithelium. Immunol Rev. 2000;173:27-38.

9. Becker MN, Diamond G, Verghese MW, Randell SH. CD14-dependent lipopolysaccharide-induced beta-defensin-2 expression in human tracheobronchial epithelium. J Biol Chem. 2000;275:29731-29736.

10. Platz J, Beisswenger C, Dalpke A, et al. Microbial DNA induces a host defense reaction of human respiratory epithelial cells. J Immunol. 2004;173:1219-1223.

11. Lefrancois L, Puddington L. Intestinal and pulmonary mucosal T cells: local heroes fight to maintain the status quo. Annu Rev Immunol. 2006;24:681-704.

12. Mellman I, Steinman RM. Dendritic cells: specialized and regulated antigen processing machines. Cell. 2001;106:255-258.

13. Bender A, Albert M, Reddy A, et al. The distinctive features of influenza virus infection of dendritic cells. Immunobiology. 1998;198:552-567.

14. Feng H, Zhang D, Palliser D, et al. Listeria-infected myeloid dendritic cells produce IFN-beta, priming T cell activation. J Immunol. 2005;175:421-432.

15. Gerna G, Percivalle E, Lilleri D, et al. Dendritic-cell infection by human cytomegalovirus is restricted to strains carrying functional UL131-128 genes and mediates efficient viral antigen presentation to CD8+ T cells. J Gen Virol. 2005;86:275-284.

16. Lambrecht BN, Pauwels RA, Fazekas De St Groth B. Induction of rapid T cell activation, division, and recirculation by intratracheal injection of dendritic cells in a TCR transgenic model. J Immunol. 2000;164:2937-2946.

17. van Rijt LS, Jung S, Kleinjan A, et al. In vivo depletion of lung CD11c+ dendritic cells during allergen challenge abrogates the characteristic features of asthma. J Exp Med. 2005;201:981-991.

18. Lambrecht BN, Salomon B, Klatzmann D, Pauwels RA. Dendritic cells are required for the development of chronic eosinophilic airway inflammation in response to inhaled antigen in sensitized mice. J Immunol. 1998;160:4090-4097.

19. Bellini A, Vittori E, Marini M, Ackerman V, Mattoli S. Intraepithelial dendritic cells and selective activation of Th2-like lymphocytes in patients with atopic asthma. Chest. 1993;103:997-1005.

20. van den Heuvel MM, Vanhee DD, Postmus PE, Hoefsmit EC, Beelen RH. Functional and phenotypic differences of monocyte-derived dendritic cells from allergic and nonallergic patients. J Allergy Clin Immunol. 1998;101:90-95.

21. Probst HC, Tschannen K, Odermatt B, Schwendener R, Zinkernagel RM, Van Den Broek M. Histological analysis of CD11c-DTR/GFP mice after in vivo depletion of dendritic cells. Clin Exp Immunol. 2005;141:398-404.

22. Miller MJ, Wei SH, Parker I, Cahalan MD. Two-photon imaging of lymphocyte motility and antigen response in intact lymph node. Science. 2002;296:1869-1873.

23. Bousso P, Robey E. Dynamics of CD8+ T cell priming by dendritic cells in intact lymph nodes. Nat Immunol. 2003;4:579-585.

24. Sumen C, Mempel TR, Mazo IB, von Andrian UH. Intravital microscopy: visualizing immunity in context. Immunity. 2004;21:315-329.

25. Holt PG, Haining S, Nelson DJ, Sedgwick JD. Origin and steady-state turnover of class II MHC-bearing dendritic cells in the epithelium of the conducting airways. J Immunol. 1994;153:256-261.

26. Vermaelen K, Pauwels R. Pulmonary dendritic cells. Am J Respir Crit Care Med. 2005;172:530-551.

27. McWilliam AS, Nelson D, Thomas JA, Holt PG. Rapid dendritic cell recruitment is a hallmark of the acute inflammatory response at mucosal surfaces. J Exp Med. 1994;179:1331-1336.

28. Stumbles PA, Thomas JA, Pimm CL, et al. Resting respiratory tract dendritic cells preferentially stimulate T helper cell type 2 (Th2) responses and require obligatory cytokine signals for induction of Th1 immunity. J Exp Med. 1998;188:2019-2031.

29. Vermaelen KY, Carro-Muino I, Lambrecht BN, Pauwels RA. Specific migratory dendritic cells rapidly transport antigen from the airways to the thoracic lymph nodes. J Exp Med. 2001;193:51-60.

30. Hammad H, de Heer HJ, Soullie T, Hoogsteden HC, Trottein F, Lambrecht BN. Prostaglandin D2 inhibits airway dendritic cell migration and function in steady state conditions by selective activation of the D prostanoid receptor 1. J Immunol. 2003;171:3936-3940.

31. Legge KL, Braciale TJ. Accelerated migration of respiratory dendritic cells to the regional lymph nodes is limited to the early phase of pulmonary infection. Immunity. 2003;18:265-277.

32. Lawrence CW, Braciale TJ. Activation, differentiation, and migration of naive virus-specific CD8+ T cells during pulmonary influenza virus infection. J Immunol. 2004;173:1209-1218.

33. Medzhitov R, Janeway CA, Jr. Innate immune induction of the adaptive immune response. Cold Spring Harb Symp Quant Biol. 1999;64:429-435.

34. MacLean JA, Sauty A, Luster AD, Drazen JM, De Sanctis GT. Antigen-induced airway hyperresponsiveness, pulmonary eosinophilia, and chemokine expression in B cell-deficient mice. Am J Respir Cell Mol Biol. 1999;20:379-387.

35. Tsitoura DC, DeKruyff RH, Lamb JR, Umetsu DT. Intranasal exposure to protein antigen induces immunological tolerance mediated by functionally disabled CD4+ T cells. J Immunol. 1999;163:2592-2600.

36. Akbari O, DeKruyff RH, Umetsu DT. Pulmonary dendritic cells producing IL-10 mediate tolerance induced by respiratory exposure to antigen. Nat Immunol. 2001;2:725-731.

37. Brimnes MK, Bonifaz L, Steinman RM, Moran TM. Influenza virus-induced dendritic cell maturation is associated with the induction of strong T cell immunity to a coadministered, normally nonimmunogenic protein. J Exp Med. 2003;198:133-144.

38. Eisenbarth SC, Piggott DA, Huleatt JW, Visintin I, Herrick CA, Bottomly K. Lipopolysaccharide-enhanced, toll-like receptor 4-dependent T helper cell type 2 responses to inhaled antigen. J Exp Med. 2002;196:1645-1651.

39. Havenith CE, Breedijk AJ, Betjes MG, Calame W, Beelen RH, Hoefsmit EC. T cell priming in situ by intratracheally instilled antigen-pulsed dendritic cells. Am J Respir Cell Mol Biol. 1993;8:319-324.

40. Kuipers H, Hijdra D, De Vries VC, et al. Lipopolysaccharide-induced suppression of airway Th2 responses does not require IL-12 production by dendritic cells. J Immunol. 2003;171:3645-3654.

41. Sallusto F, Lenig D, Forster R, Lipp M, Lanzavecchia A. Two subsets of memory T lymphocytes with distinct homing potentials and effector functions. Nature. 1999;401:708-712.

42. Freytag LC, Clements JD. Mucosal adjuvants. Vaccine. 2005;23:1804-1813.

43. Holmgren J, Czerkinsky C, Eriksson K, Mharandi A. Mucosal immunisation and adjuvants: a brief overview of recent advances and challenges. Vaccine. 2003;21 Suppl 2:S89-95.

44. Klinman DM. Immunotherapeutic uses of CpG oligodeoxynucleotides. Nat Rev Immunol. 2004;4:249-258.

45. Yamamoto S, Yamamoto T, Kataoka T, Kuramoto E, Yano O, Tokunaga T. Unique palindromic sequences in synthetic oligonucleotides are required to induce IFN [correction of INF] and augment IFN-mediated [correction of INF] natural killer activity. J Immunol. 1992;148:4072-4076.

46. Krieg AM, Yi AK, Matson S, et al. CpG motifs in bacterial DNA trigger direct B-cell activation. Nature. 1995;374:546-549.

47. Klinman DM, Yi AK, Beaucage SL, Conover J, Krieg AM. CpG motifs present in bacteria DNA rapidly induce lymphocytes to secrete interleukin 6, interleukin 12, and interferon gamma. Proc Natl Acad Sci U S A. 1996;93:2879-2883.

48. Hemmi H, Takeuchi O, Kawai T, et al. A Toll-like receptor recognizes bacterial DNA. Nature. 2000;408:740-745.

49. Takeshita F, Leifer CA, Gursel I, et al. Cutting edge: Role of Toll-like receptor 9 in CpG DNA-induced activation of human cells. J Immunol. 2001;167:3555-3558.

50. Bauer S, Kirschning CJ, Hacker H, et al. Human TLR9 confers responsiveness to bacterial DNA via species-specific CpG motif recognition. Proc Natl Acad Sci U S A. 2001;98:9237-9242.

51. Ishii KJ, Takeshita F, Gursel I, et al. Potential role of phosphatidylinositol 3 kinase, rather than DNA-dependent protein kinase, in CpG DNA-induced immune activation. J Exp Med. 2002;196:269-274.

52. Takeshita F, Ishii KJ, Ueda A, Ishigatsubo Y, Klinman DM. Positive and negative regulatory elements contribute to CpG oligonucleotide-mediated regulation of human IL-6 gene expression. Eur J Immunol. 2000;30:108-116.

53. Yamamoto M, Sato S, Mori K, et al. Cutting edge: a novel Toll/IL-1 receptor domain-containing adapter that preferentially activates the IFN-beta promoter in the Toll-like receptor signaling. J Immunol. 2002;169:6668-6672.

54. Takeshita F, Klinman DM. CpG ODN-mediated regulation of IL-12 p40 transcription. Eur J Immunol. 2000;30:1967-1976.

55. Hacker H, Vabulas RM, Takeuchi O, Hoshino K, Akira S, Wagner H. Immune cell activation by bacterial CpG-DNA through myeloid differentiation marker 88 and tumor necrosis factor receptor-associated factor (TRAF)6. J Exp Med. 2000;192:595-600.

56. Aderem A, Ulevitch RJ. Toll-like receptors in the induction of the innate immune response. Nature. 2000;406:782-787.

57. Gursel M, Verthelyi D, Gursel I, Ishii KJ, Klinman DM. Differential and competitive activation of human immune cells by distinct classes of CpG oligodeoxynucleotide. J Leukoc Biol. 2002;71:813-820.

58. Hornung V, Rothenfusser S, Britsch S, et al. Quantitative expression of toll-like receptor 1-10 mRNA in cellular subsets of human peripheral blood mononuclear cells and sensitivity to CpG oligodeoxynucleotides. J Immunol. 2002;168:4531-4537.

59. Kadowaki N, Ho S, Antonenko S, et al. Subsets of human dendritic cell precursors express different toll-like receptors and respond to different microbial antigens. J Exp Med. 2001;194:863-869.

60. Demedts IK, Bracke KR, Maes T, Joos GF, Brusselle GG. Different roles for human lung dendritic cell subsets in pulmonary immune defense mechanisms. Am J Respir Cell Mol Biol. 2006;35:387-393.

61. Iwasaki A, Medzhitov R. Toll-like receptor control of the adaptive immune responses. Nat Immunol. 2004;5:987-995.

62. Kerkmann M, Costa LT, Richter C, et al. Spontaneous formation of nucleic acid-based nanoparticles is responsible for high interferon-alpha induction by CpG-A in plasmacytoid dendritic cells. J Biol Chem. 2005;280:8086-8093.

63. Hartmann G, Weeratna RD, Ballas ZK, et al. Delineation of a CpG phosphorothioate oligodeoxynucleotide for activating primate immune responses in vitro and in vivo. J Immunol. 2000;164:1617-1624.

64. Vollmer J, Weeratna R, Payette P, et al. Characterization of three CpG oligodeoxynucleotide classes with distinct immunostimulatory activities. Eur J Immunol. 2004;34:251-262.

65. Hartmann G, Krieg AM. Mechanism and function of a newly identified CpG DNA motif in human primary B cells. J Immunol. 2000;164:944-953.

66. Sparwasser T, Koch ES, Vabulas RM, et al. Bacterial DNA and immunostimulatory CpG oligonucleotides trigger maturation and activation of murine dendritic cells. Eur J Immunol. 1998;28:2045-2054.

67. Sparwasser T, Miethke T, Lipford G, et al. Macrophages sense pathogens via DNA motifs: induction of tumor necrosis factor-alpha-mediated shock. Eur J Immunol. 1997;27:1671-1679.

68. Lipford GB, Bauer M, Blank C, Reiter R, Wagner H, Heeg K. CpG-containing synthetic oligonucleotides promote B and cytotoxic T cell responses to protein antigen: a new class of vaccine adjuvants. Eur J Immunol. 1997;27:2340-2344.

69. Davis HL, Weeratna R, Waldschmidt TJ, Tygrett L, Schorr J, Krieg AM. CpG DNA is a potent enhancer of specific immunity in mice immunized with recombinant hepatitis B surface antigen. J Immunol. 1998;160:870-876.

70. Moldoveanu Z, Love-Homan L, Huang WQ, Krieg AM. CpG DNA, a novel immune enhancer for systemic and mucosal immunization with influenza virus. Vaccine. 1998;16:1216-1224.

71. Elkins KL, Rhinehart-Jones TR, Stibitz S, Conover JS, Klinman DM. Bacterial DNA containing CpG motifs stimulates lymphocyte-dependent protection of mice against lethal infection with intracellular bacteria. J Immunol. 1999;162:2291-2298.

72. Gramzinski RA, Doolan DL, Sedegah M, Davis HL, Krieg AM, Hoffman SL. Interleukin-12- and gamma interferon-dependent protection against malaria conferred by CpG oligodeoxynucleotide in mice. Infect Immun. 2001;69:1643-1649.

73. Krieg AM, Love-Homan L, Yi AK, Harty JT. CpG DNA induces sustained IL-12 expression in vivo and resistance to Listeria monocytogenes challenge. J Immunol. 1998;161:2428-2434.

74. Zimmermann S, Egeter O, Hausmann S, et al. CpG oligodeoxynucleotides trigger protective and curative Th1 responses in lethal murine leishmaniasis. J Immunol. 1998;160:3627-3630.

75. Horner AA, Ronaghy A, Cheng PM, et al. Immunostimulatory DNA is a potent mucosal adjuvant. Cell Immunol. 1998;190:77-82.

76. McCluskie MJ, Davis HL. Oral, intrarectal and intranasal immunizations using CpG and non-CpG oligodeoxynucleotides as adjuvants. Vaccine. 2000;19:413-422.

77. Pal S, Davis HL, Peterson EM, de la Maza LM. Immunization with the Chlamydia trachomatis mouse pneumonitis major outer membrane protein by use of CpG oligodeoxynucleotides as an adjuvant induces a protective immune response against an intranasal chlamydial challenge. Infect Immun. 2002;70:4812-4817.

78. Bozza S, Gaziano R, Lipford GB, et al. Vaccination of mice against invasive aspergillosis with recombinant Aspergillus proteins and CpG oligodeoxynucleotides as adjuvants. Microbes Infect. 2002;4:1281-1290.

79. Jain VV, Kitagaki K, Businga T, et al. CpG-oligodeoxynucleotides inhibit airway remodeling in a murine model of chronic asthma. J Allergy Clin Immunol. 2002;110:867-872.

80. Choudhury BK, Wild JS, Alam R, et al. In vivo role of p38 mitogen-activated protein kinase in mediating the anti-inflammatory effects of CpG oligodeoxynucleotide in murine asthma. J Immunol. 2002;169:5955-5961.

81. Hayashi T, Beck L, Rossetto C, et al. Inhibition of experimental asthma by indoleamine 2,3-dioxygenase. J Clin Invest. 2004;114:270-279.

82. Broide D, Schwarze J, Tighe H, et al. Immunostimulatory DNA sequences inhibit IL-5, eosinophilic inflammation, and airway hyperresponsiveness in mice. J Immunol. 1998;161:7054-7062.

83. Juffermans NP, Leemans JC, Florquin S, et al. CpG oligodeoxynucleotides enhance host defense during murine tuberculosis. Infect Immun. 2002;70:147-152.

84. Edwards L, Williams AE, Krieg AM, Rae AJ, Snelgrove RJ, Hussell T. Stimulation via Toll-like receptor 9 reduces Cryptococcus neoformans-induced pulmonary inflammation in an IL-12-dependent manner. Eur J Immunol. 2005;35:273-281.

85. Deng JC, Moore TA, Newstead MW, Zeng X, Krieg AM, Standiford TJ. CpG oligodeoxynucleotides stimulate protective innate immunity against pulmonary Klebsiella infection. J Immunol. 2004;173:5148-5155.

86. Harandi AM, Eriksson K, Holmgren J. A protective role of locally administered immunostimulatory CpG oligodeoxynucleotide in a mouse model of genital herpes infection. J Virol. 2003;77:953-962.

87. Raghavan S, Nystrom J, Fredriksson M, Holmgren J, Harandi AM. Orally administered CpG oligodeoxynucleotide induces production of CXC and CC chemokines in the gastric mucosa and suppresses bacterial colonization in a mouse model of Helicobacter pylori infection. Infect Immun. 2003;71:7014-7022.

88. Rappuoli R, Pizza M, Douce G, Dougan G. Structure and mucosal adjuvanticity of cholera and Escherichia coli heat-labile enterotoxins. Immunol Today. 1999;20:493-500.

89. Katz JM, Lu X, Young SA, Galphin JC. Adjuvant activity of the heat-labile enterotoxin from enterotoxigenic Escherichia coli for oral administration of inactivated influenza virus vaccine. J Infect Dis. 1997;175:352-363.

90. Marinaro M, Riccomi A, Rappuoli R, et al. Mucosal delivery of the human immunodeficiency virus-1 Tat protein in mice elicits systemic neutralizing antibodies, cytotoxic T lymphocytes and mucosal IgA. Vaccine. 2003;21:3972-3981.

91. Zurbriggen R, Metcalfe IC, Gluck R, Viret JF, Moser C. Nonclinical safety evaluation of Escherichia coli heat-labile toxin mucosal adjuvant as a component of a nasal influenza vaccine. Expert Rev Vaccines. 2003;2:295-304.

92. Giuliani MM, Del Giudice G, Giannelli V, et al. Mucosal adjuvanticity and immunogenicity of LTR72, a novel mutant of Escherichia coli heat-labile enterotoxin with partial knockout of ADP-ribosyltransferase activity. J Exp Med. 1998;187:1123-1132.

93. Pizza M, Giuliani MM, Fontana MR, et al. Mucosal vaccines: non toxic derivatives of LT and CT as mucosal adjuvants. Vaccine. 2001;19:2534-2541.

94. Baudner BC, Balland O, Giuliani MM, et al. Enhancement of protective efficacy following intranasal immunization with vaccine plus a nontoxic LTK63 mutant delivered with nanoparticles. Infect Immun. 2002;70:4785-4790.

95. Baudner BC, Giuliani MM, Verhoef JC, Rappuoli R, Junginger HE, Giudice GD. The concomitant use of the LTK63 mucosal adjuvant and of chitosan-based delivery system enhances the immunogenicity and efficacy of intranasally administered vaccines. Vaccine. 2003;21:3837-3844.

96. Beignon AS, Briand JP, Rappuoli R, Muller S, Partidos CD. The LTR72 mutant of heat-labile enterotoxin of Escherichia coli enhances the ability of peptide antigens to elicit CD4(+) T cells and secrete gamma interferon after coapplication onto bare skin. Infect Immun. 2002;70:3012-3019.

97. Ugozzoli M, Santos G, Donnelly J, O'Hagan DT. Potency of a genetically detoxified mucosal adjuvant derived from the heat-labile enterotoxin of Escherichia coli (LTK63) is not adversely affected by the presence of preexisting immunity to the adjuvant. J Infect Dis. 2001;183:351-354.

98. Ugozzoli M, Mariani M, Del Giudice G, Soenawan E, O'Hagan DT. Combinations of protein polysaccharide conjugate vaccines for intranasal immunization. J Infect Dis. 2002;186:1358-1361.

99. Tierney R, Beignon AS, Rappuoli R, Muller S, Sesardic D, Partidos CD. Transcutaneous immunization with tetanus toxoid and mutants of Escherichia coli heat-labile enterotoxin as adjuvants elicits strong protective antibody responses. J Infect Dis. 2003;188:753-758.

100. Jakobsen H, Adarna BC, Schulz D, Rappuoli R, Jonsdottir I. Characterization of the antibody response to pneumococcal glycoconjugates and the effect of heat-labile enterotoxin on IGg subclasses after intranasal immunization. J Infect Dis. 2001;183:1494-1500.

101. Bonenfant C, Dimier-Poisson I, Velge-Roussel F, et al. Intranasal immunization with SAG1 and nontoxic mutant heat-labile enterotoxins protects mice against Toxoplasma gondii. Infect Immun. 2001;69:1605-1612.

102. Peppoloni S, Ruggiero P, Contorni M, et al. Mutants of the Escherichia coli heat-labile enterotoxin as safe and strong adjuvants for intranasal delivery of vaccines. Expert Rev Vaccines. 2003;2:285-293.

103. Simmons CP, Hussell T, Sparer T, Walzl G, Openshaw P, Dougan G. Mucosal delivery of a respiratory syncytial virus CTL peptide with enterotoxin-based adjuvants elicits protective, immunopathogenic, and immunoregulatory antiviral CD8+ T cell responses. J Immunol. 2001;166:1106-1113.

104. Ryan EJ, McNeela E, Murphy GA, et al. Mutants of Escherichia coli heat-labile toxin act as effective mucosal adjuvants for nasal delivery of an acellular pertussis vaccine: differential effects of the nontoxic AB complex and enzyme activity on Th1 and Th2 cells. Infect Immun. 1999;67:6270-6280.

105. Stephenson I, Zambon MC, Rudin A, et al. Phase I evaluation of intranasal trivalent inactivated influenza vaccine with nontoxigenic Escherichia coli enterotoxin and novel biovector as mucosal adjuvants, using adult volunteers. J Virol. 2006;80:4962-4970.

106. Di Tommaso A, Saletti G, Pizza M, et al. Induction of antigen-specific antibodies in vaginal secretions by using a nontoxic mutant of heat-labile enterotoxin as a mucosal adjuvant. Infect Immun. 1996;64:974-979.

107. Douce G, Fontana M, Pizza M, Rappuoli R, Dougan G. Intranasal immunogenicity and adjuvanticity of site-directed mutant derivatives of cholera toxin. Infect Immun. 1997;65:2821-2828.

108. Jakobsen H, Bjarnarson S, Del Giudice G, Moreau M, Siegrist CA, Jonsdottir I. Intranasal immunization with pneumococcal conjugate vaccines with LT-K63, a nontoxic mutant of heat-Labile enterotoxin, as adjuvant rapidly induces protective immunity against lethal pneumococcal infections in neonatal mice. Infect Immun. 2002;70:1443-1452.

109. Baudner BC, Morandi M, Giuliani MM, et al. Modulation of immune response to group C meningococcal conjugate vaccine given intranasally to mice together with the LTK63 mucosal adjuvant and the trimethyl chitosan delivery system. J Infect Dis. 2004;189:828-832.

110. Ryan EJ, McNeela E, Pizza M, Rappuoli R, O'Neill L, Mills KH. Modulation of innate and acquired immune responses by Escherichia coli heat-labile toxin: distinct pro- and anti-inflammatory effects of the nontoxic AB complex and the enzyme activity. J Immunol. 2000;165:5750-5759.

111. Simmons CP, Mastroeni P, Fowler R, et al. MHC class I-restricted cytotoxic lymphocyte responses induced by enterotoxin-based mucosal adjuvants. J Immunol. 1999;163:6502-6510.

112. Neidleman JA, Vajdy M, Ugozzoli M, Ott G, O'Hagan D. Genetically detoxified mutants of heat-labile enterotoxin from Escherichia coli are effective adjuvants for induction of cytotoxic T-cell responses against HIV-1 gag-p55. Immunology. 2000;101:154-160.

113. Williams AE, Edwards L, Humphreys IR, et al. Innate imprinting by the modified heat-labile toxin of Escherichia coli (LTK63) provides generic protection against lung infectious disease. J Immunol. 2004;173:7435-7443.

114. Walzl G, Tafuro S, Moss P, Openshaw PJ, Hussell T. Influenza virus lung infection protects from respiratory syncytial virus-induced immunopathology. J Exp Med. 2000;192:1317-1326.

115. Chen HD, Fraire AE, Joris I, Brehm MA, Welsh RM, Selin LK. Memory CD8+ T cells in heterologous antiviral immunity and immunopathology in the lung. Nat Immunol. 2001;2:1067-1076.

116. Karrer HE. The ultrastructure of mouse lung: the alveolar macrophage. J Biophys Biochem Cytol. 1958;4:693-700.

117. Lutz MB, Kukutsch N, Ogilvie AL, et al. An advanced culture method for generating large quantities of highly pure dendritic cells from mouse bone marrow. J Immunol Methods. 1999;223:77-92.

118. Krieg AM. CpG motifs in bacterial DNA and their immune effects. Annu Rev Immunol. 2002;20:709-760.

119. Suzuki K, Suda T, Naito T, Ide K, Chida K, Nakamura H. Impaired toll-like receptor 9 expression in alveolar macrophages with no sensitivity to CpG DNA. Am J Respir Crit Care Med. 2005;171:707-713.

120. Lappin MB, Weiss JM, Delattre V, et al. Analysis of mouse dendritic cell migration in vivo upon subcutaneous and intravenous injection. Immunology. 1999;98:181-188.

121. Kirby AC, Raynes JG, Kaye PM. CD11b regulates recruitment of alveolar macrophages but not pulmonary dendritic cells after pneumococcal challenge. J Infect Dis. 2006;193:205-213.

122. Vermaelen K, Pauwels R. Accurate and simple discrimination of mouse pulmonary dendritic cell and macrophage populations by flow cytometry: methodology and new insights. Cytometry A. 2004;61:170-177.

123. Krieg AM, Davis HL. Enhancing vaccines with immune stimulatory CpG DNA. Curr Opin Mol Ther. 2001;3:15-24.

124. Li J, Ma Z, Tang ZL, Stevens T, Pitt B, Li S. CpG DNA-mediated immune response in pulmonary endothelial cells. Am J Physiol Lung Cell Mol Physiol. 2004;287:L552-558.

125. Chen L, Arora M, Yarlagadda M, et al. Distinct responses of lung and spleen dendritic cells to the TLR9 agonist CpG oligodeoxynucleotide. J Immunol. 2006;177:2373-2383.

126. Luster AD. The role of chemokines in linking innate and adaptive immunity. Curr Opin Immunol. 2002;14:129-135.

127. Khader SA, Partida-Sanchez S, Bell G, et al. Interleukin 12p40 is required for dendritic cell migration and T cell priming after Mycobacterium tuberculosis infection. J Exp Med. 2006;203:1805-1815.

128. Nakano H, Yanagita M, Gunn MD. CD11c(+)B220(+)Gr-1(+) cells in mouse lymph nodes and spleen display characteristics of plasmacytoid dendritic cells. J Exp Med. 2001;194:1171-1178.

129. Asselin-Paturel C, Boonstra A, Dalod M, et al. Mouse type I IFN-producing cells are immature APCs with plasmacytoid morphology. Nat Immunol. 2001;2:1144-1150.

130. Bangs SC, McMichael AJ, Xu XN. Bystander T cell activation--implications for HIV infection and other diseases. Trends Immunol. 2006;27:518-524.

131. Hemmi H, Kaisho T, Takeuchi O, et al. Small anti-viral compounds activate immune cells via the TLR7 MyD88-dependent signaling pathway. Nat Immunol. 2002;3:196-200.

132. Jurk M, Heil F, Vollmer J, et al. Human TLR7 or TLR8 independently confer responsiveness to the antiviral compound R-848. Nat Immunol. 2002;3:499.

133. Zuniga EI, McGavern DB, Pruneda-Paz JL, Teng C, Oldstone MB. Bone marrow plasmacytoid dendritic cells can differentiate into myeloid dendritic cells upon virus infection. Nat Immunol. 2004;5:1227-1234.

134. Colonna M, Trinchieri G, Liu YJ. Plasmacytoid dendritic cells in immunity. Nat Immunol. 2004;5:1219-1226.

135. Tritto E, Muzzi A, Pesce I, et al. The acquired immune response to the mucosal adjuvant LTK63 imprints the mouse lung with a protective signature. J Immunol. 2007;179:5346-5357.

136. Chapman TJ, Castrucci MR, Padrick RC, Bradley LM, Topham DJ. Antigen-specific and non-specific CD4+ T cell recruitment and proliferation during influenza infection. Virology. 2005;340:296-306.

137. Roman E, Miller E, Harmsen A, et al. CD4 effector T cell subsets in the response to influenza: heterogeneity, migration, and function. J Exp Med. 2002;196:957-968.

138. Yamamoto N, Suzuki S, Shirai A, et al. Dendritic cells are associated with augmentation of antigen sensitization by influenza A virus infection in mice. Eur J Immunol. 2000;30:316-326.

139. Gill MA, Palucka AK, Barton T, et al. Mobilization of plasmacytoid and myeloid dendritic cells to mucosal sites in children with respiratory syncytial virus and other viral respiratory infections. J Infect Dis. 2005;191:1105-1115.